GROUNDWATER RECHARGE MECHANISM, GROUNDWATER-SURFACE WATER CONNECTION AND GROUNDWATER DYNAMICS AROUND LAKE SIBAYA , NORTH EASTERN KWAZULU-NATAL.

Thobeka Nsibande (216010937)

Supervisor: Professor Seifu Kebede Gurmessa

and

Co-Supervisor: Susan Janse van Rensburg

Submitted in partial fulfilment of the requirements

For the degree of Master of Science in Hydrology

Centre for Water Resources Research

University of KwaZulu-Natal

Pietermaritzburg

South Africa

Date: June 2023

ABSTRACT

The Maputaland Coastal Plain (MCP) within catchment W071A has South Africa's largest freshwater Lake Sibaya, a topographically closed lake fed by groundwater from the surrounding aquifers. The lake has substantially declined in water volume, area, and depth. The cause of the lake shrinking has been attributed to changes in rainfall pattern, increased abstraction by people or land use –land cover or a combination of these. As the lake is a groundwater dependent lake, to better understand the cause of the lake level decline, it is important to understand the relationship between rainfall and the response of the groundwater to rainfall. Groundwater models would be more realistic if the hydrological responses using a well-constructed realistic conceptual model of interconnectivity between aquifers were understood. This study aims to construct a conceptual groundwater recharge and flow model for Lake Sibaya, which will inform the ongoing numerical groundwater flow model using coupled ACRU-MODFLOW tools. Stable isotope $\delta^{18}O$ and $\delta^{2}H$, piezometer, well-log and water chemistry data were used to achieve the study objectives. Daily rain, monthly groundwater (from community boreholes and community dug-wells), and monthly surface water samples were collected between July 2021 to August 2022 and analysed. Vertical interconnectivity between aquifers was studied using measurements done on nested (shallow and deep borehole) boreholes. The $\delta^{18}O$ showed that rainfall is the primary source of groundwater recharge and occurs episodically when rainfall events exceed 30mm/day. This implies that Lake Sibaya catchment groundwater largely depends on the frequency of extreme rainfall events. The isotope, piezometer, well log data, water chemistry data $\delta^{18}O$ obtained from nested boreholes (shallow and deep borehole) indicated aquifers are interconnected, indicating two aquifer layer must be accounted for when groundwater flow models are to be parametrized.

Key words: *Conceptual modelling, isotopes, Lake Sibaya, groundwater recharge, aquifer to aquifer interactions.*

PREFACE

The research contained in this MSc dissertation was completed by the candidate while based in the Discipline of Hydrology, School of Agricultural, Earth and Environmental Sciences of the College of Agriculture, Engineering and Science, University of KwaZulu-Natal, Pietermaritzburg campus, South Africa. The research was financially supported by Water Research Commission and South African Environmental Observation Network.

The contents of this work have not been submitted in any form to another university and, except where the work of others is acknowledged in the text, the results reported are due to investigations by the candidate.

_____

Signed :

Date:

DECLARATION 1: PLAGIARISM

I, Thobeka Nomfundo Nsibande, declare that:

(a) The research reported in this document, except where otherwise indicated, is my original work.

(b) This document has not been submitted for any degree or examination at any other university.

(c) This document does not contain text, data, figures, pictures, graphs or tables from another document, unless it is specifically acknowledged as being sourced the original document. Where other sources have been quoted, then:

(i) their words have been paraphrased/re-written, and the general information attributed to them has been referenced, and

(ii) where their exact words have been used, their writing has been placed inside quotation marks, and referenced.

(d) Where I have reproduced a publication, of which I am an author, co-author or editor, I have indicated, in detail, which part of the publication was actually written by myself alone and I have fully referenced such publications.

(e) This document does not contain text, graphics or tables copied and pasted from the Internet, unless they are specifically acknowledged and the source is detailed, both in the document and in the References section.

Signed:  Date: 31/10/2023

Supervisor: 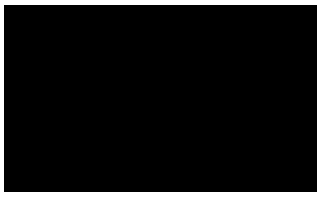 Date:

Co-Supervisor: Date:

ACKNOWLEDGEMENTS

I would like to express my sincere gratitude to my Supervisor, Professor Seifu Kebede Gurmessa, for his guidance and support throughout this project. His insights and feedback were invaluable, and I am genuinely grateful for the Mentorship.

I would also like to thank Susan Janse van Rensburg from the South African Environmental Observation Network for her guidance, support, feedback, and relevant reports for the study area and geological information. The opportunities she provided me throughout this project and her encouragement to attend and present at different conferences.

Water Research Commission (WRC) and South African Environmental Observation Network SAEON for providing me with financial support during this study.

Finally, I would like to thank all my friends and family for their support and love. Their encouragement and understanding helped me persevere through this project challenges. They all became my pillar of support through my studies. To all my colleagues from SAEON, Siphiwe Mfeka and Nosihle Mkhize from South African Environmental Observation Network, Mkholo Maseko, Amanda Nyawose, Sabelo Nxumalo, and Baba Mdletshe. I would not have been able to do this without your support and assistance through fieldwork.

This dissertation would not have been possible without these people's help. I am deeply indebted to them.

LIST OF ABBREVATION

amsl	Above mean sea level
EC	Electrical conductivity (mS/m)
GMWL	Global Meteoric Water Line
LMWL	Local Meteoric Water Line
VSMOW	Vienna Standaed Mean Ocean Water
$\delta^{18}O$	Oxygen-18 (‰)
$\delta^{2}H$	Deuterum (‰)
MCP	Maputaland Coastal Plain

Table of content

LIST OF FIGURES

LIST OF TABLES

1. INTRODUCTION

South Africa is a water-scarce, semi-arid country with an estimated average rainfall of around 500 mm/a, which is less than 60% of the world average (Makiwane, 2019). In many circumstances, surface water has proven to be an increasingly unreliable water source due to climate change and poor water infrastructure development in certain regions (Kulsawat and Nochit, 2019). Groundwater has emerged as a crucial natural water resource for production of freshwater in many areas and nations around the world (He *et al*., 2020; Li *et al*., 2019; Su *et al*., 2020; Wu *et al*., 2020). According to Mpenyana-Monyatsi *et al.* (2012), between 13% and 15% of South Africa overall water needs are met by groundwater.

The National Water Act (Act 36 of 1998) recognizes that water resources are interconnected, and that they must be managed as a whole. This means that surface water, groundwater, and unconventional water resources must all be considered when making decisions about water management. The Act also recognizes that water resources must be developed and used in an environmentally responsible manner, which means that the ecological processes that sustain water must be protected. A better understanding of water resources and the hydraulic and ecological processes that sustain them is therefore required.

Heavy rainfall have been observed to result to higher groundwater recharge rates given the conducive properties of the soil. Maréchal *et al*. (2006) found that the more rainy days during the monsoon, the more likely the groundwater recharge would occur. Several studies in Africa have found that heavy rainfall has a disproportionate contribution to groundwater recharge (Leblanc *et al*., 2008; Favreau *et a*l., 2009; Owor *et al*., 2009; Taylor *et al*., 2013; Galle *et al*., 2018; Cuthbert *et al*., 2019; MacDonald *et al.,* 2021). The frequency and intensity of heavy precipitation events are projected to increase almost everywhere in Africa with additional global warming (IPCC *et al*., 2021). As a result, it is necessary to comprehend how recharge would behave locally under heavy rainfall, specifically by determining the extent of recharge dependence on rainfall amount .

A number of ecologically significant coastal lakes distinguishes Maputaland Coastal Plain. These coastal lakes, such as Lake Sibaya, are significant hydrological features with significant scientific and commercial significance. Climate has a strong influence on the water resources of Maputaland Coastal Plain and the surface water and groundwater in the region is a direct response to local climate conditions. The system is recharged through precipitation.

Hydrological process such as groundwater recharge rate are strongly influenced by the type of rainfall and frequency. Given that the water resources in the region are strongly influenced by precipitation and during the drought periods are recharge by groundwater, there is still a lack in understating the relationship between them. The understanding of the relationship between rainfall and the response of groundwater is poorly understood and the roles of cyclones and other extreme rainfall events in replenishing groundwater while speculated as important, have as yet not been explicitly addressed, with appropriate data and evidence in this region.

Surface water-groundwater relationship has long been the primary focus of development and exploitation in MPC, including the studies by Weitz and Demlie (2014) and Kelbe and Germishuye (2010). These studies found the groundwater and surface water highly connected. Aquifer has been one of the MPC feature that has been explored however; the connectivity between aquifers has yet not been confirm. Instead, patchy well-logs have been used to delineate the number of aquifers, including work by Weitz and Demlie (2014).

Over the years, considerable research has contributed to understanding various aspects of the hydrological processes associated with Lake Sibaya and surrounding areas. Weitz and Demile (2014), developed a conceptual model of Lake Sibaya (Figure 1.1). The conceptual model constructed by Weitz and Demlie (2014) focused on surface water and groundwater interaction and lacks details on groundwater recharge mechanism, aquifer-aquifer interactions. The model indicated the lake recharges the aquifers on the east. However, no model has determined the recharge of the lake from the dune cordon through field observations and if the conceptualization in the model is correct. Therefore, this study intends to provide additional details on groundwater recharge mechanism and aquifer interconnectivity by producing high quality spatially and temporally dense data using stable water isotopes, chemistry and piezometer data.

.

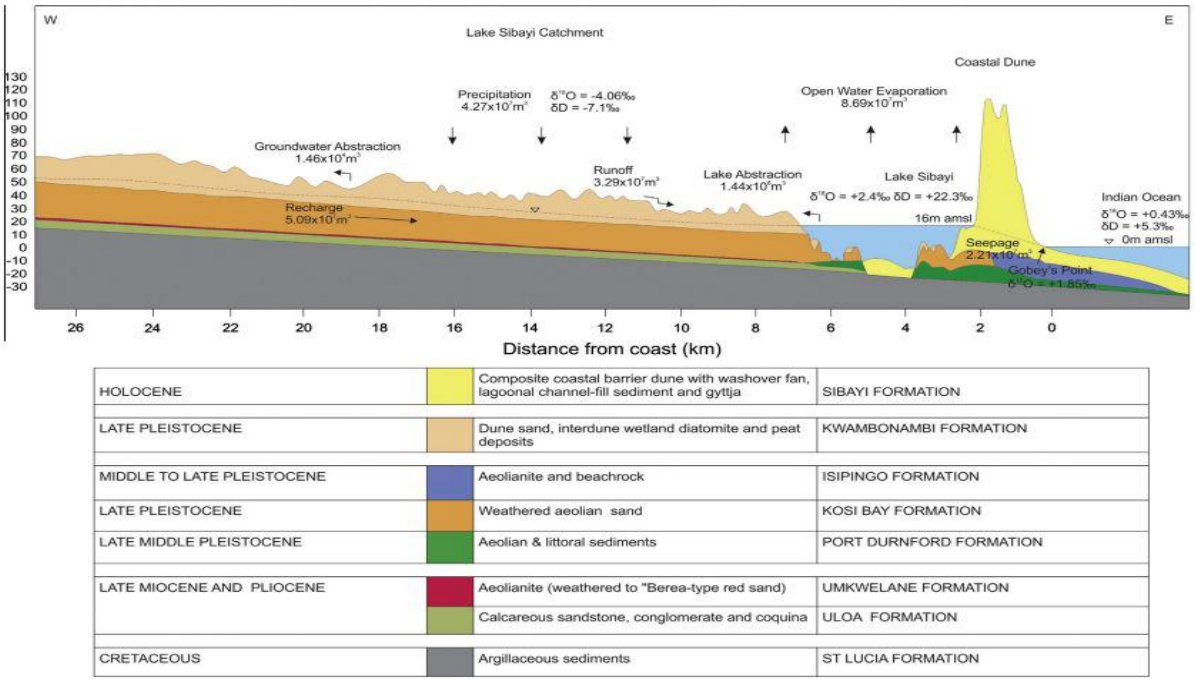

HOLOCENE		Composite coastal barrier dune with washover fan, lagoonal channel-fill sediment and gyttja	SIBAYI FORMATION
LATE PLEISTOCENE		Dune sand, interdune wetland diatomite and peat deposits	KWAMBONAMBI FORMATION
MIDDLE TO LATE PLEISTOCENE		Aeolianite and beachrock	ISIPINGO FORMATION
LATE PLEISTOCENE		Weathered aeolian sand	KOSI BAY FORMATION
LATE MIDDLE PLEISTOCENE		Aeolian & littoral sediments	PORT DURNFORD FORMATION
LATE MIOCENE AND PLIOCENE		Aeolianite (weathered to "Berea-type red sand)	UMKWELANE FORMATION
		Calcareous sandstone, conglomerate and coquina	ULOA FORMATION
CRETACEOUS		Argillaceous sediments	ST LUCIA FORMATION

Figure 1-1Hydrogeological conceptual model of Lake Sibaya Catchment (Weitz and Demile, 2014).

1.1 Significance of the study

Recharge assessment is an essential aspect of hydrological systems, and it is critical in the development, proper utilization, management, and protection of groundwater resources (Manna *et al.*, 2017).

Groundwater in the MPC has been utilized for many years, as the region is the groundwater-based system where lake, streams and wetlands are also groundwater discharge areas, thus, aquifer systems in this area are extremely important and need to be used sustainably. Understanding the recharge process is critical to managing the groundwater system in MPC under changing climate and land use. Understanding recharge process would aid in predicting how the groundwater availability responds to land use and climate changes. Although many studies on this region has been conducted since the late 1960's, there is still a limited knowledge, particularly on groundwater response on different rainfall patterns, and the interaction between aquifers.

1.2 Research Questions

This research primarily aims to answer the question, what is the cause of the recent water (groundwater, lake, and wetland) availability decline in the Lake Sibaya system? It attempts to answer the following research questions, which will allow the provision of better insight and understanding, groundwater recharge mechanism, and determine interconnectivity of the aquifer system contained within the MPC. Specific research questions are:

- What is the predominant groundwater recharge mechanism? Diffuse or focused recharge? From all rainfall events or selective recharge from heavy rains? What is the lowest minimum rainfall amount contributing to groundwater recharge? In which specific season of the year and the groundwater recharge takes place.
- Are different aquifers interconnected? Is the aquifer system one interconnected body separated by tiny lenses of impermeable units or are these different aquifers layers disconnected from each other and responding to pumping and climatic pressures independently?
- How valid are the parameterization of the existing groundwater numerical models and the outputs of existing numerical flow models?

1.3 Research Aims and Objectives

1.3.1 Aim:

This research aims to construct a conceptual groundwater recharge and flow model for the Lake Sibaya area for eventual use in informing the ongoing numerical groundwater flow model using coupled ACRU-MODFLOW tools. It aims to use and generate new integrated baseline isotope hydrology, piezometry, well-log and water chemistry data for use under the current work and for future research as part of larger collaborative WRC project.

More specifically the research aims to refine the existing conceptual model to develop an updated conceptual groundwater recharge, flow and discharge model for the MPC.

To achieve the above aim and answer the research questions of this study, which will ensure the success of the project, the following objectives will have to be met.

1.3.2 Objectives:

The research objectives are to:

- To provide an analysis of the groundwater recharge mechanism
- Determine interconnectivity between the different aquifers
- Construct a conceptual groundwater recharge and flow model accounting for all its components

1.4 Thesis structure

Chapter 1: Chapter introduces the dissertation and provides a brief overview on the global knowledge on rainfall and groundwater recharge. It also describes the study problem, significance of the study, research question, aims, and the objectives.

Chapter 2: Chapter provides a literature review related to groundwater recharge mechanism, factors influencing the groundwater with a specific attention to climate-rainfall on how extreme rainfall events affect the groundwater recharge and how extreme rainfall events has affected the MPC region with specific to Lake Sibaya Catchment. The other topics covered on this chapter are aquifer-aquifer interaction, methodologies to investigate their interaction, environmental isotopes, conceptual modelling and hydrological units.

Chapter 3: Chapter describes the study area, in terms of its location, climate, geology, hydrogeology, morphology, physiography, vegetation and land use, and wetlands.

Chapter4: Chapter outlines the research approaches, methodology and material used in the study to collect, analyse and present the data obtained.

Chapter 5: Chapter provides the summary of the results from the investigations and provides the description of the results.

Chapter 6: Chapter provides the detailed discussions of the results. This chapter concluded by developing the groundwater flow conceptual model and the hydrogeological conceptual mode of the study site.

Chapter 7: Chapter presents the conclusions of the research, the implications of the findings and recommendations.

Chapter 8: Chapter includes comprehensive list of references and appendixes.

2. LITERATURE REVIEW

Understanding the relationship between rainfall amount and groundwater recharge is essential in forecasting the impact of future climate change on groundwater resources availability (Kotchoni *et al*., 2019). Studies have shown a strong correlation between annual precipitation and the amount of recharge (Taylor *et al*., 2013; Cuthbert *et al.*, 2019), implying that more rainfall will result in more recharge and, thus, aquifer replenishment. However, infiltration rate varies depending on the type of soil cover, initial moisture content, rainfall intensity and duration, depth to the water table, aquifer effective porosity, and conductivity (Taylor *et al*., 2013). In arid and semi-arid environments groundwater recharge tends to occur during extreme or heavy precipitation events depending on the favourable condition for recharge (Thomas *et al.*, 2016). The MPC coastal plain being a humid region with a primarily sandy aquifer with no drainage, the relation between the role of extreme rainfall events on groundwater recharge and aquifer-aquifer interaction needs to be investigated .

2.1 Groundwater Recharge Mechanism

Groundwater recharge is the process of water from rainfall and surface water bodies enter into the groundwater system (Kelbe and Germishuyse, 2010; Merz, 2012). Healy (2010) defined *recharge* as the downward flow of water that reaches the water table, adding to the groundwater storage. Groundwater recharge occur through two main mechanisms: diffuse and focused mechanisms (Healy, 2010). Diffuse recharge refers to the recharge over large areas due to precipitation infiltrating the soil surface and percolating through the unsaturated zone to the water table. Diffused recharge is also known as local recharge (Allison, 1988) or direct recharge (Simmers, 1998). Focus recharge is water movement from surface water bodies, such as streams and lakes, to underlying aquifers (Healy, 2010). This type of recharge varies significantly in space and time, and as the degree of aridity in a particular area increases, focused recharge becomes more critical (Xu and Beekman, 2003).

2.2 Factors influencing groundwater recharge

Groundwater recharge is controlled by a number of environmental factors, including climate, soils and geology, vegetation and land use, and depth to the water table. These factors interact

to create specific conditions that result in recharge. In this study, the focus is on the climate, specifically rainfall.

2.2.1 Climate

Water availability at the land surface is controlled by the spatial and temporal variability of climate (Scanlon *et al*., 2022). Climate variability is a key factor that controls groundwater recharge, as precipitation is the primary source of recharge. Precipitation trends such as timing, duration, and intensity can all affect groundwater recharge. Recharge is more likely to take place when precipitation rates exceed evaporation rates.

Climate change is predicted to alter rainfall patterns in various parts of the world. These changes in rainfall patterns include prolonged drought periods interrupted by heavy rainfall events, where a significant portion of the yearly rainfall can fall in hours (He *et al*., 2022). The Intergovernmental Panel on Climate Change (IPCC) Sixth Assessment Report finds that the frequency and intensity of heavy rainfall events have increased over most land areas in recent decades and those heavy rainfall events are likely to become even more frequent and intense with continued global warming. This shows high chances of the extreme events increasing in frequency and magnitude in the future (IPCC *et al*., 2021). Many studies have examined the frequency and magnitude of South African floods over the last half-century (Alexander, 2002 as cited by Grab and Nash, 2022; Ntanganedzeni and Nobert, 2021). In the broader context, Dube *et al*. (2022) mentioned that extreme weather events associated with climate change have intensified and become more frequent over the recent decade (2010-2020). Floods with considerable damage generally occur every two years in South Africa, with more widespread catastrophic floods occurring every 10-15 years (Viljoen and Booysen, 2006).

2.3 Impact of extreme rainfall events on groundwater recharge

Multiple studies have found a strong correlation between annual precipitation and the amount of recharge (Doll and Fiedler, 2008; Taylor *et al*., 2013; Cuthbert *et al*., 2019). Tayler *et al*. (2013) studied the dependence of groundwater resources on extreme rainfall in East Africa. The projected extreme monthly rainfall using the model were responsible for recharge. According to Cuthbert *et al*. (2019), extreme annual recharge is commonly associated with intense and flooding events, driven by climate controls. Obadala and AL-Abri, 2011 evaluated

the groundwater recharge with respect to Gonu 2007 cyclone to assess the potential of recharge induced by such cyclones in the arid zones. The study showed that the cyclone resulted in a significant water table rise; however, the water table rise was subjected to favourable geological and structural setting. This was justified by the piezometer, which were located in less favourable zone, which showed minimum rise of water table. However, Obadala and AL-Abri, 2011 mentioned that when the recharge from the cyclonic event was compared with the frequent precipitation along favourable zone produced a significant recharge compared with cyclonic events where surface water residence time is shorter to allow for efficient infiltration. In a study by Boas and Mallants, 2022, highlighted that only 150 to 200 mm events generated noticeable recharge. The recharge was linked to extreme rainfall associated with monsoonal cyclones.

Region such as northern eastern of KwaZulu-Natal has favourable geological setting containing sandy soils, which is expected to allow high infiltration and less runoff. Extreme rainfall such as cyclonic events are expected to increase groundwater recharge and this work aims to prove the increase in groundwater recharge accompanying heavy rains. Været *et al*. (2008) cited by Weitz (2016), provides climate predictions ending in the year 2100 for the area of Lake St Lucia, which is south of Lake Sibaya and indicated a 5 – 10% precipitation increase and a 2 to 3 °C temperature increase, as well as an overall climate that is warmer and wetter. Furthermore, Janse van Rensburg (2019b) states that since the year 2000, there has not been rainfall from cyclonic storms that would be considered significant and projections by researchers indicate potentially less input from rainfall due to cyclone belt shifts in the northern direction. Other studies suggest northward (Malherbe *et al*., 2013) westward (Malherbe *et al*., 2012), and southward (Fitchett and Grab, 2014) directions about tropical cyclone shifts, therefore indicating conflicting projections.

2.4 Extreme rainfall events impacted MPC

Almost to all of South Africa, the MPC is classified as summer rainfall region and is prone to drought and occasional events (Mpungose *et al*., 2022). Reason *et al.* (2000) mentioned that some of this variability in rainfall in the MPC might be associated with ENSO, which affects the sub-continent strongly in summer, leading to above average rainfalls during El Nino and below average rainfall during La Nino episodes.

Lake Sibaya water (situated in the MPC) water levels have decreased significantly over the last past two decades, exposing large areas that were once covered by water. The lake is currently 15.1 (SAEON) as compared to 21 amsl, when full (Hill, 1979 cited by Mpungose *et al*., 2022). It is not yet clear, whether the lake decline is due to changes in land use or the changes in rainfall patterns, or both. However, extreme rainfall events can have an impact on groundwater recharge, resulting in an increase in the lake levels, as well as cause severe floods and damages or loss of life (Bopape *et al*., 2021). A better understanding of the impact of extreme rainfall events in the MPC (Lake Sibaya Catchment) is needed to make informed decision about water resources in the region.

Weitz (2016) mentions that previous extreme weather events such as floods which occurred in the mid-1980 were from Cyclone Imboa and Domonia, as well as from cut-off lows. These floods were reflected by lake level increases. Significant cyclones in South Africa that had a hydrologic impact were Domoina, which occurred in January 1984, Imboa in February 1984, and Eline in February 2000. Schapers (2018), mentioned that in January of 1984, Cyclone Domoina deposited three-quarters of the annual rainfall over the Coastal plain in under a week, followed to a lesser extent two weeks later by Cyclone Imboa. The highly transmissive KwaMbonambi Formation could not accommodate the volumes, and most of the Coastal plain became a shallow lake, allowing massive storage of water in on the surface of the Maputaland geological formations. Since the year 2000 and prior to 2019, it was documented that there had not been any significant rainfall from cyclonic storms (Janse van Rensburg, 2019a). During the course of the current project one cyclone activity occurred (Cyclone Eloise 2021) (Mawren *et al*., 2022) and a Subtropical Depression Issa, 2022 (Mühr *et al*., 2022) have contributed to rainfall amounts in northern KwaZulu-Natal, with storm event Issa generating floods. Other significant contributors to the MPC rainfall includes both cut-off lows (Reason, 2006; Favre *et al*., 2012) and meso scale convective system (MCS) (Blamey and Reason, 2009; Morake *et a*l., 2021).

2.5 Aquifer-aquifer interconnectivity

Aquifer-aquifer connectivity describes the degree to which groundwater can flow between two aquifers that are separated by aquitard also known as inter-aquifer leakage. (Pandey *et al*., 2020). This Aquifer connectivity is how groundwater can transfer water laterally or vertically between two or more adjacent aquifers. This interconnectivity between aquifers can be caused by man-made and natural activities that trigger the hydraulic interaction between aquifers. Human activities that can increase aquifer connectivity include poorly constructed wells that allow water to seep along the well casting (Van der Schyff *et al*., 2020). Water extraction from an aquifer can also alter water pressure, which can lead to aquifer leakage in some cases. Natural vertical cracks in the rock that separates two aquifers can allow water to flow between aquifers. The connectivity of aquifers depends on the type of rock and sediment that makes up the aquifers and aquitards, as well as the integrity and continuity of these layers (Priestley *et al*., 2017). Inadequately sealed boreholes, faults, and fractures can also create preferential flow path between aquifers, meaning water is likely to flow between these pathways.

2.5.1 Aquifers

The National Water Act No 36 of 1998 defines aquifers as geological formations with structures or textures that can store and transmit water. They can also be described as permeable geological layers that transmit water sufficiently to sustain pumping from a well (Salako *et al*., 2018). Aquifers often feed lakes and rivers. They receive water from rainfall, river connections, canals, and drains. The ability of the aquifer to yield water depends on the aquifer rock formation (Kelbe *et al*., 2016).

2.5.2 Types of Aquifers

Aquifers have been traditionally classified into two types either unconfined or confined systems depending on the presence or absence of water.

2.5.2.1 Unconfined Aquifer

Unconfined aquifers have a water table that varies in undulating form and slope depending on recharge and discharge areas and the hydraulic properties of the porous medium (Kelbe and Germishuyse, 2010). There are frequently areas within the aquifer with low permeable strata where soil moisture concentrations lead to perched water tables. The majority of alluvial deposits along flood plains of large river systems are unconfined aquifers that are inextricably linked to river recharge and discharge (Kelbe and Germishuyse, 2010). The largest primary aquifer in South Africa is located along Maputaland Coastal Plain (MPC) (Midgley *et al*., 1994; Kelbe and Germishuyse, 2010).

2.5.2.2 Confined Aquifers

A confined aquifer is an aquifer bounded above and below by confining units of distinctly lower permeability than that of the aquifer itself. The pressure in confined aquifers is greater than atmospheric pressure (Harrington *et al*., 2014). This is because the water is underpressure from the water and the water below it. They are also aquifers under pressur, where groundwater is confined between impermeable (confining) layers, (Kelbe and Germishuye, 2010).

2.2.1 Hydraulic Characterisation of Aquifers

Aquifer parameters such as transmissivity (T), storativity (S) and hydraulic conductivity (K) are basic information required for aquifer analysis and modelling of groundwater (Mondal *et al.*, 2008). Transmissivity (T) is the rate at which groundwater flows horizontally through an aquifer. Storativity (S) is the volume of water released from storage per unit decline in hydraulic head in the aquifer, per unit are of the aquifer. Hydraulic conductivity (K) is the constant of proportionally that defines fluid flows through a porous media, which is dependent on the permeability and physical properties of the media.

Experimentally, on-site measurements such as pumping tests can be used to determine the aquifer parameters as hydraulic conductivity (K).

2.4.5 Hydrostratigraphic Units

For the aquifers to be categorized into well-defined hydrogeological units, sufficient hydraulic properties and varying combinations of sands, clay and silts are required (Kelbe *et al*., 2013). The essential information requirements in determining aquifer connectivity are primarily associated with geology, including the lithology and structure, groundwater hydrology, aquifer permeability, groundwater level, pressure gradients, and potential influence of anthropogenic structures and discrete geology (Pandey *et al*., 2020).).

In general, the subsurface is divided into hydrostratigraphic units (HSUs) based on similar properties with regard to groundwater transmission and storage, based on the permeability and porosity that characterize the rock structures (Mukherjee, 2011; Merz, 2012). However, these geological structures are frequently described for non-aquatic purposes and may not be adequate for aquifer delineation. Various studies are used in conjunction with these geological logs to delineate physical boundaries for hydrologically similar units (Kelbe and Germishuyse, 2010). These units are defined by fractures or interstices interconnections, rock structure arrangements, shapes, sizes, and numbers, and their occurrence in soils or rocks is recognized by the magnitude, extent, and nature of their occurrence. (Mukherjee, 2011). To depict the hydrostratigraphy within a terrain, panel and/or cross-sectional diagrams are commonly used. MODFLOW has been used more often than other computer software for hydrostratigraphic 3D model simulations (Mukherjee, 2011). Similar hydraulic features are used to evaluate geological formations, delineate boundaries, and group zones with similar properties into single hydrostratigraphic units (HSUs); however, geological and hydrological variations within HSUs may persist. HSU boundaries are defined using well logs, cross-sections of geological formations, and geological maps. The geomorphological and hydrogeological information used in the interpolation and interpretation of bounding surfaces during mapping is made up of conceptual model inferences, river cross sections, and bathymetric surveys (Kelbe and Germishuyse, 2010).

Alternative methods in determining the connectivity between aquifers the hydraulic methods are conducted in the field. The test includes a single well test (which is useful for obtaining hydraulic properties near borehole) and geochemical methods, including stable isotopes. One of the limitations to the measurement of aquifer connectivity is the inability to directly observe the subsurface other than at discrete points or lines such as boreholes (Peeters *et a*l., 2014).

2.6 Environmental Isotopes to determine groundwater recharge dynamics and aquifer to aquifer interaction

2.6.1 Stable Isotopes

The invention of the mass spectrometer in the 1950‘s made it possible to accurately the relative abundance of isotopes in samples with high precision. Isotopes are atoms of the element that have different numbers of neutron (Weaver *et al*., 2009; Fetter, 2001). This means they have the same atomic number but different atomic weights. Stable isotopes are isotopes that do not decay. The use of stable isotopes, such as ^{2}H and ^{18}O in hydrology is based on the principle of water fractionation during phase changes. Water fractionation is the process by which the different isotopes of water are separated during phase changes. For example when water evaporates the lighter isotopes ($\delta H^{1}\ ^{16}O$) has a higher vapour pressure and more likely to vaporize than the heavier isotopes ($\delta H^{2}\ ^{18}O$) (Hunt *et al*., 2005). This means that the water that remains behind is enriched in heavier isotopes. The different degrees of fractionation caused by different processes, ^{2}H and ^{18}O can be used to investigate hydrologic systems in a variety of ways (Levy, 2009). For example, the stable isotope composition of groundwater can be used to trace the source of groundwater and to identify processes that have affected the groundwater, such as evaporation or mixing with surface water (Clark and Fritz, 1997). Stable isotopes are also used to study the interaction between groundwater and surface water. The isotopic composition of groundwater and surface water can be used to identify where the two water bodies are mixing.

Water from various sources, such as precipitation, rivers, and groundwater, has different isotopic signatures (Aggarwal *et al*., 2007). This means that the water molecules from each source have different amounts of the heavier isotopes of Deuterumand oxygen. Stable isotopes ^{18}O and ^{2}H are ideal tracers of water movement, because they are part of the water molecule and do not change during phase changes (Hunt *et al*., 2005). As a result, these isotopes have been used to locate and confirm groundwater discharge locations (Oxtobee and Novakowski, 2002), quantify groundwater discharge to surface water (Space *et al*., 1991), and differentiate the sources of groundwater recharge (Blasch and Bryson, 2007).

The δ Notation

Stable isotopic compositions are typically reported as delta (δ) values which are expressed in parts per thousand (denoted as ‰ or permil). The ratio defined by the δ notation is calculated by taking the ratio of the heavy to light isotope in the sample and subtracting it from the ratio of the heavy to light isotope in the standard, then multiplying by 1000:

Equation 1

$$\delta = (R_{sample} / R_{standard} - 1) \times 1000$$

Where "R" is the ratio of the heavy to light isotope. A positive delta value means the sample has a higher ratio of heavy isotopes than the standard (enriched in the heavy isotope). In contrast, a negative value means that the sample has a lower ratio of heavy to light isotopes than the standard (depleted in the heavy isotope). The isotopic compositions of δ^2H and $\delta^{18}O$ values are typically reported relative to the SMOW standard (Standard Mean Ocean Water) or the equivalent VSMOW (Vienna-SMOW) standard. In practice, each laboratory has its standard or set of standards calibrated relative to the international standard SMOW. When a sample is measured, its isotopic ratio is compared to that of the laboratory standard and the result is recalculated to the VSMOW scale.

The Global Meteoric Water Line

Craig (1961) observed that there is a linear relationship between the abundance of ^{18}O and ^{2}H in water relative to VSMOW, which is the standard for Vienna Standard Mean Ocean Water. Equation 2 below represents the relationship.

Equation 2

$$\delta^2H = 8\delta^{18}O + 10$$

The Global Meteoric Water Line (GMWL), described in *equation 1,* provides a reference for comparing local differences in water and thus aids in interpreting water origin. If water samples are evaporated, the $\delta\ ^2H$ and $\delta\ ^{18}O$ relationship no longer plots on the GMWL due to the non-equilibrium kinetic effects of evaporation causing the fractionation of H and O isotopes to occur in different proportions (Kendall and McDonnell, 1998). Waters often develop unique isotopic composition "fingerprints" because of fractionation processes. These fingerprints can indicate the water source or the processes that formed it (Kendall and McDonnell, 1998).

The need to understand the processes by which fractionation occurs is essential for the interpretation of isotope data. By understanding these processes, it will be easy to use isotope data to track the movement of water through the hydrological cycle and understand the water source. The fractionation of water isotopes begins with the evaporation of water from the ocean's surface with $\delta^{18}O$ and $\delta^{2}H$ values similar to VSMOW. The evaporated water is usually lighter or more depleted in isotopes than the water left behind because the lighter isotopes of Deuterumand oxygen are more likely to vaporize than the heavier isotopes meaning the water remaining behind is enriched in the heavier isotopes.

A number of factors (Mook, 2006; Clark and Fritz, 1997) determines the actual ^{18}O values of precipitation reaching the ground

Latitude: Colder temperatures reduce the likelihood of heavier water condensing and falling as precipitation. As a result, the higher the latitude, the more depleted the precipitation is in $\delta^{18}O$, which does not affect the isotopic ratios in this study. The heavy isotope composition of precipitation at high latitudes frequently resembles that of water near the equator, which typically has high ^{16}O levels because of fractionation brought on by evaporation (Gibson, Fekete, and Bowen, 2010)

Altitude: Precipitation becomes isotopically depleted at higher altitudes because of the cooler temperatures experienced there, especially in mountainous areas. This effect results from the constant pseudo-adiabatic cooling of air masses below the dew point in an orographic precipitation system, which increases rainfall at higher elevations. Precipitation that is more depleted in $\delta^{18}O$ typically occurs when colder temperatures are experienced at higher elevations.

Season: Stronger seasonal variations in precipitation isotopic composition are caused by the greater seasonal temperature extremes. The seasonal variations in the values are brought on by temperature, relative humidity, and evaporation variations. Colder temperatures in winter lead to precipitation generally depleted in $\delta^{18}O$ (the heavier isotopes). While seasonal fluctuations are minimal in coastal regions, the seasonal effect is more pronounced in inland regions.

Amount: Large rainfall events tend to be lower in $\delta^{18}O$ than small rains. The intensity and duration of rainfall events will result in different isotopic ratios, which will influence the isotopic signature. Because heavy isotopes preferentially rain out before light isotopes, studies

of the isotopic composition of meteoric water collected throughout a rainstorm event discovered that precipitation becomes more depleted with time (e.g. Gedzelman and Lawrence, 1990). The more depleted numbers correspond to the middle and end of the storm event as precipitation rains out of an air mass (Gat, 2010). The water that falls later in a storm event is depleted in those values because the water molecules loaded with the heaviest isotopes, ^{18}O and ^{2}H, rain out at the front of the air mass when air masses shift and precipitation falls (Liu, Bowen and Welker, 2010).

Due to all the above variables, local precipitation will have a slightly different relationship between ^{18}O and ^{2}H. In order to establish the Local Meteoric Water Line (LMWL) against which isotopic values from water in other portions of the hydrologic cycle can be compared, it is essential to sample local precipitation throughout time in any local field research (Kendall and McDonnell, 1998). In order to evaluate whether a recharge is immediate or delayed, as well as to pinpoint potential processes that changed the isotopic composition of precipitation prior to recharging the groundwater, it is feasible to use the groundwater's ^{2}H and ^{18}O values and their relationship to the MWL. Stable Isotopes are useful tracers in groundwater recharge studies.

The local meteoric water line (LMWL) usually serves as a reference line that is used to interpret the stable isotopes composition of water. The amount-weighted average precipitation value is regarded as the meteoric input signal (Bagheri *et al*., 2019). The slope of LMWL is determined by the temperature of the air mass that produced the precipitation. The stable water isotope method can be used to estimate recharge by tracing the origin, pathway, and behaviour of water (Paces and Wurster, 2014). Oxygen and Deuterumare ideal conservative tracers for aquifer recharge because they are the components of water molecules and remain unchanged except in water phase changes or isotope fractionation in the hydrological cycle (Li *et al*., 2018). Variations in the isotopic composition of water can be used to track the movement of water precipitation, groundwater and surface water, allowing the connection of groundwater in aquifers to its origin (Lemma *et al*., 2020).

Weitz and Demile (2015) adopted the environmental isotopic analysis in determining the intricate relationship between various water resources in the Lake Sibaya catchment.

This study will utilize stable isotopes to determine the relationship between rainfall and groundwater recharge. They are suitable for this study because the ratios of oxygen and

Deuterumin water have long been considered powerful paleoclimate indicators they have been utilized in several studies; Rozanski *et al.* (2017) used isotopes to analyse the relationship between long-term trends of the oxygen-18 isotope composition of precipitation and climate. He mentioned that there is a good relationship between precipitation and isotope composition. The stable isotopes of water provide a convenient alternative approach to analysing the impact of high-intensity rainfall on groundwater recharge (Cherry *et al*., 2019; Jasechko *et al*., 2014, 2017; Tasechko and Taylor, 2018). In studies by (Cherry *et al*., 2019; Jasechko *et al*., 2014, 2017; Tasechko and Taylor, 2018), the isotopic composition of groundwater compared to precipitation signal and deviations are considered indicative of a predominance of recharge in certain seasons by a specific precipitation type. Muller *et al*. (2020) states that the stable isotope technique works in hindsight. One can evaluate the groundwater isotopic composition as an integral; hence, the technique applies to modern water and old groundwater (Nicholson *et al*., 2020).

2.7 Conceptual modelling of Groundwater

The qualitative representation of the groundwater flow system (including hydrochemical, hydrological, and geophysical information) and associated hydrogeological units based on principles of hydrogeology is referred to as a conceptual model (Baalousha *et al*., 2008; Betancur, 2012; Kiptum *et al*., 2017). A cross-section, plan view, or block diagram is commonly used to represent the system of groundwater flow in a graphical representation known as a conceptual model (Merz, 2012; Weitz, 2016). The model or conceptual understanding of a system will determine the success of the quantification of the groundwater/surface water interactions. The conceptual model considers boundary conditions delineation, the receiving environments response, and the aquifers main characteristics to readily analyse the system through simplifications based on field data and associated field parameters. Three steps need to be followed for the successful construction of a conceptual model, these include stratigraphic units' delineation, water budget preparation, and flow system design (Weitz, 2016).

Weitz and Demlie (2014) used geological, hydrological, physical, hydrochemical, and environmental isotope data to successfully develop a hydrogeological conceptual model for the Lake Sibaya catchment. The goal was to use the conceptual hydrogeological model to understand the interaction between surface water and groundwater in the Lake Sibaya catchment. The conceptual model, in conjunction with the water balance, showed that the

groundwater and surface water are highly connected, and that abstraction of either source could have negative impact on the environment.

2.8 Previous studies conducted in MPC relevant to current study

Numerous hydrogeological and hydrological have been conducted in different parts of the Maputaland Coastal Plain (MPC). The Water Research Commission commissioned many hydrological studies of the aquifer, which were carried out by the University of Zululand carried out (Kelbe *et al*., 2001; Kelbe and Germishuyse, 2010). On the study conducted by Rawlins and Kelbe (1992) investigated the relationship rainfall and groundwater in the St Lucia area. The study found that a water table 2-3 meters below the surface would only respond to rainfall event of more than 10 mm. The study also found that only the first 50 mm of rainfall per day would enter and contribute directly to percolation into the shallow groundwater system in Richards Bay. Another study conducted by Kelbe and Germishuyse (2010) in the Richards Bay area along the coastal plain, found that the groundwater/piezometric surface was very responsive to rainfall fluctuations. This finding could apply to the Lake Sibaya system, given the similar conditions.

The studies mentioned above suggest that rainfall is an important factor in groundwater recharge in the MPC. However, the amount of rainfall that is actually recharged into the groundwater system is limited. Only the first few millimeters of rainfall per day will actually enter the groundwater system, and the water table will only respond to rainfall events of more than 10 mm

Estimates of groundwater recharge have been reported by many researchers in MPC. According to Meyer *et al*. (2001), Worthington (1978) utilized a Water Balance approach and calculated the recharge in the vicinity of Richards Bay to be approximately 24% of the mean annual precipitation (MAP). Meyer and Kruger (1987) reported a recharge of 21% of MAP using Bredenkamp (1985) rainfall recharge relationship technique which is solely based on the MAP. Meyer *et al*. (2001) established the rainfall-recharge relationship, indicating that recharge varied with distance from the coast. The recharge was presented as a percentage of maps varying from 18% at the coast to 5% at a distance of 50 km inland. Weitz and Demlie (2014), utilized chloride mass balance method (CMB) to estimate the recharge for the Lake Sibaya catchment and the result compared with estimates published maps, they estimated the recharge to be126 mm (12% MAP) against 95 mm/a (10% MAP) estimated using published naps.

Many studies have shown that groundwater recharge in the MPC is influenced by rainfall, with heavy rainfall events being particularly important. However, more research is needed to better understand the factors that control groundwater recharge in the area.

Studies conducted in MPC has shown that there is a strong connection between surface water and groundwater. Worthington (1978) used the distribution of aquifer transmissivity in conjunction with potentiometric levels map to estimate the subsurface seepage into Lake Mzingazi. Worthington (1978) estimated that 30% of Lake Mzingazi replenishment comes from groundwater seepage, which indicated the lake is recharged by groundwater. Similar results were found by Weitz and Demlie (2014) based on the conceptual model of Lake Sibaya. They found that Groundwater and surface water are highly connected and that lake receives a subsurface recharge through the sandy substrate. Weitz and Demlie (2014) findings were supported by the isotopic signature of groundwater sample collected along the dune cordon, which was similar to the isotopic signature of the lake. In addition, Meyer *et al*. (2001) found the same results, where it was reported that the water of the Lake was found to have a direct hydraulic connection with seepage water occurring along the coastal dune.

The studies mentioned in the previous paragraph (above paragraph) have shown that groundwater is an essential source of recharge for the Lakes in Maputaland Coastal Plain (MPC). However, not enough research has looked at the importance of heavy rainfalls and their connection to groundwater recharge.

3. DESCRIPTION OF THE STUDY SITE

3.1. Introduction

The physical characteristics of MPC plays an import ant role on groundwater recharge and Surface water- groundwater interaction. The climate, geomorphology and aquifers of the MPC all influence how water moves through the system. By understanding, these physical characteristics it will be easy to better understand how groundwater recharge and its interaction with surface water works. This chapter focuses on the physical characteristics of the MPC, including location, climate, lake morphology, physiography and drainage, and vegetation and land cover. This study mainly focuses on the Lake Sibaya and ssurrounding area of Mbazwane and Mseleni.

3.2 Location

The MPC, located in the northern-eastern KwaZulu-Natal province, is known for its biodiversity, conservation areas, and its status as a world Heritage site. The area is home to a variety of fresh and saline water wetlands, including swamp forest, saline reed swamp, salt marsh, submerged macrophyte beds, and magrooves (Kelbe *et al*., 2016). The Northern MPC (NMCP) is a component of the nationally significant Zululand Coastal Plain Groundwater Strategic Water Source Area (Le Maitre *et al*., 2018). The study area is located within Quaternary Catchment W70A, which includes the Lake Kosi, Lake Sibaya, and Mgobezeleni systems. It is exemplified by the lack of rivers importing water from upper catchments. W70A is located in the Umhlabuyalingana Local Municipality (ULM) and the uMkhanyakude District Municipality (UKDM).

The study area has a unique and fragile coastal landscape in the Indian Ocean Coastal Belt Biome South Africa. It contains a large aquifer, classified as a Strategic Water Source Area (SWSA) of national and provincial importance and provides local people access to fresh water throughout the year. Aquifer dependent ecosystems typify the region including a diversity of estuarine, wetland, freshwater and terrestrial ecosystems, connected to the marine ecosystem through subsurface flows (Botha, 2015).

The study areas include Lake Sibaya, which is a coastal freshwater lake situated on the seaward margin of the MPC along the northern KwaZulu-Natal coastline. The lake is located between 27°15° and 27°25°S and 32°33° to 32°43°E, about 180 km north of Richards Bay and

60 km from the Mozambique border (Weitz, 2016). The Lake Sibaya catchment falls within the uMhlabuyalingana Local Municipality in the UMkhanyakude District, situated in the northeastern part of the KwaZulu-Natal Province. The other areas are in the neibouring rural towns of Mbazwana and Mseleni town, which are located around the periphery of the lake.

According to Weitz and Demile, (2013), the imagery satellite (Google Earth, 2014) the lake surface has been significantly reduced in recent years, and currently has an average surface area of 56 km at a time of this study.

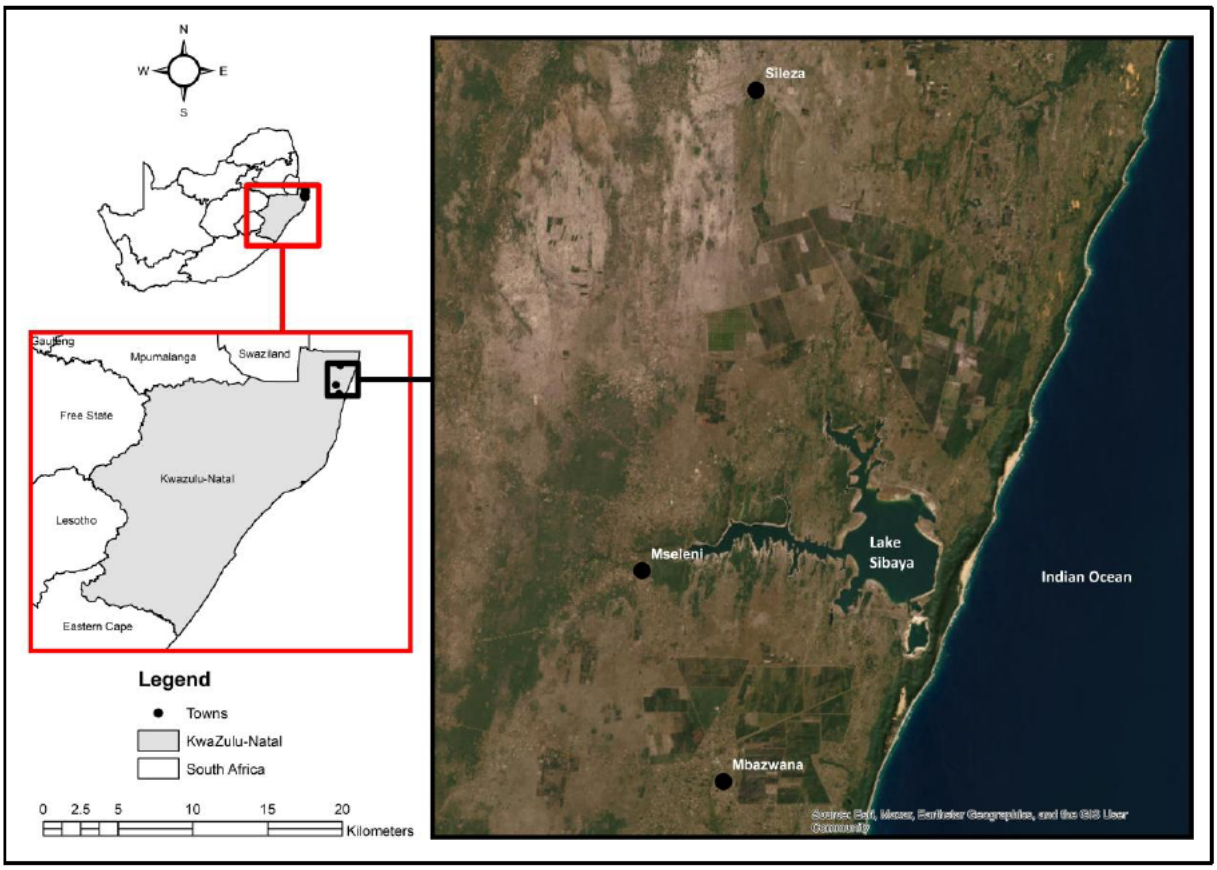

Figure 3-1. Location map showing Lake Sibaya and neighbouring sampling points

3.3 Climate

The study area (Catchment W70A) is a climate sensitive region receiving rainfall from a variety of different systems, including occasional heavy tropical rainfall input. The region is characterised by humid and wet subtropical climates with warm summer temperatures (Money, 1998). Mucina and Ruthford (2006) reported that 60% of the rainfall in the Maputaland Coastal Plain (MPC) occurs during summer months (November to March) and 40% during winter

months (April to October). Over lake Sibaya, the averages rainfall is 900 mm/a, but it varies from 1200 mm/a in the southeast and 700 mm in the west (Pitman and Hutchinson cited by Wright *et al*., 2000). The latest rainfall data shows the precipitation in the region increases from 700 mm/year along the western edge of the catchment to 1000 mm/year along the coast. Annual pan evaporation data ranged between 1400 mm/year and 1500 mm/year for the S class pans and between 1800 mm/year and 2000 mm/year for the A class pans. Temperatures also showed seasonal variation, but less than rainfall. Temperatures peaked in the summer months with the highest mean monthly temperature experienced in February (26.1°C), while the lowest temperatures were experienced in July (18.4°C).

The most important rain-producing weather systems for the region are cloud bands (or tropical-temperate troughs (TTTs)) (Hart *et al.*, 2013), tropical lows (and occasionally tropical cyclones), cut-off lows (Singleton and Reason, 2007), ridging anticyclones, and mesoscale convective system scale convective systems (Blamey and Reason, 2009, 2013). The region lies south of the typical landfall location of tropical cyclones and storms in central Mozambique, but north of the coastal region that typically receives significant rainfall from onshore flow associated with ridging anticyclones (Hart *et al.*, 2013). This makes it an interesting transition zone. Although the region does typically receive tropical cyclones, when they do occur, they can cause widespread heavy rainfall (Malherbe *et al*., 2012). The heavy rainfall are likely to play an important role in recharging groundwater resources.

3.4 Geological Setting

The study area is part of the Maputaland Coastal Plain Formation which is made up of Mesozoic and Cenozoic soils that extend north and south along the Mozambican Coastal Plain (Botha *et al*., 2013). The geology of the area is made of Quaternary and Tertiary sediments of the Maputaland Group, which are flat to undulating Cretaceous sandstones. The Cretaceous sandstones are primarily underlain by marine siltstones, which are part of the St. Lucia Formation.

According to Botha *et al*. (2013), geological processes that produced a sedimentary succession of unconsolidated formations during times of marine regressions and transgressions were responsible for the creation of the MPC. Subsequent Aeolian depositions formed paleo-dune ridges parallel to the coast, as did more recent high frontal dunes along the shore. The Jurassic

basalts and rhyolitic rocks that make up the coastal plain are distinguished by a series of sediments that cover them and generally slope at an angle of around 3° to the east (Boha *et al*., 2013; Botha, 2015). Much of the region was submerged during the Cretaceous Period, resulting in the formation of the Zululand Group, an aquifer with residual brackish water that is composed of clay stones and siltstones with very low hydraulic conductivity, porosity, and storability.

The Uloa Formation was deposited in the late Miocene and continued into the Pleistocene (Maud and Orr, 1975). The Uloa Formation is made up of a lower coquina layer and an upper calcarenite layer. The base of the Uloa Formation consists of a 2.5-m-thick basal conglomerate bed that rests unconformably on the eroded surface of the St. Lucia Formation siltstones (Dingle *et al*., 1983). The basal conglomerate, which suggests deposition in deep marine waters, is overlain by the Pecten Bed (glauconite-rich and fossiliferous calcrites), also known as the Coquina (Maud and Orr, 1975). The Pecten 18 Bed has a thickness of about 5 m (Dingle *et al*., 1983). The coquina is overlain by up to 20 m of aeolian cross-bedded calcarenites (Wright *et al*., 2000), which was initially thought to be the Upper Uloa Formation (Frankel, 1966; Maud and Orr, 1975; Cooper and McCarthy, 1988).

Because there is a distinct lithological break between the calcarenites and the underlying coquina (Maud and Orr, 1975). Botha (1997) proposed that, this unit be designated as a separate formation, namely the Umkwelane Formation.

The UMkwelane Formation is made up of course, light grey sand interlaminated with calcareous sandstone, or Calcarenite with shell fragments. The Uloa Formation is significant in hydrogeology because it is one of the main aquifers in the stratigraphic sequence (Worthington, 1978). The Umkwelane Formation is a beach or marine succession of coarse-grained sedimentary rocks overlain by aeolian cross-bedded hard, light gray calcarenites that overlies the Uloa Formation (Maud and Orr, 1975). The Umkwelane Formation is karstified on the upper surface and has a thickness of about 4 m (Dingle *et al*., 1983).

The transition from a beach or marine depositional environment to an aeolian depositional environment confirms the separation of the Uloa and Umkwelane Formations (Maud and Orr, 1975).

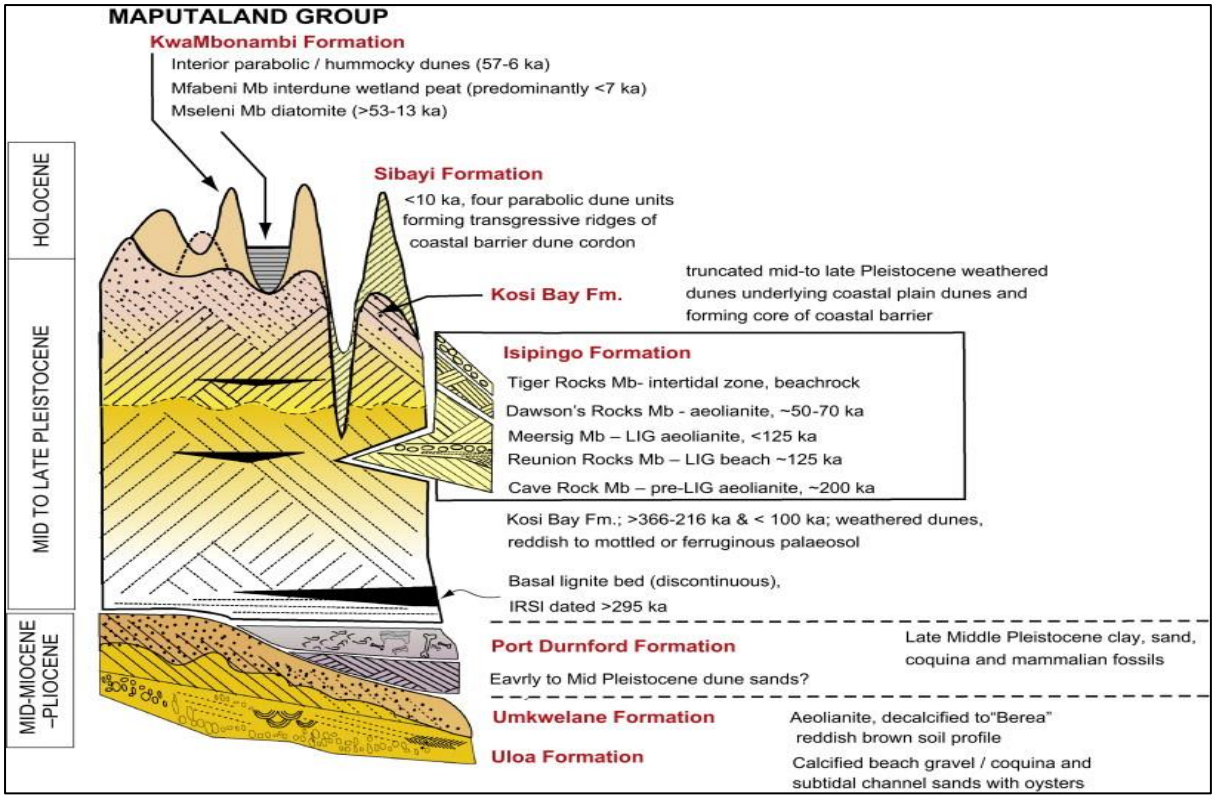

Figure 3-2 Schematic representation of the Maputaland Ground lithostratigraphic units (after Porat and Botha, 2008)

Hobday and Orme (1974) reported that remnants of the Uloa and Umkwelane Formations are unconformably overlain by Port Dunford Formation sediments. The Port Dunford Formation basal component in the Richards Bay area is made up of coarse beach rocks (Maud and Orr, 1975). The Port Durnford Formation is comprised of marine clay, silt, and sand deposits that have lower hydraulic conductivity and storage than the Uloa Formation. It is made up of confined leaky aquifers that are hydraulically connected to the Indian Ocean (Kelbe and Germishuyse, 2010). Hobday and Orme (1974) indicated that the upper portion of the Port Dunford Formation constitutes a 10 m thick marine and terrestrial fossil-ferrous grey and black mud with sandy lamina often referred to as the "Lower Argillaceous Member". The "Lower Argillaceous Member" is overlain by the "Lignite Bed," a 0.2 m to 2.5 m thick lignite layer (Hobday and Orme ,1974). A thin layer of marine sands defines the "Upper Arenaceous Member" of the Port Dunford Formation. The "Upper Arenaceous Member" is now defined as Kosi Bay Formation (Roberts *et al*., 2006).

The Kosi Bay Formation, which is composed primarily of non-calcareous, uncemented sediments that rest unconformably on the Uloa, Umkwelane, and Port Durnford Formations, is a composite, multiphase dune-sand deposit. These deposits form the foundation of both the

coastal dune cordon and the lower inland dune cordon exposed around coastal lakes (Roberts *et al*., 2006).

The KwaMbonambi Formation is group of sediments that were deposited during late Pleistocene to Holocene transition (Botha and Porat, 2007). These sediments include decalcified dune sediments, redistributed sand, coastal wetland deposits, and freshwater diatomite accumulations (Botha, 1997). The eastern margin of the coastal plain is dominated by relic cordons of late Pleistocene dunes, particularly in the Lake Sibaya region, creating a distinctive low undulating topography (Wright, 1995; Miller, 1998; Wright *et al*., 2000). Freshwater diatomite deposits and calcareous clays banked up against late Pleistocene dunes on the western shores of Lake Sibaya near Mseleni and south of Mbazwana reach thicknesses of up to 4m and formed between 45 000 and 25 000 years ago (Maud 1993; Miller 1996; Miller 2001; Porat and Botha, 2008). The surface of the 143-meter-high Tshongwe Sihangwane sand megaridge (Figure 3.2), which is located inland of the coastal lakes of Lake Sibaya and Kosi Bay, is made up of low KwaMbonambi Formation parabolic dunes (Botha and Singh, 2012).

Thus, according Maud and Botha (2000), the Isipingo Formation is made up of calcified dunes and beach deposits that formed in response to sea level fluctuations and are found along the eastern coast. The Isipingo Formation is the primary component of the coastal barrier dune cordon (Maud and Botha, 2000).

The Holocene Sibaya Formation is a high coastal barrier dune that stretches from the St Lucia estuary to the Mozambique border. It is a composite aeolian deposit made up of a core of Kosi Bay and Isipingo Formation dune sands that has been overlain by at least four phases of parabolic dune accretion over the last 10,000 years (Porat and Botha, 2008). In some areas, the Sibaya Formation can reach a thickness of 150 m. (Maud and Botha, 2000; Porat and Botha, 2008).

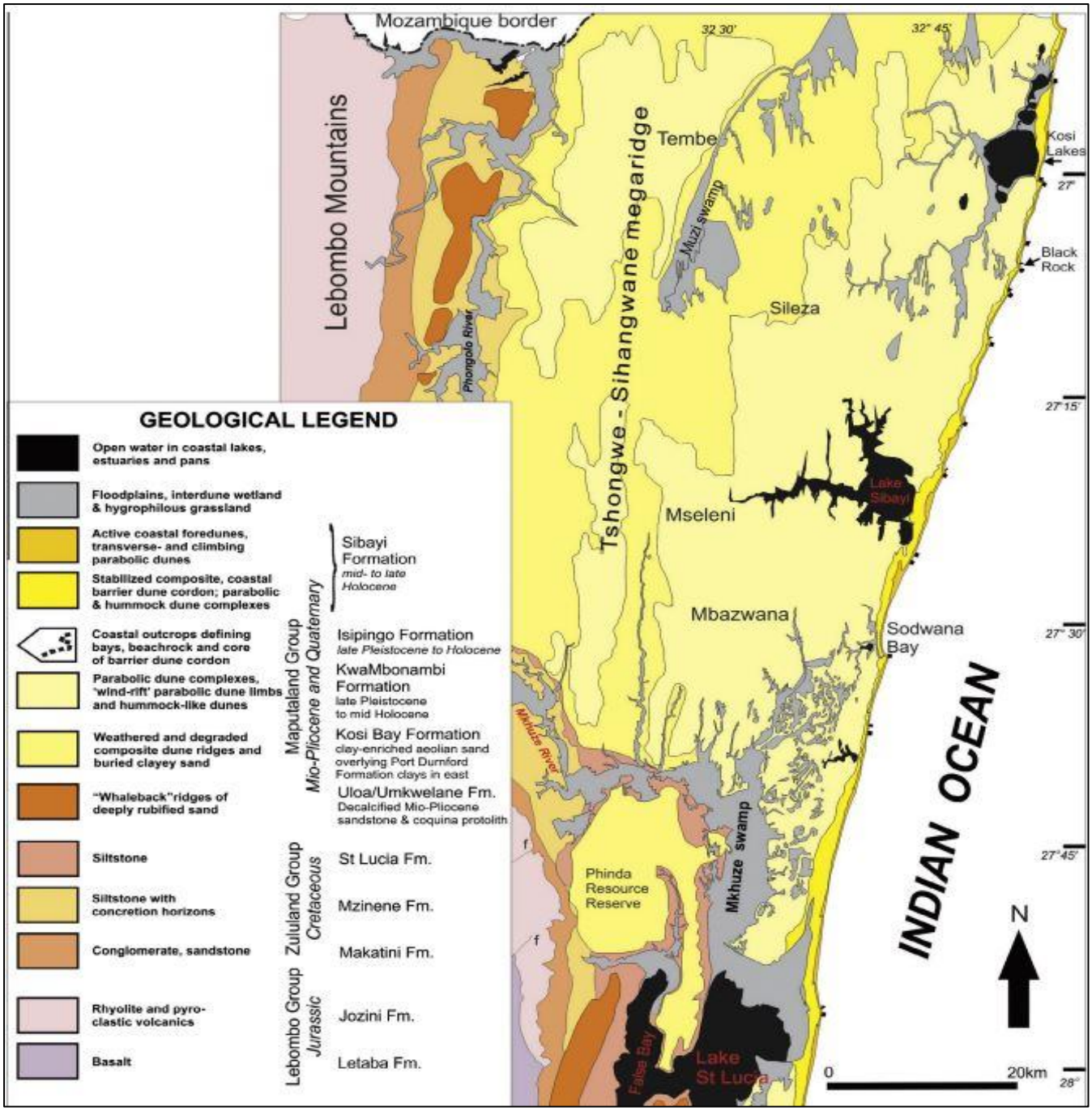

Figure 3-3 Geology of the study area (after Porat and Botha, 2008)

3.5 Hydrogeology

According to Kelbe and Germishuye, (201), the primary aquifer of Maputaland comprises shallow marine, alluvial and Aeolian sediments overlying the Cretaceous sediments. The Miocene to Holocene strata of the Maputaland Group are underlain by a Cretaceous-age succession known as the Zululand Group, which is composed primarily of fine siltstones,

conglomerates, and sandstones. The Zululand Group can be thought of as the impermeable basement to the underlying sediments due to its extremely low permeability, groundwater quality, and abundance. (Meyer and Godfrey, 2003).

The northern eastern of KwaZulu-Natal where Lake Sibaya located, is distinguished by sedimentary successions that create a multi-stockwork of aquifer layers and a regional aquiclude as the hydrogeological basement. These formations display different mixtures of marine, alluvial, and aeolian-derived sand, silt, and clay. They can be divided into separate hydrogeological units because they have sufficiently different hydraulic characteristics (Kelbe *et al*., 2013). Primary aquifers in the area are made up of these sedimentary layers from the Mio-Pliocene and Quaternary eras (Meyer and Godfrey, 1995). The region has two most productive aquifer system which are the shallow KwaMbonambi and Deep Uloa Formation (Meyer and Godfrey, 1995; Meyer *et al*., 2009) .

The Late Pleistocene KwaMbonambi Formation's unconfined superficial dune sands, which were deposited in reaction to polyphase dune mobilisation events, make up the first aquifer unit. This unit extends to varying depths and is commonly utilized by the local community through hand-dug wells (Botha and Porat, 2007; Porat and Botha, 2008); (Meyer and Godfrey, 1995). The upper aquifer intergranular units have little variance in their grain size and porosity, and their permeabilities range from 0.87 to 15.6 m/d (Meyer and Godfrey, 1995) .

The Upper Cretaceous St. Lucia Formation siltstone lies beneath the lowermost and most productive aquifer layer. Although there is little hydrogeological knowledge about this formation, it is thought to be the impermeable hydrogeological basement to the overlying aquifers because of its poor yields and low permeability. Table 3.1 obtained from Weitz, (2016) provides a summary of the major reservoirs that support the Lake Sibaya system .

Table 3-1Hydraulic characteristics of the different aquifer units present (compiled from different sources) (Weitz, 2016)

Aquifer name	Thickness (m)	K (m/d)	T (m^2/day)	Borehole yields (l/s)
Sibayi and KwaMbonambi Formations	20-30*	0.87-15.6 (mean: ~5)	1490	0.5-5
Kosi Bay/Port Durnfort Formation	15-20*	4-5 (mean: 4.3)	-	2-10
Uloa/Umkwelane Formation	5-20	0.5-25 (mean: 4.5)	116	5-25
St Lucia Formation	900	-	-	<1

3.6 Lake Sibaya Morphology

Lake Sibaya can be divided into five morphological regions, the Main Basin, Northern Arm, Western Arm, South-Western Bay and Southern Basin (Figure 3.3). The Main basin is the largest, accounting for nearly 60% of the lake's surface area and containing the deepest water (Hill, 1979). The Main Basin is roughly oval, with straight or gently curving shorelines punctuated by sand bodies or dune ridges (Hill, 1979; Miller, 2001). The South-Western Bay and Southern Basin, two smaller regions in the south, account for about 9% of the lake area (Weitz, 2016). The Northern and Western Arms are extremely dendritic, accounting for 12 to 20% of the lake surface area (Weitz, 2016). The bathymetric profile running across the bottom of the Main Basin appears to be continuous with the Northern and Western Arms, as well as the South-Western Bay. The Southern Basin, on the other hand, does not continue and is nearly isolated from the Main Basin (Hill, 1979).

The northern arm is fed by the Velindlovu, and the KuMzingwane streams, the eastern arm fed by the Mseleni River (Figure 3.4). The western arms northern and southern portions are fed by the Umsilalane stream and the Iswati and Umtibalu streams, respectively. The close relationship between the groundwater and surface water in the catchment is due to a water table that is shallow, a topography that is flat, and the catchments sandy substrate (Smithers et al., 2017; Carnie, 2020). Groundwater and surface water in the catchment close relationship is due to a water table that is shallow, a topography that is flat, and the catchments sandy substrate (Smithers *et al.*, 2017; Carnie, 2020). However, because there is no upstream river feeding into this catchment, the rivers mentioned above rely on rainfall within the Lake Sibaya catchment,

similar to the lake and groundwater system (Weitz, 2016; Smithers *et al*., 2017). Due to a limited amount of surface runoff due to the sandy substrate, groundwater inflow largely maintains lake water levels (allows for rapid infiltration of water). According to Smithers *et al.*, (2017), 569 km^2 of the area contributes groundwater to the lake, which is greater than the size of the catchment that contributes surface water, emphasizing the importance of focusing on the entire extent of the groundwater catchment due to a higher groundwater head, the lake is fed by groundwater on its western shores. On the eastern side of the lake, the lake feeds into the groundwater due to a higher lake stage.

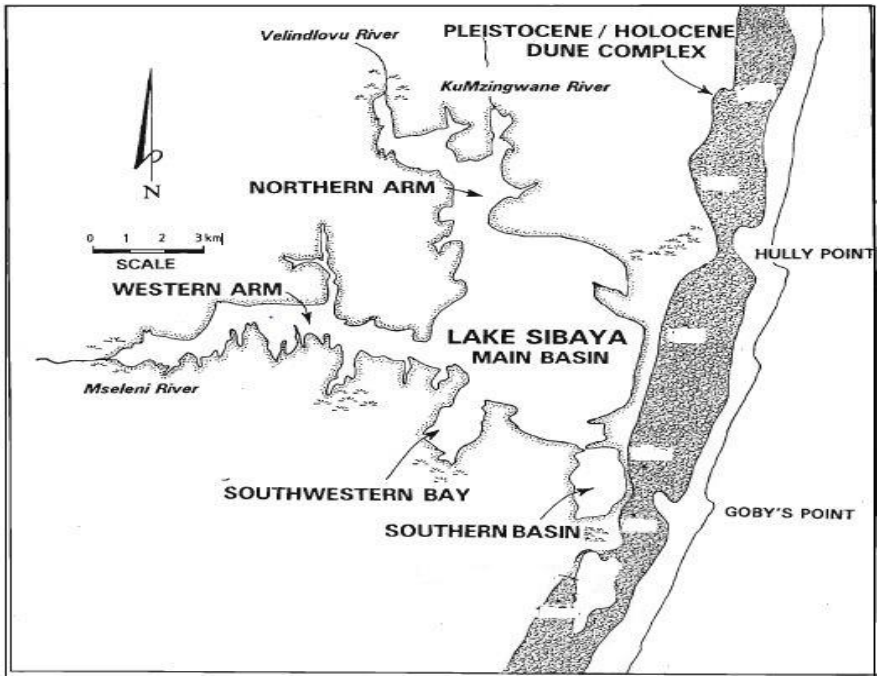

Figure 3-4 Morphology of lake Sibaya (after Miller, 1998).

3.7 Physiography and Drainage

The MPC topography consists of ancient to young sandy dunes with relatively elevated topography and low-lying plains to the east, and a series of rugged terraces deeply incised by river valleys in the central and western parts (Weitz, 2016). The recent, infertile, wind-distributed (Aeolian) sands cover most of the region. As a result, a series of north-south trending dune ridges parallel to the current coastline formed (Goodman, 1990; Weitz, 2016) (Figure 3.5).

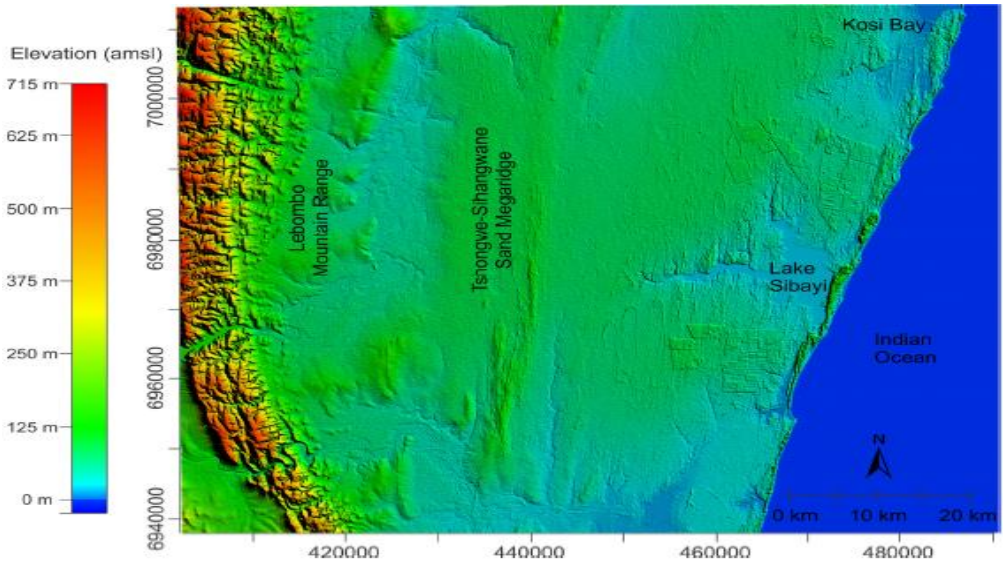

Figure 3-5 Topographic Surface of the area surrounding Lake Sibaya with significant regional features (adopted from Weitz, 2016)

The sandy substrate in a Lake Sibaya catchment, combined with relatively flat topography and shallow water table, results in a close relationship between lake surface waters and groundwater. This relationship is evident because the lake is a surface expression of groundwater (Meyer *et al*., 2001). Unconsolidated to semi-consolidated fine sands that cover the majority of the MPC (Weitz, 2016) primarily support the lake. The lake is separated from the sea by a series of high north south trending forested sand dunes, and thus has no connection to the sea. Near Ntambama, opposite the lake, the dune ridge reaches a maximum height of 172 m. The dunes separated the Lake Sibaya system from the sea during its evolution, allowing it to transition from a saline lagoon to a freshwater system (Roberts *et al*., 2006).

3.8 Vegetation and Land cover

Lake Sibaya catchment area falls within Maputaland Coastal Lake Zone. This area is distinguished by a series of barrier lakes, lagoons, and swamps located behind high-vegetated dunes. The catchment's vegetation is dominated by grassland (natural and degraded), with forests along the coastal dune cordon, dense bush along the western extremes and exotic plantations to the north and south of the lake. The lake and a large portion of the eastern coast are protected as part of the Isimangaliso Wetland Park.

The area surrounding the Lake Sibaya contains a large number of endemic species that are important for biodiversity conservation in the region's coastal environment. Smithers *et al.* (2017) found that 30% of forestry plantation was under Pinus elliottii, 50% was under Eucalyptus camaldulensis and Eucalyptus grandis, and the remaining 20% was under clear-field compartments. The most prominent plantations in the area are the Manzengwenya and Mbazwana plantations, which are located on the northern and southern sides of Lake Sibaya, respectively (Smithers *et al*., 2017). Furthermore, afforestation in this catchment that began in the 1990s has been attributed to a 1.4 m drop in lake levels, but the main cause of lake level decline was the 2001 to 2011 period with below-average rainfall (Smithers *et al*., 2017). Plantations have higher evapotranspiration rates than natural vegetation (Albaugh *et al*., 2013), so any expansion of the plantation would increase the loss of water from the catchment (Smithers *et al*., 2017; Ramjeawon *et al*., 2020). According to Ramjeawon *et al*. (2020), the development rate increased in the previous decade, and the extent of wetlands decreased by 47.9% between 2001 and 2019. Habitats in the Vasi Pan (slightly north of Lake Sibaya) have been lost due to groundwater level declines, affecting hippos, fish, and crocodiles that lived there (Janse van Rensburg, 2019a).

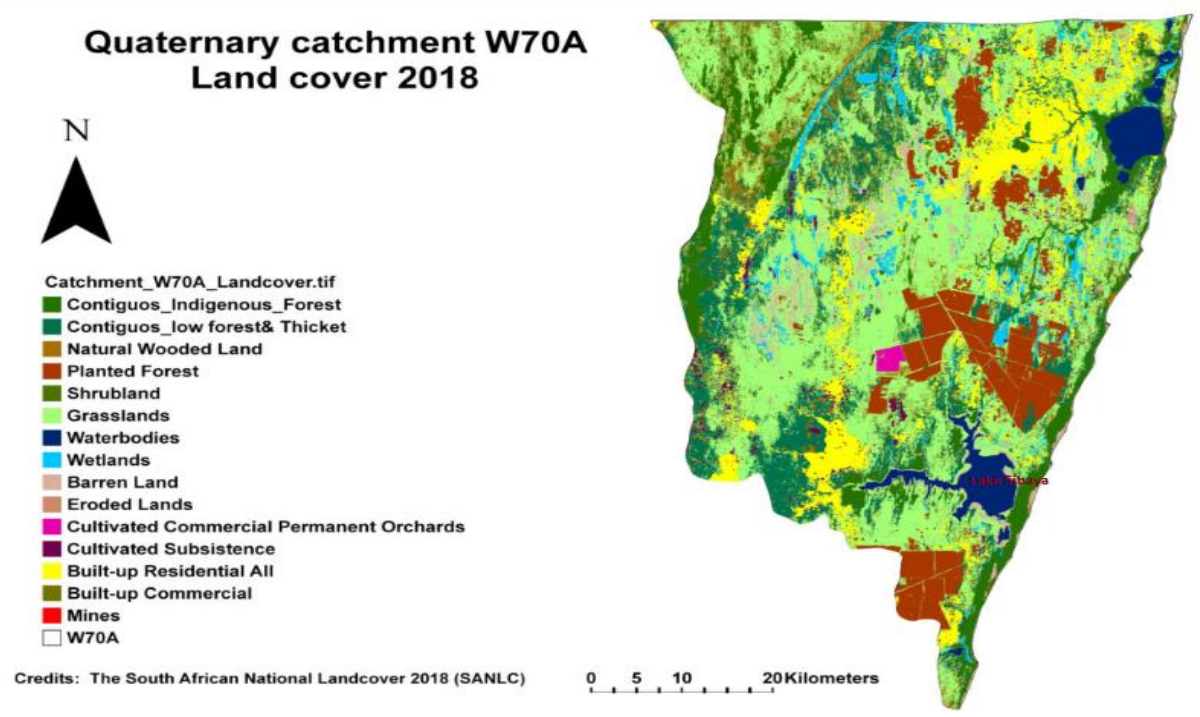

Figure 3-6 Different vegetation types and land cover surrounding the study area (SANLC, 2018).

3.9 Wetland

Wetlands form when water remains at or near the land surface for an extended period, promoting hydric soils and supporting vegetation communities adapted to wet conditions (Kelbe *et al*., 2016). These conditions can occur when the hydrogeomorphic setting and climate result in a high-water table connected to the regional groundwater regime or when perched water tables intersect the surface topography (Kelbe *et al.,* 2016). The MPC is a low-relief, undulating sandy dune landscape in the north-eastern region of South Africa, KwaZulu-Natal Province (Grundling *et al*., 1998). It contains the most wetland area per province area in South Africa and 60% of South Africa known peatlands (Grundling *et al*., 1998; Grundling *et al*. 2013). The study area contains a diverse range of wetland types, ranging from permanent wetlands with peat or high organic soil substrates to seasonal wetlands with mineral soils.

The MPC (Northern eastern of KwaZulu-Natal) is home to a diverse range of wetlands that provide valuable ecosystem services to an expanding population and tourist demand. The apparent distribution of wetlands varies in response to water surpluses or drought periods. It has been reduced over time by developed resources (e.g., agriculture, forestry) and infrastructure (e.g., urbanization). The MPC has aeolian sand soil, which is leached and low in nutrients, which results in low agricultural activities in the region (Grundling *et al*. 2013). This results in local communities heavily relying on wetlands for their daily livelihoods, especially peat-dominated wetlands such as swamp forests. However, land use changes such as cultivation and forest plantation affect the permanent wetlands (Swamp Forests) and temporary sedge/moist grassland wetlands in the region (Grundling *et al*., 2013).

Changes in groundwater dynamics at the regional scale will affect both wetland and terrestrial systems. Large areas of unique peatlands have also dried out, exacerbated by extensive fires. The peatlands in MPC, estimated to be many years old, play an essential role in retaining and gradually releasing moisture from heavy rainfall (Carnie, 2020). Many of the wetlands in the study area have been damaged due to extensive substantial farming.

3.9.1 Permanent Wetland

Permanent wetlands are wetlands that are constantly saturated with water throughout the year (Botha and Porat, 2007). During a drought, they shrink in size. In the MPC, permanent

wetlands include peatlands, swamp forests, and reed or sedge wetlands. Organic-rich soil and peat occur in permanent wetlands (Botha and Porat, 2007). These wetlands are often high in carbon and peaty in character and permanently saturated, they are also used for subsistence agriculture.

3.9.2 Seasonal Wetland

Season wetlands occur on the deep sandy soil areas where the water table fluctuations are greater, conditions which are not ideal for the development of peat. Their boundaries may appear to grow or shrink in wet or dry periods potentially causing them to be underestimated in periods of water shortage. These wetlands serve as vital recharge areas for the groundwater resources in the region (Grundling *et al*., 2013). They are characterized by slightly undulating Lala Palm, with a water table that vary from 1-3 m (Grundling *et al*., 2013). Seasonal wetlands appear to grow or shrink in wet or dry periods (Begg, 1989), potentially underestimating their area in times of water scarcity (Grundling *et al*., 2013a). Some areas, including wetlands, may be seasonal inundated with pools of open water during extremely wet years. This is referred to as "seasonally open water" (Grundling *et al*., 2013).

4. RESEARCH METHODOLOGY

This chapter describes the methods used in this study to achieve the aim of this study and, in turn, answers the research questions posed. The method included a desktop study, research approach, field sampling procedures, techniques in which raw data are acquired, and the laboratory analysis methods. This chapter aims to demonstrate the research setup, which aided in conceptualizing the groundwater recharge mechanism and aquifer interconnectivity in the study area. The methodology explained in this chapter employed to analyse and interpret the raw data.

4.1 Desktop review

A desktop review comprised a thorough examination of all existing and available hydrochemical, hydrogeological, and hydro-meteorological data. The review involved gathering relevant meteorological and groundwater level data from the South African Environmental Observation Network (SAEON monitored Met Stations) and borehole logs

from TERRASTES (2019). The review has been presented in the preceding literature review section. The references of all the literature reviewed is listed in the reference list.

4.2 Research Approach

Four methods have been employed in the current study. These are stable isotopes of water, use of borehole water level monitoring data from three pairs of nested boreholes, re-analysis of well logs and field chemistry data.

The stable water isotopes ($\delta^{18}O$ and $\delta^{2}H$) method was used as a primary tool to achieve the aim and answer the research questions posed. This approach was used because $\delta^{18}O$ and $\delta^{2}H$ can provide helpful information for understanding groundwater recharge processes and aquifer interconnectivity. This is because meteoric processes leave its fingerprints on water isotopic composition giving the opportunity to study groundwater origin, seasonality of recharge, and a threshold of rain amount that can contribute to recharge (Clark and Fritze, 1997). They can also be used in age determination. The stable isotopes are very effective in identifying processes that change the isotopic composition of rainfall prior to infiltration, such as evaporation or mixing from different rainfall events (Clark and Fritz, 1997). Thus, the isotopic composition of groundwater and rainfall were used to establish the groundwater recharge mechanism and aquifer connectivity. Additionally, the isotopic composition of surface water from streams and lakes is compared to groundwater to identify surface-water interaction.
Initially, groundwater pumping and recovery tests were conducted on six boreholes to determine aquifers' transmissivity (T) and hydraulic conductivity (K) characteristics. However, due to the minimal drawdown (under one minute) created during the pumping, the data has not yet been used to compute K and T. Recovery was also extremely fast (in the order of less than 1 min). The fast recovery did not allow its reasonable measurement. Therefore, the pumping and recovery test data generated under the current work were not used to analyse aquifer interconnectivity and its characteristics. The other method employed was a geological log analysis since it is the primary record of the geologic formations penetrated by the borehole. The sequence of the geologic logs has been visually inspected to assess the number of potential aquifers, confining layers, and the potential interconnection between the aquifer. Groundwater levels data were also used to interpret the interconnectivity between the aquifers, observing

how they respond to the recharge. The water level data was combined with the daily rainfall data to indicate groundwater dynamics.

4.3 Field sampling

A total of 245 water samples from 35 sampling points were collected from groundwater and surface water monthly for 5 months. Rainfall samples were collected daily. Five sampling trips occurred during 2021 (September, October) and 2022 (April, May, and August), with 94 samples collected from 20 boreholes, 78 surface water samples, and 92 rainfall samples across the study area. Samples were collected monthly from each sampling point, the rainfall was collected daily. The sampling of groundwater, surface water, and rainfall procedure is briefly discussed in the following sections.

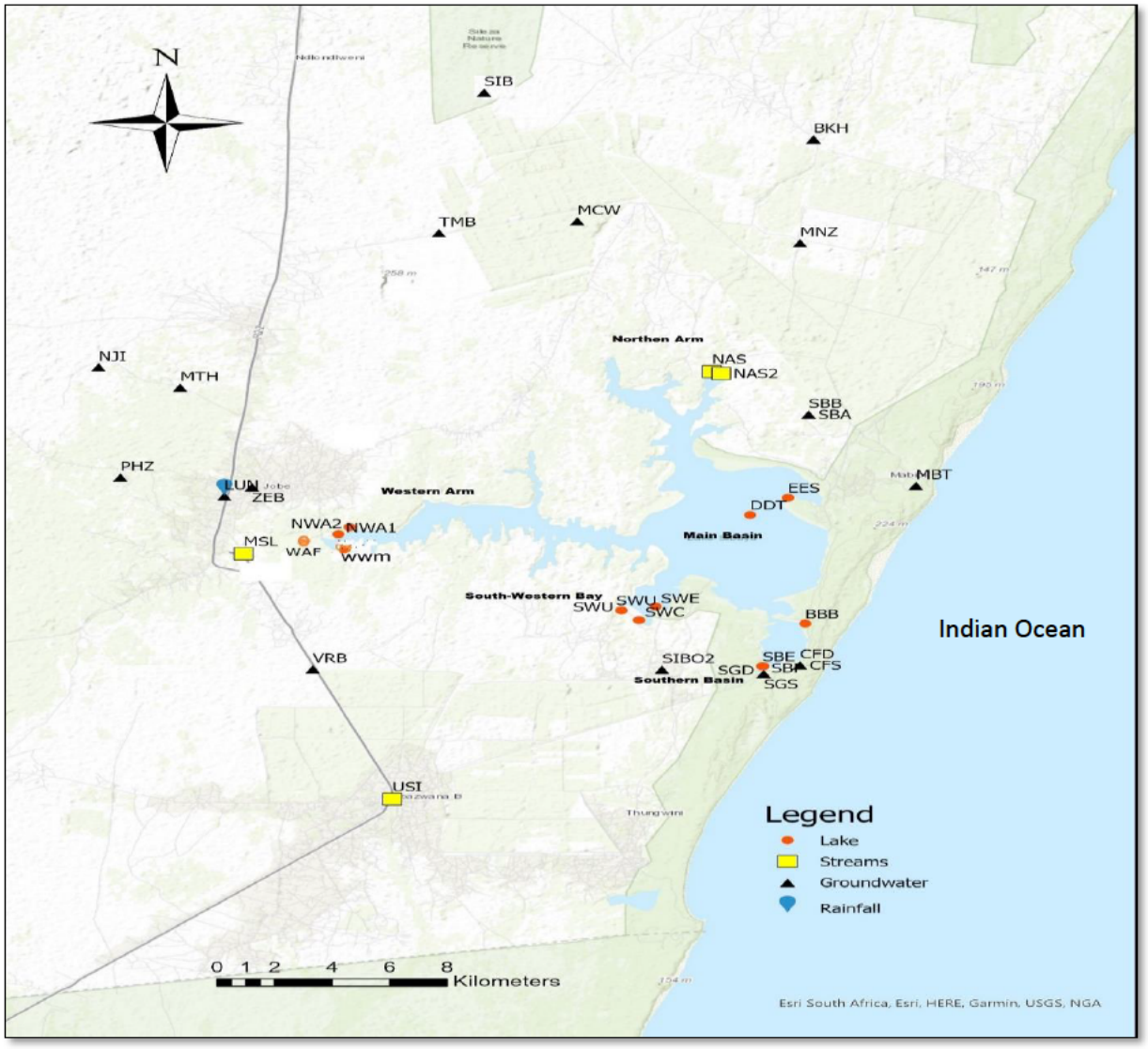

Figure 4-1 A map representing all the sampling points for this project.

4.3.1 Groundwater sampling

Monthly groundwater samples were collected from 20 boreholes (active and inactive boreholes) representative of the aquifer system contained within the study area. The samples were collected for 5 months. Out of the twenty boreholes six are pairs of nested boreholes (3x) drilled to different depth at the same location allowing the monitoring of the water isotopes, chemistry and water level across the sampling period.

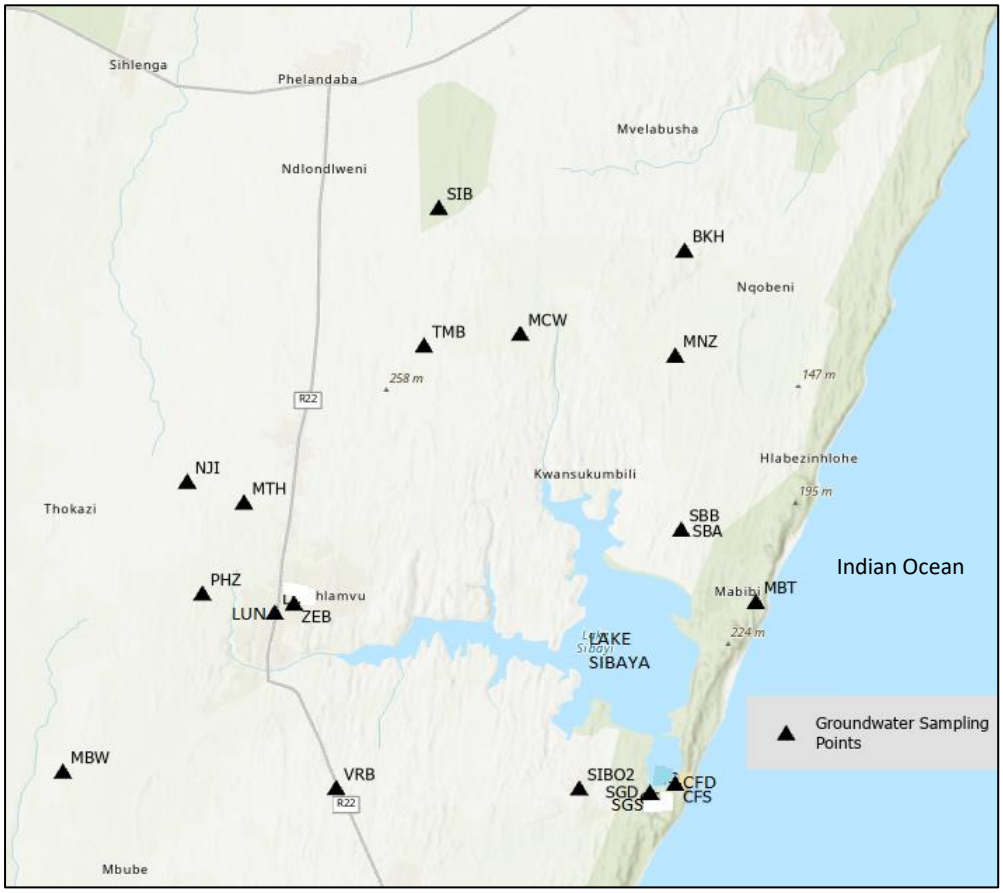

Figure 4-2 Groundwater sampling sites

Before sampling the groundwater level within a borehole, the depth to the water below the borehole casing was measured using the electronic water level meter (dip meter). The instrument consisted of a sensor attached to the end of a double connector wire. When the sensor encounters water, it makes a sound. Depth to water level is then taken directly from the tape at the top of the borehole casing. The inactive (monitoring) boreholes were purged using the 12 Volt STAINLESS STEEL MEGA-MONSOON XL Pump (figure 4-3). They were

purged according to the procedures set out by Groundwater Sampling Manual (WRC, 2017) as outlined in Weaver *et al*. (2007).

Figure 4-3 Dip meter used to measure groundwater level

The groundwater level measurements were used to understand the temporal responses of the aquifer to rainfall and to calculate the height of the water column in the borehole = *borehole depth – depth to water level*. Then the standing volume of water in liters was calculated by substituting the formula below (*equation 3*):

Equation 3

$V = \pi \times d^2 (h/4000)$

Where *d* is the diameter of the inner casing in mm, and *h* is the water level in meters subtracted from the depth of the borehole.

After the volume calculations, the pump was installed above the main water strike to avoid cascading, then the pumping rate was calculated, then using the volume calculated, the pumping time needed to remove the three volumes of water was calculated (spreadsheet example in Appendix A). Then the borehole was pumped into a 10L bucket using a 12 Volt STAINLESS STEEL MEGA-MONSOON XL Pump. This was to aid in calculating the pumping time needed to remove the stagnant water. Then continuous pH, EC, DO, and ORP were recorded using the Hanna H19828 multipara meter until they stabilized. The stabilization of the field parameters helps indicate when to take the samples at the borehole site. After the field parameters had stabilized the samples were collected directly from the pump using a 50

ml bottle. Care was taken to avoid headspace in the sample bottle and to prevent the sample from contacting air. For active boreholes such as community, farm, and school boreholes, water was left to run out for 10 minutes, the samples were collected.

Figure 4-4 Pump used to purge the inactive (monitoring) boreholes

The nested boreholes included the shallow and the deep aquifer located 5m apart. The nested monitored boreholes allowed the assessment of their log information as they represent different aquifers shallow and deep aquifers. Following is a brief description of these nested boreholes:

a) SG01A (shallow) and SG01B (deep) are located at 27.42089, 32.69809, on the South basin of Lake Sibaya. The site consists of shallow and deep boreholes drilled 5 m apart. The shallow well was drilled at 20.4 m with a diameter of 100m and static water level at the drilling date of 11.28. The deep well (SG01B) was drilled at 53 m with a borehole diameter of 100 static water level at the drilling date of 11.26 (TERRASTES, 2019).

b) CF01 boreholes are located on the eastern edge of the South basin of Lake Sibaya. The site consists of one shallow and one deep borehole. The deep borehole as CF01B (CFD) located at -27.41662, 32, and 32.70964 was drilled at 66 m with a borehole diameter of 100 m. CF01A (CFS) (shallow) is located at -27.41658, 32.70941 drilled at 36 m and a borehole diameter of 100 m (TERRASTES, 2019).

c) SIB01A&B (SBB and SBA) boreholes are located on the northern arm of Lake Sibaya. The site consists of shallow and deep boreholes. The site consists of shallow and deep

boreholes. They are both located at 27° 17' 42.8"S and 32° 42' 43.3"E. SIB01B was drilled at 46 m at an altitude of 44 m, and SIB01A was drilled at 26 m (TERRASTES, 2019).

4.3.2 Surface water sampling

Surface water samples were collected directly from the water bodies (lakes (59 samples) and streams (19 samples). To prevent collecting floating debris, stream samples were collected manually below the surface (about 30 cm). They were collected in areas with little human activity and less flow. Lake samples were collected using a pop bottle tied with a rope on the lake arms. To collect samples representing the lake, the pop bottle was thrown as far as feasible. During boat operations on the lake centre, samples were collected at 1m using the bailer. After collecting the samples with the pop bottle, they were put into 100 ml bottles and labelled with the site name (code). Onsite EC, pH, DO, ORP, and temperature measurements were recorded using the Hanna HI 9828 multipara meter water quality probes.

After each sample was taken from groundwater and surface water, they were stored in a cooler box with Ice until they were transferred to an air-conditioned room with the refrigerator in the University of KwaZulu-Natal Water laboratory.

4.3.3 Rainfall water Sampling

Daily rainfall was sampled using three rainfall samplers. Two samplers, a glass bottle rain gauge set 1.5 meters above the ground (GRS), and a rooftop rain gauge set at roughly 2.1 m (RFS)was set up in July 2021 in the Mseleni area (27.33482E, 32.52963S). The third sampler, a Palmex Rain Sampler RS1 (PRS), was set up in October 2021 (Figure 4-5). This sampler was selected as the standard sampler since it was designed for collecting monthly or daily samples as requested for stable isotope precipitation networks and is evaporation free. Samples were collected daily at 8 am. Depending on the water received, they were collected from the sampler using a 50 ml or 100 ml bottle. Care was taken to avoid headspace in the sample bottle and to prevent the sample from contacting with the air.

Figure 4-5 Three rainfall samplers used to collect rain water.

Figure 4-6 Palmex Rain Sampler RS1 (selected as a standard sampler).

The

4.3.4 Laboratory measurement

The stable isotope analysis of the rainfall, groundwater, stream, and lake samples was performed at the University of Stellenbosch (BIOGRIP water and soil node) using the Los Gatos T-L-WIA-45-EP stable Isotope instrument (*Figure 4.7*). To prepare the samples for analysis 1.9 mL liquid sample was filtered using a syringe filter (0.22 Filter Bio cellulose acetate syringe filter, with a diameter of 25 mm) for each sample in 2 mL glass vials and PTFE septum caps. The system was primed using the deionized water followed by three LGR working standards (two calibration standards (1E and 5E) and control standard (3E) as shown in Table 4.1, ten unknowns, and then another standard. This array of standards and unknowns

was repeated up to 4 times (40 unknowns) for a single run. Each standard or unknown was individually measured with nine injections. Then the results from each vial were averaged.

Table 4-1 LGR working standards vs VSMOW

Standards	$\delta^{2}H$ (‰)	$\delta^{17}O$ (‰)	$\delta^{18}O$ (‰)
1E	-165.7 ± 0.5	-11.26 ± 0.15	-21.28 ± 0.15
3E	-79.6 ± 0.5	-5.83 ± 0.15	-11.04 ± 0.15
5E	-9.9 ± 0.5	-1.52 ± 0.15	-2.99 ± 0.15

Figure 4-7 Los Gatos T-L-WIA-45-EP stable Isotope's instrument

4.3.5 Isotopic data analysis

To aid the interpretation of the isotopes regarding the groundwater recharge mechanism and aquifer interconnectivity, the rainfall isotope data has been used to construct the Local Meteoric Water Line (LMWL). When used along with the information about the range of isotope ratios, the LMWL can provide a reference scheme for interpreting the isotope ratios measured in groundwater, river, or lake waters. Comparing the groundwater isotope data with the LMWL is the basis for deciphering seasonality in groundwater recharge, the importance of evaporative water loss prior to recharge, and determining the minimum threshold rainfall amount that contributes to groundwater recharge. Additionally, the presence of isotopic rainfall effects in terms of the amount, seasonality, and temperature effects was analysed to investigate the seasonality of recharge and the minimum threshold rainfall amount contributing to groundwater recharge.

4.3.5.1 Amount effect

The amount effect has been used to determine the minimum rainfall required to recharge the groundwater. The stable isotope amount effect has been invoked to explain patterns of isotopic composition in rainfall in the tropics. The amount effect means that the more rainfall there is, the lower the $\delta^{18}O$ amount and the more depleted it is. Less intense rainfall resulted in enriched rainfall and high $\delta^{18}O$ levels. The time series analysis was done from a plot with rainfall amount on the X-axis and stable isotope signature on the Y-Axis to visualize the amount effect each day. Comparing the isotopic composition of the groundwater with the $\delta^{18}O$ amount plot or rainfall serves as the basis for pinpointing the rainfall threshold responsible for groundwater recharge.

4.3.5.2 Seasonality effect

The amount-weighted monthly stable isotope signatures were calculated using the daily stable isotope signature and the daily rainfall amount. The monthly amount-weighted isotope signature was determined by first calculating the fraction of daily rainfall amount to the total rainfall for that month and multiplying the fraction by the isotope signature ($\delta^{2}H$ and $\delta^{18}O$) of rainfall for that day to get the isotopic weight of daily rainfall. The isotopic composition of the groundwater was then compared to the weighted mean to understand the relation between different rainfall intensities and groundwater recharge. In situations whereby selective heavy rainfall contributes to groundwater recharge, the isotopic composition of the groundwater tends to reflect the composition of the high (intensity/amount) rainfall events.

4.3.6 Chemistry Data Analysis

This study measured EC, pH, and DO in surface and groundwater samples. However, for the interest of this study, only electrical conductivity was analysed. The analysis of electrical conductivity was conducted to assess the aquifer interconnectivity. However, chemistry is not a good evidence to reveal the aquifer interconnectivity.

4.3.7 Geological Log Analysis

The geological logs were obtained from Terrastest (2019), Lake Sibaya Report. The geological log analysis was conducted since it is the primary record of the geological geologic formations penetrated by the borehole. The sequence of the geologic logs has been visually inspected to assess the number of potential aquifers, confining layers, and the potential interconnection between the aquifer.

4.3.8 Water Level Fluctuation

The groundwater level data was sourced from SAEON. The level measurements taken by SAEON from 2019 to 2022 with a monitoring frequency of 30 minutes were used to determine the correlation between rainfall and observed groundwater level response from the six monitored boreholes. The data was converted from 30-minute frequency to a daily data, using the Microsoft Excel (Pivot Table). The water levels also assisted in analysing if the shallow and deep boreholes responded the same in different rainfall amounts. The rainfalls were plotted in a bar graph, and water levels were plotted in a line graph. Groundwater levels data were also used to interpret the interconnectivity between the aquifers, observing how they respond to the recharge.

5 RESULT

This chapter presents the results and analysis of the data collected during this research. Original data collected during this research are complemented with the secondary data. These datasets are collated and presented in the forthcoming sections

5.1 The slope of local meteorological water line and the composition of the rainfall

When used along with information about the range of isotope ratios, the LMWL can provide a reference scheme for interpreting the isotope ratios measured in ground, river, or lake waters.

The results in figure 5.1 show the plot of $\delta^{18}O$ versus $\delta^{2}H$ for the three rainfall samplers, PRS, RFS and GRS. The $\delta^{18}O$ values varied from -9.0 ‰ to 0.40‰, and $\delta^{2}H$ values ranged from -55.22 to 15.28‰ for PRS. RFS $\delta^{18}O$ varies from - 0.56 to 0.96‰, and $\delta^{2}H$ ranged from -55.33 to 15.28 ‰. GRS $\delta^{18}O$ varies from -8.85 to 1.91%, and $\delta^{2}H$ ranged from 51.17 to 16.56‰. In all the three instances, the slopes of the Local Meteoric Water Line (varying between 6.34 to 7.13) constructed using the three samplers is less than the slope of the Global Meteoric Water Line (slope =8).

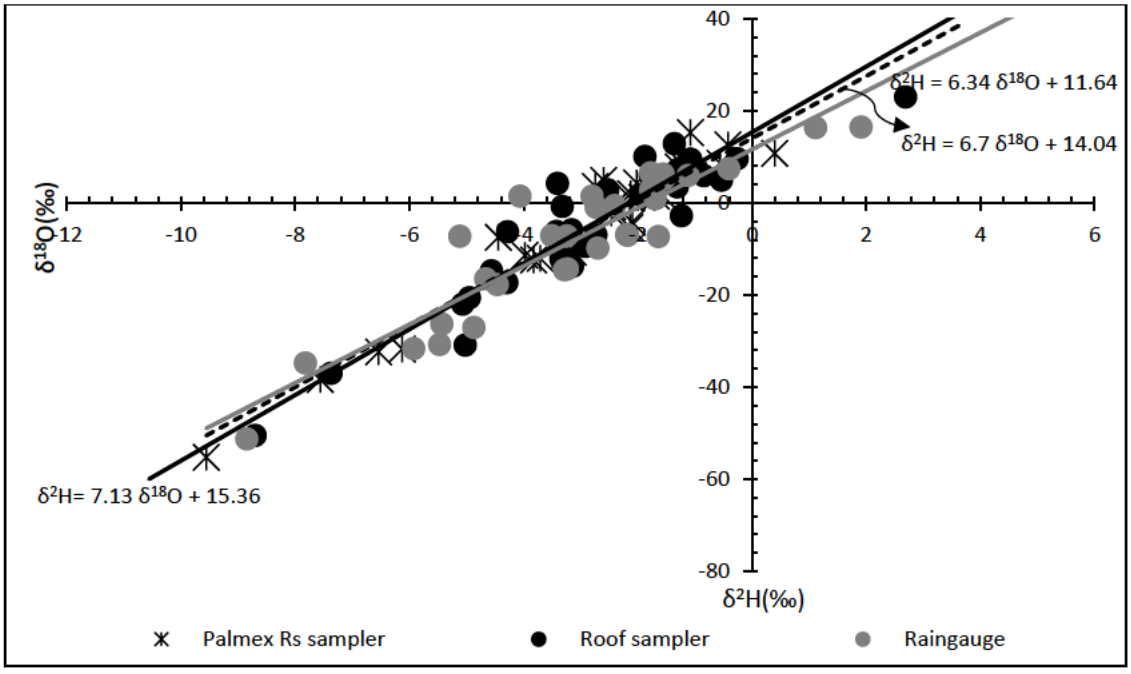

Figure 5-1 Plot of $\delta^{2}H$ versus $\delta^{18}O$ for samples collected using Palmex Rs Sampler, Roof sampler and Rain gauge (1.5 m).

The samplers provide slightly different regression line (local meteoric water line). The PRS sampler yields a higher slope compared to the RFS and GRS samplers. The relatively lower slope of RFS and GRS reveals the involvement of evaporative fractionation of the collected waters before sampling. As the result, the best-fit line through rains collected using the PRS sampler has been used as the Local Meteoric Water Line of the MPC region. There was no difference in the isotopic composition of samples obtained using the RFS and GRS samplers. The design of both samplers was similar and placed at different heights, indicating that the sampling height did not affect the isotopic composition. These were untested custom-made samplers, which should be avoided in such investigations.

5.1.1 Amount effect in the isotope dataset

Figure *5.2*, shows the isotopic composition of rainfall vs amount of rainfall. It can be seen in figure 5.2 that as the amount of rainfall increases the isotope signatures of rainfall becomes more depleted. The more depleted isotope signatures plotted on rainfall amounts higher than 30 mm/day. The enriched samples plotted in rainfalls below 30 mm/day. The low rainfall amount produced enriched rainfall with high $\delta^{18}O$.

The negative slope suggests that an increase in rainfall generally corresponds to the depletion of heavy isotopes, whereas a reduction in rainfall corresponds to an enrichment of heavy isotopes. Rainfall less than 30 mm/day is classified as light rains more prone to re-evaporation, allowing the light isotope to evaporate and leaving the heavy enriched isotope. Heavy rains (>30mm/day) are less prone to re-evaporation, resulting in a more depleted isotopic composition. The observed amount of effect in the enriched section of the plot could be due to post-condensation rainfall re-evaporation, which is particularly effective for light rainfall (Clark and Fritz, 1997). When the rainfall exceeds 30mm/day, the amount effect becomes more pronounced than when the rainfall is less than 30mm/day. The presence of a strong amount effect (R^2=0.73) in daily rainfall reveals the potential of use of isotopes to determine groundwater recharge threshold.

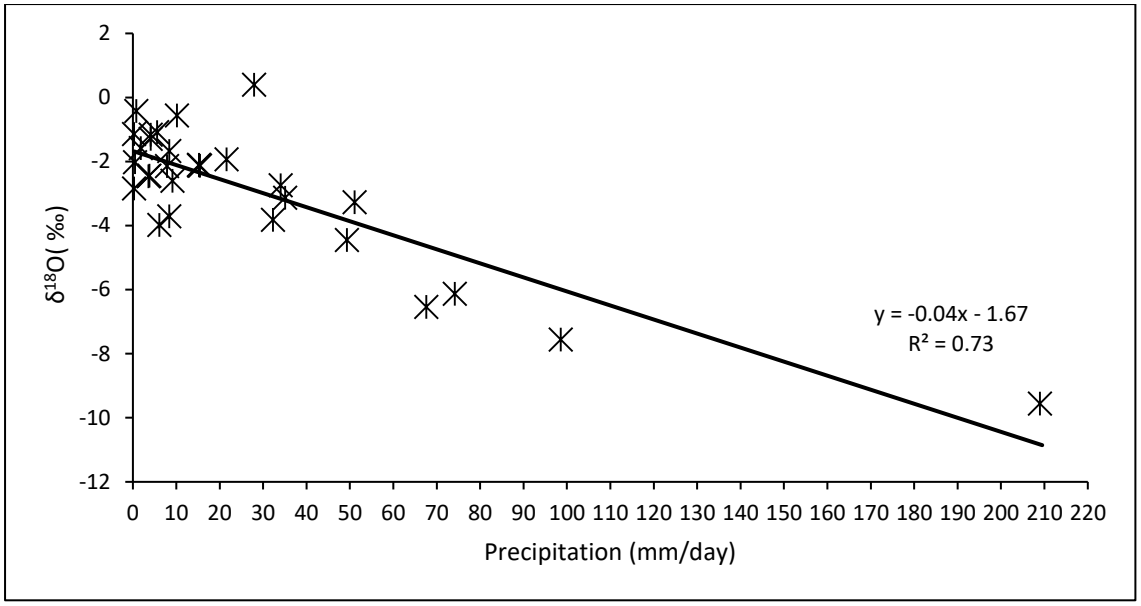

Figure 5-2 Amount effect graph indicating threshold to recharge groundwater

Plotting the rainfall isotopic composition as a time series plot along with the daily rainfall amount reveals some other noticeable features (figure 5.3). On January 29 2021, marked with a total rainfall amount of 98.6 mm in a single day the $\delta^{18}O$ was -7.56 ‰, and $\delta^{2}H$ of -38.2‰. This unusually high depletion is related to the exceptional rain of the day. Similarly, the heaviest rain recorded on April 12, 2022 amounting to 209 mm in a single day resulted in the most depleted isotopic composition recorded in the data set (with $\delta^{18}O$ of -9.56‰, and $\delta^{2}H$ of -55.2‰). Rainfall was enriched in months with lower rainfall totals. The other rains, which produced highly depleted values, are in the week of 12-19 April 2022. These heavy rainfalls are believed to correspond to subtropical storms (Karisruhe *et al*, 2022) and even other researchers attribute the rains of the week of 12 April to a cyclonic event.

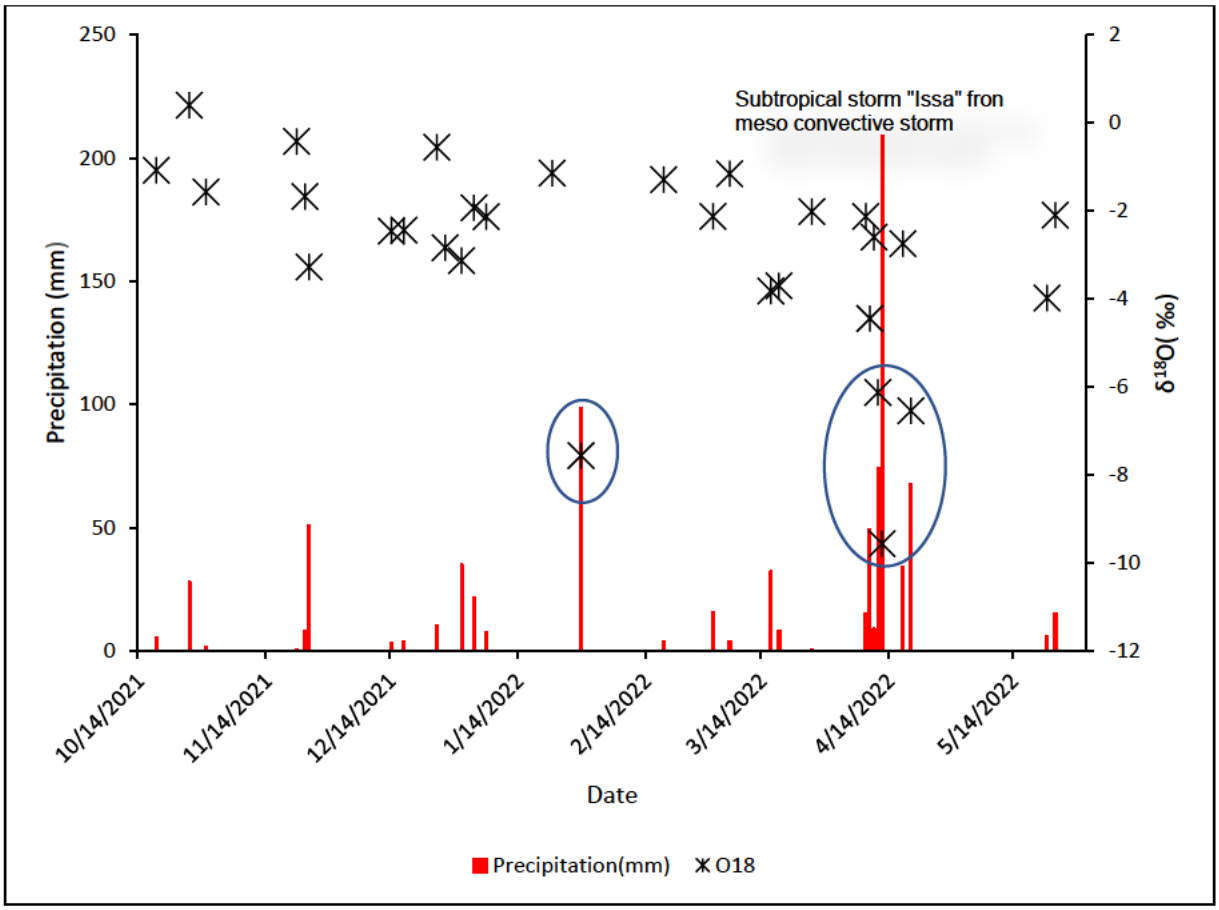

Figure 5-3 Plot of rainfall daily amount and the isotopic composition of rainfall

5.1.2 The weighted average δ ^{18}O and δ ^{2}H composition of the rainfall

Figure 5-4 shows the plot of amount weighted $\delta^{18}O$ and $\delta^{2}H$ in rainfall dataset. The amount-weighted values were calculated based on the following formula.

Equation 4

$$\text{Amount-weighted} = \sum p_i / \sum \delta^{18}O \text{ or } \delta^{2}H$$

Where *pi* is precipitation daily

The amount weighted value plot at the lower slope of the LMWL with a $\delta^{18}O$ of -5.63‰ and $\delta^{2}H$ of -25.64 ‰. The skewness towards the depleted end of the LMWL is caused by the highly depleted heavy sub-tropical storms which accounted for 60% of the total rains observed during the sampling period. Figure 5-5. Shows the weighted isotopic composition of each month over which the data has been collected.

Compared to months with little precipitation, months with high precipitation had depleted weighted averages isotopes composition (figure 5-5). The month of October2021 with the least rainfall amount shows the most enriched value with $\delta^{18}O$ of 0.07‰ and $\delta^{2}H$ of 11.05 ‰. The months of April and January show the most depleted compositions. However, no clear pattern was observed in the other rainy months such as in December, February and March. This mean the month of the year is not an important control on the isotopic composition of the rainfalls. Rather the presence of exceptional heavy rainfall events controls the temporal variation in the isotopic signals. Nevertheless, the months which receive the heaviest rains show depleted signal compared to the months with low rainfall.

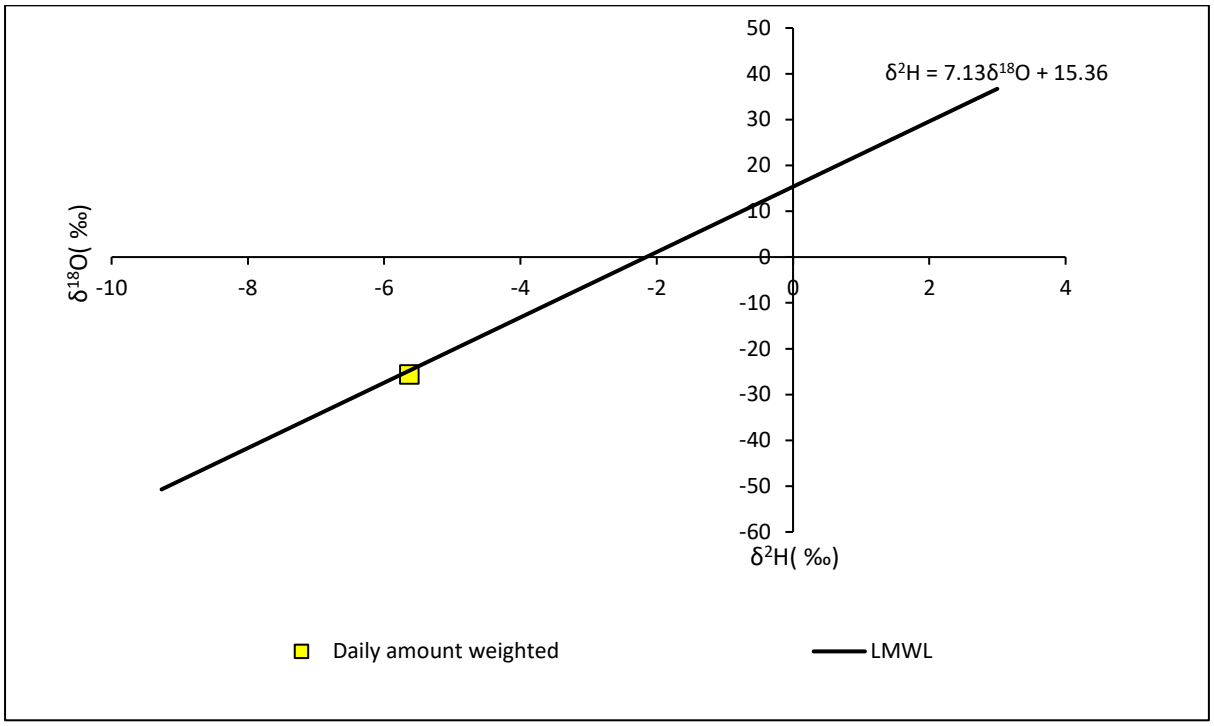

Figure 5-4 the amount weighted $\delta^{18}O$ and $\delta^{2}H$ of rainfall.

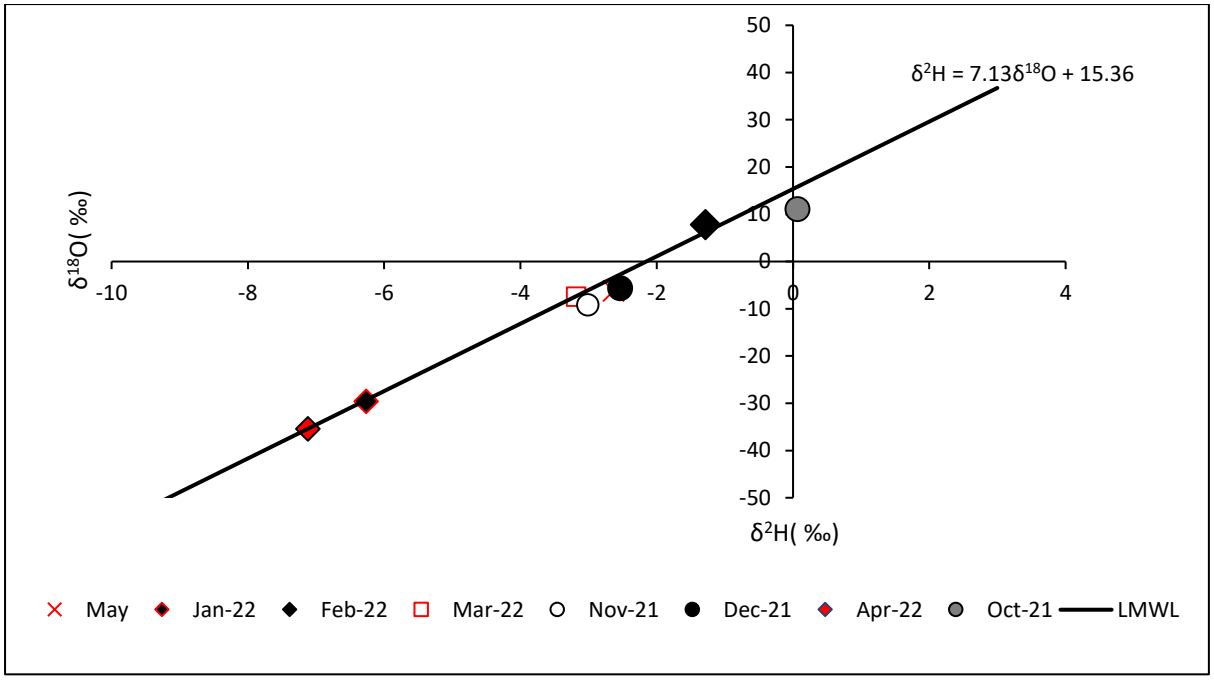

Figure 5-5 the plot of weighted monthly and amount weighted $\delta^{18}O$ and $\delta^{2}H$ of rainfall.

5.2 Isotopic composition of groundwater

Groundwater samples were obtained from 20 sites surrounding the Lake Sibaya. The groundwater samples clustered into three groups (figure 5.6) established with respect to distance from the LMWL. In all the cases, the $\delta^{18}O$ vs. $\delta^{2}H$ for all groundwater sampled plotted below the LMWL populating the best fit slope of 5.4 typical of indicating the groundwater had undergone some evaporation prior to recharge. It is to be noted that a slope of 5.4 is typical of evaporation line produced when a liquid water evaporates (Craig, 1965).

Group one groundwater samples, named as CFS and CFD boreholes collected in the nested boreholes east of the South Basin of the lake Sibaya with the most positive $\delta^{18}O$ and $\delta^{2}H$ values. The stable isotopes for group one boreholes range from 1.22 ‰ to 2.18‰ for $\delta^{18}O$ and 16.63 ‰ to 20.62 ‰ for $\delta^{2}H$, as will be demonstrated below (figure 5-6), in similar range as that of the Lake water. The similarity with the Lake water isotopic composition reveals the connection of the groundwater to the Lake. Group 2 located on the eastern coastal dunes of the main basin of the Lake Sibaya named as MBT, they fall below the LMWL but with a less pronounced degree of isotopic enrichment with a $\delta^{18}O$ and $\delta^{2}H$ ranging from -1.898 to -2.75 ‰ and -4.68‰ to -7.47‰ respectively. Considering the location of the boreholes and their static water level far above the Lake Sibaya level, the enrichment is not the result of lake water mixing but rather is the result of recharge from isotopically enriched coastal rains. Coastal rains are generally

enriched compared to inland rains. Group 3 consisting of the inland boreholes named as "inland BH", with a $\delta^{18}O$ and $\delta^{2}H$ ranging from -3.05 to -5.27‰ and -10.47‰ to 25.04‰, respectively. The depleted values can be observed in the inland boreholes, while enriched samples are dominant on the CFS and CFD located on the east South Basin part of the Lake Sibaya. Regardless of the relatively depleted composition when compared to the coastal boreholes, the inland boreholes also show a plot below the LMWL revealing the importance of evaporation prior to recharge. Since evaporation that happens in the soil zone generally produce a much lower slope (Allison *et al.*,1983) of around 2-3, the evaporative enrichment observed in the aquifers is most likely caused by evaporation in open waters. This reveals that the importance of flood waters and wetland waters as the primary source of groundwater recharge in the area.

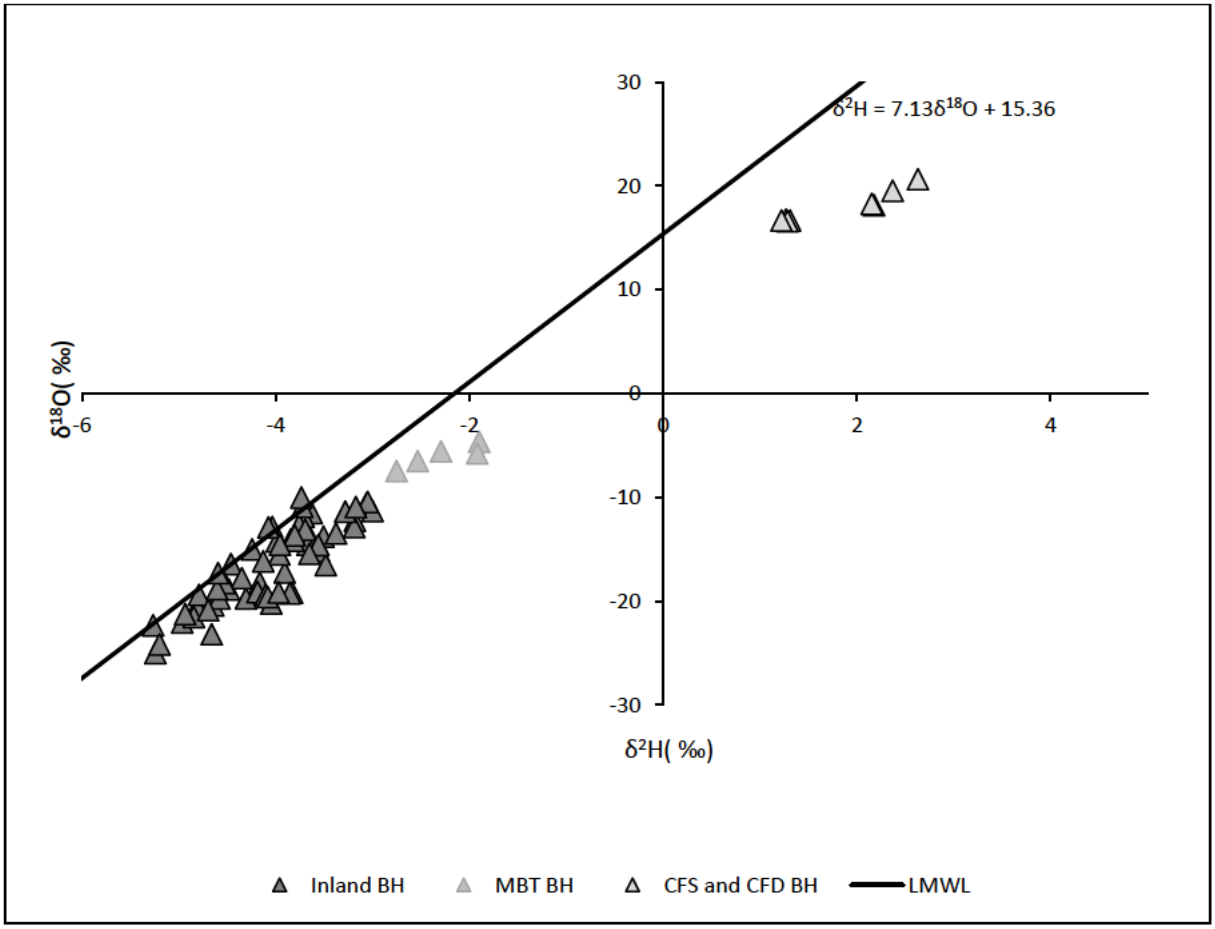

Figure 5-6 Isotope data of groundwater samples clustered into three groups established with respect to distance

5.2.1 Comparing rainfall and groundwater isotopic composition

Figure 5.7 shows the plot of weighted monthly and amount weighted $\delta^{18}O$ and $\delta^{2}H$ in rainfall together with the groundwater samples. The October and November rains are too enriched to resemble the isotopic composition of the groundwater samples. This may indicate that rainfall in less rainy months are not involved in groundwater recharge, while recharge occurs during the heavy rainfall season between December and April (summer months/season). The rains in the month of February might be involved but coincidentally there was little rainfall in the month of February when the current study was conducted.

The seasonality of groundwater recharge cannot be specified due to the limited data collection. On the other hand, the Figure provides a general notion and helps clear out low rainfall months from being involved in groundwater recharge. The mean original isotopic composition of the groundwater can be deduced from the intersection point between the best fit line to the groundwater data points and the Local Meteoric Water Line. The intersection point falls around a $\delta^{18}O$ and $\delta^{2}H$ of -6 ‰ and -26 ‰ respectively. This point is slightly more depleted than the weighted mean isotopic composition of the rainfalls indicating the fact that the groundwater is recharged from selective heavy rains. Generally, the groundwater falls towards the depleted end of the rainfall isotope signal already insinuating the involvement of selective groundwater recharge from heavy rainfall only. For example, the types of rains observed in December, February, March, November 2021 and 2022 are not sufficient to produce the isotope signal observed in the groundwater. In these months, the rainfall rarely exceeds 30 mm/day indicating rainfall in excess of 30 mm/day may be required to recharge the groundwater. However, this is an indication and to reach a conclusion a detailed water level monitoring is required.

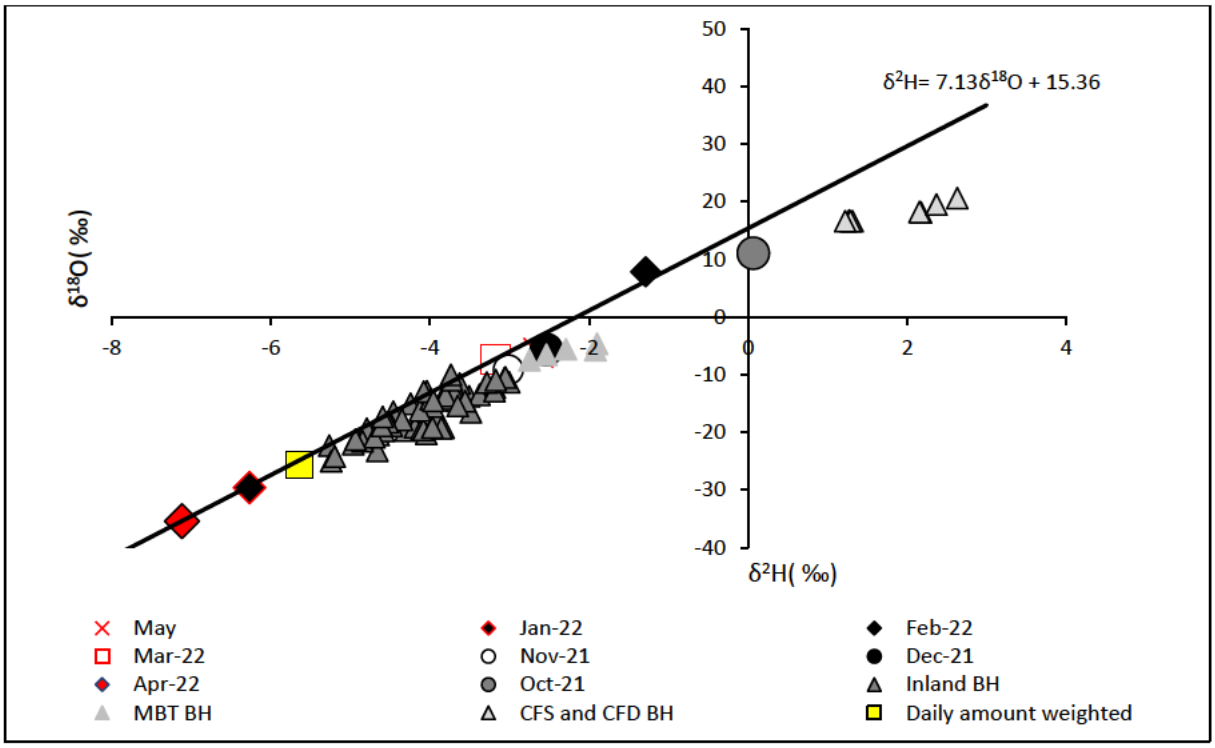

Figure 5-7 the plot of monthly a month weighted average vs isotopic composition of groundwater.

5.2.2 Aquifer interconnectivity revealed from isotopic composition of nested boreholes

In this study shallow and deep groundwater were isotopically analysed to assess the connectivity between aquifers. Nested boreholes (see section 4) drilled into the different presumed layers of the aquifers have been monitored over the period of 5 months for their water level, chemistry and isotopic composition. It is to be noted that each nested borehole was located at different sides of the Lake. The CFD-CFS nested borehole pairs are located below the dunes on the east of the South Basin of the lake. The SGD-SGS pairs are also located on the South Basin of the lake. Lastly SBB-SBA located on the Northern arm of the lake (see figure 4-1 for location). In previous conceptual and numerical models, the MCP has been considered as having three distinct aquifers. The current sampling of the nested boreholes was thus meaning to refine this conceptual model.

Figure 5.8 shows a plot of $\delta^{18}O$ vs. $\delta^{2}H$ for the nested boreholes used to analyse the aquifer interconnectivity between aquifers in the study area. The results show no statistically significant difference between the isotopic signature of the shallow and the deep well at all locations (figure 5.8). This similarity of the shallow and deep boreholes reveals the interconnectivity of the aquifers and lack of confining layer that limit vertical exchange of water between the aquifers. The isotopic data reveals that the aquifers have similar isotopic composition which is an indication of an interconnected aquifer systems getting recharge from similar sources.

The behaviour of isotopic similarity between the shallow and deep boreholes/aquifers is observed across all the seasons. It appears that the aquifers respond in a similar fashion (scale and direction) to the exceptionally heavy rains lasting between 12 and 19 April indicating the interconnection between the aquifers. After the heavy rainfall from April (the subtropical storm ISSA), their isotopic signatures decreased, indicating the contribution of recharge of the two aquifers from heavy rains of the Month of April. The changes are shown with the black arrows

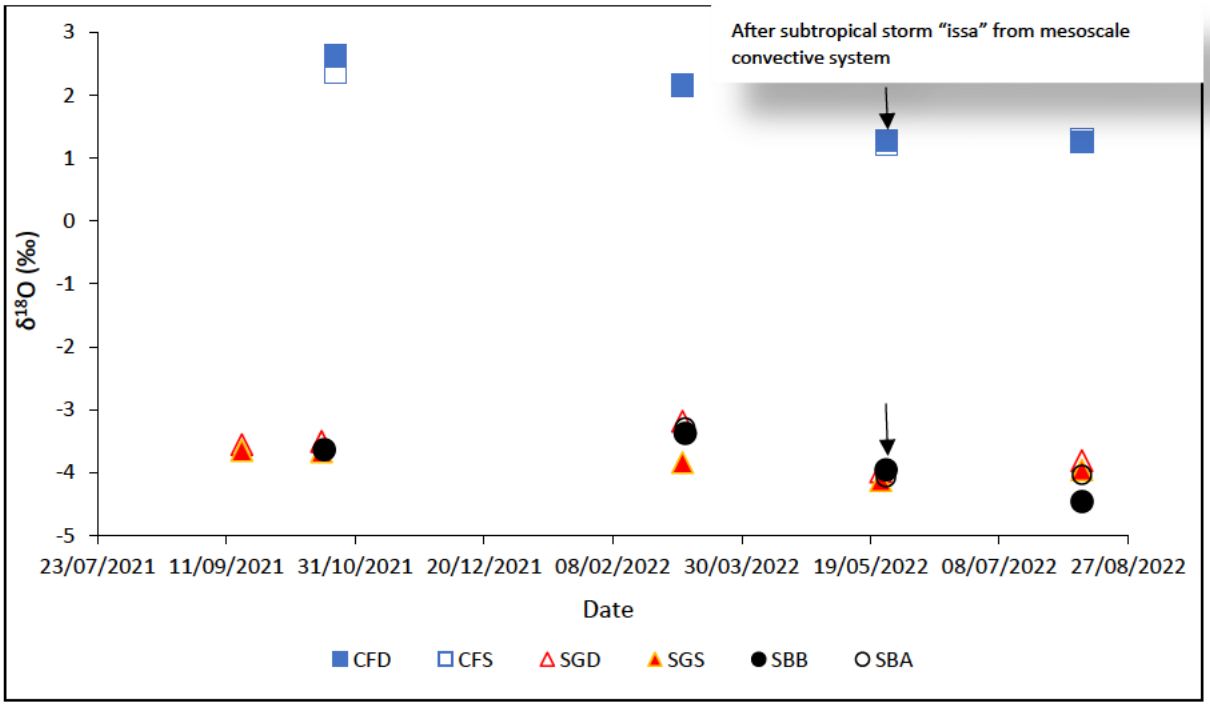

Figure 5-8 isotopic composition of the nested boreholes (shallow and deep borehole).

5.3 Isotopic composition of all water resources sampled

Figure 5-9 depicts the isotopic signatures of all lake, stream, and groundwater samples collected. The isotopic signatures of stream water samples (Figure 5-9) were identical to those of groundwater samples, revealing the source of stream water and subsequent discharge of the streams to the Lake without extra significant evaporation. Western Arm wetlands also had similar isotopic signature as groundwater samples, revealing a recharge from groundwater. Groundwater from CFS and CFD had similar isotopic signatures as the lake samples indicating a mixture of lake water and groundwater and lake recharging the groundwater. Samples from unknown lake from the South Western Bay plotting on the lower slopes, showing depletion. The lake samples collected showed a large spread in isotopic composition, showing poor mixing around the sampling points due to samples collected on the lakeshores. The Eastern and Main basin of the lake showing high enrichment compared to the western arm and southwestern bay, which shows that the inflow to the lake is from the western, southern, and northern parts.

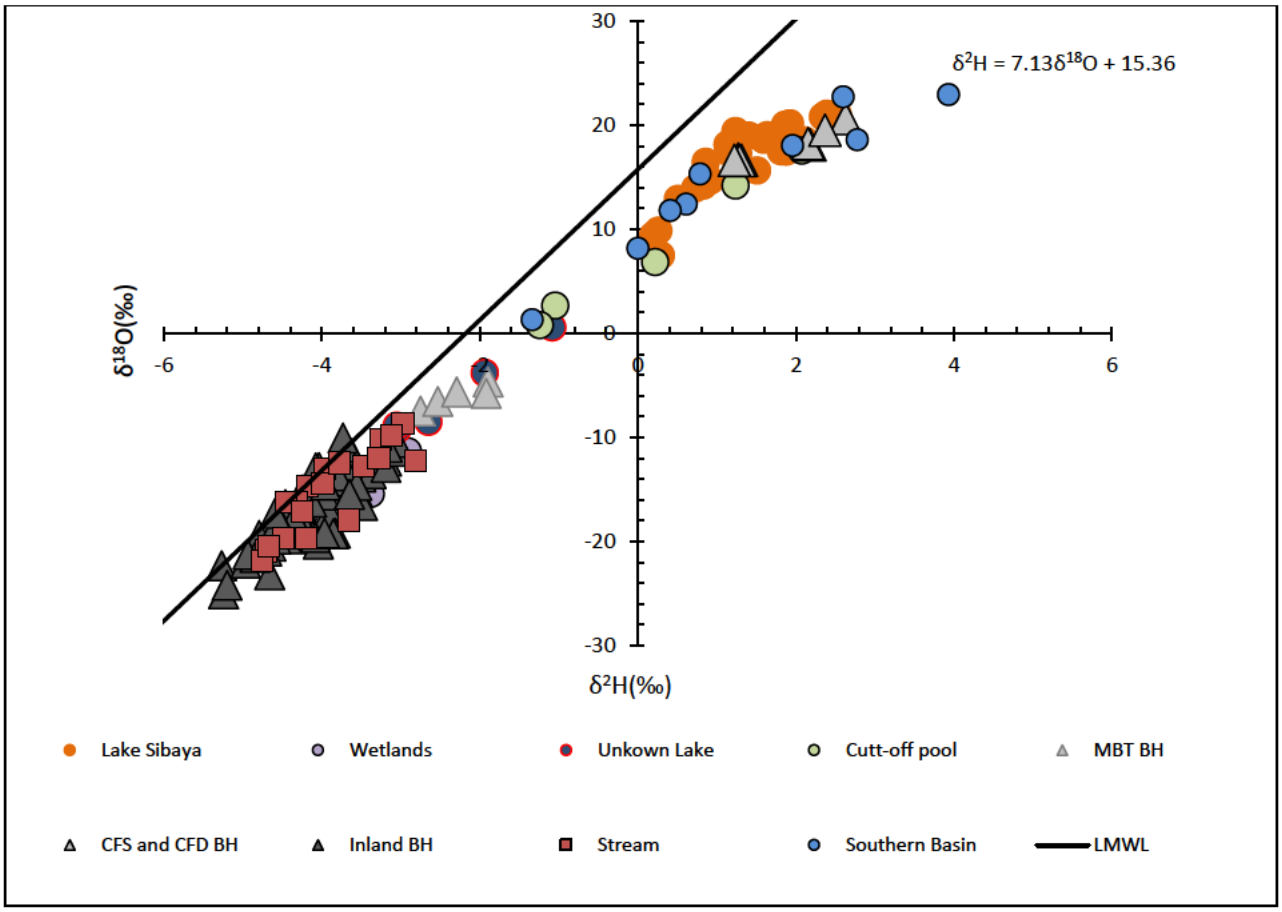

Figure 5-9 A summary plot between $\delta^{18}O$ and $\delta^{2}H$ from various water resources sampled within the study are in relation to the LMWL.

5.4 Evidence of aquifer interconnectivity and groundwater recharge processes from groundwater level fluctuation

Each nested borehole was located from different sides of the Lake Sibaya, CFD, CFS located below the dunes on the east of the south basin of the lake. SGD and SGS also located on the south basin of the lake. Lastly SBB and SBA located on the Northern arm of the lake. The water level data was acquired from SAEON.

5.4.1 Groundwater Level data

Figure 5-10, 11 and 12 shows the groundwater level vs. the daily rainfall. The water levels constantly fluctuate in response to varying amounts of rainfall. The shallow and deep boreholes indicate similarities in trends. During high rainfall, the groundwater increases, and during small rains, there is a lack of response from both boreholes (shallow and deep boreholes). Both shallow and deep boreholes had different heads but responded in similar patterns, this happens when the leaky aquifer is present, and head patterns are the same, but the heads of the aquifers are different. The response in water levels to rainfall from the nested boreholes can be observed in day when rainfall exceeds ~ 30mm/d and above, matching the results obtained from the analysis of isotopes (amount effect). A substantial rise in water level can be seen from rainfall occurred in 12 April 2022 with an amount of 207, resulted from the subtropical storm “Issa” from mesoscale convective system.

Following the dry season in May-July 2019 the water level in SGS and SGD boreholes continued to decline with minor increases corresponding to the rainfalls, which exceed 30mm/day. The first major sharp increase in water table came after two consecutive rainy days in January where rainfall exceeded 60mm/day. The time between January 29, 2021 and 12 April a sharp increase in water table.

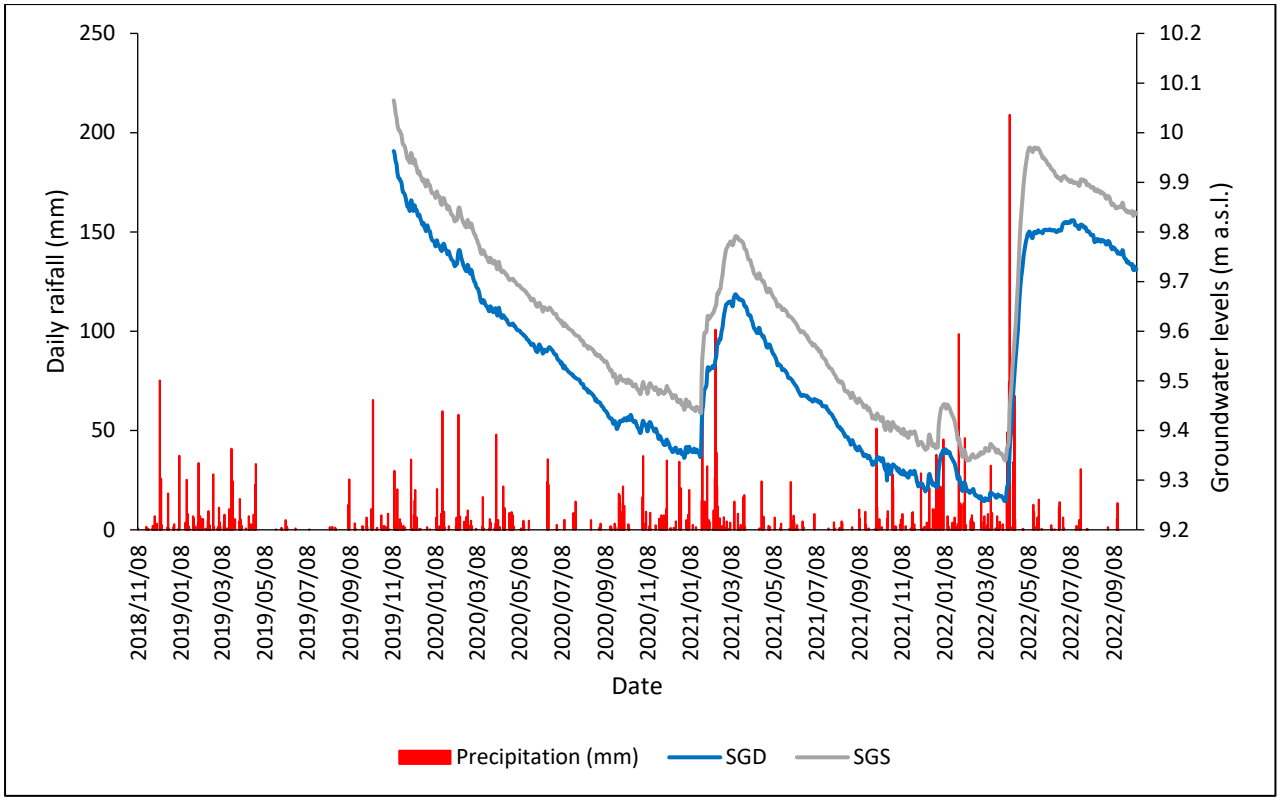

Figure 5-10 water levels of SGD and SGS boreholes vs Daily rainfall amount Vasi Science Centre weather station.

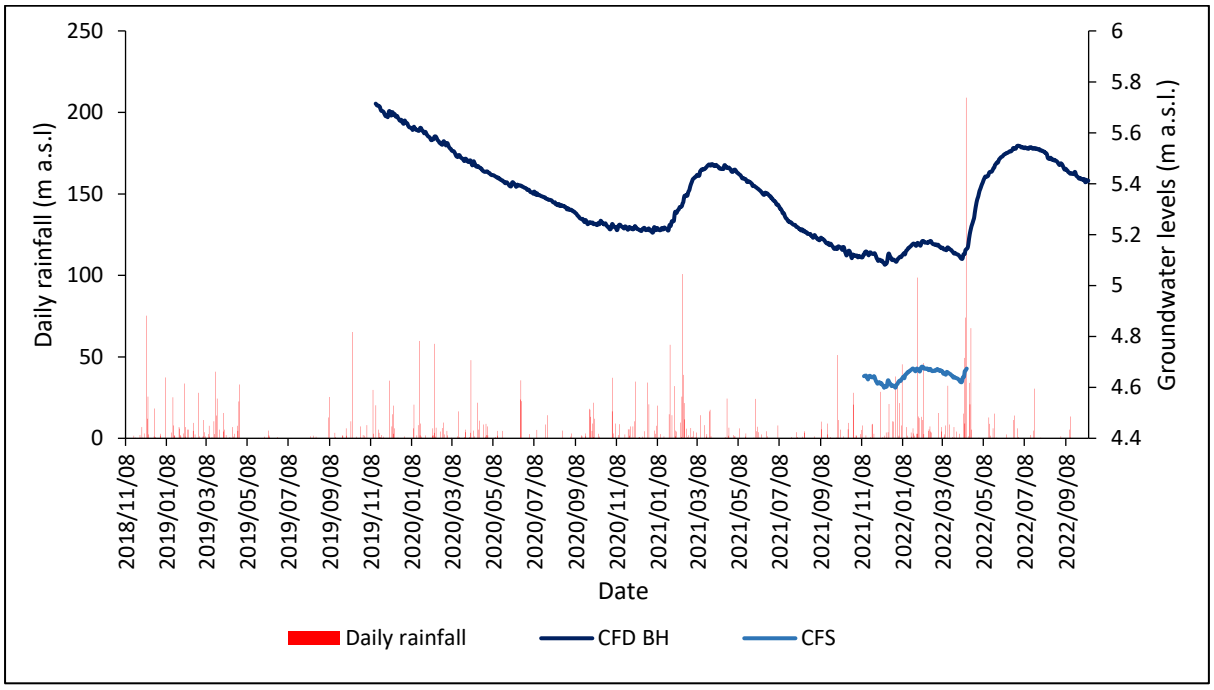

Figure 5-11 Groundwater levels of CFD and CFS boreholes vs Daily rainfall amount from Vasi Science Centre weather station.

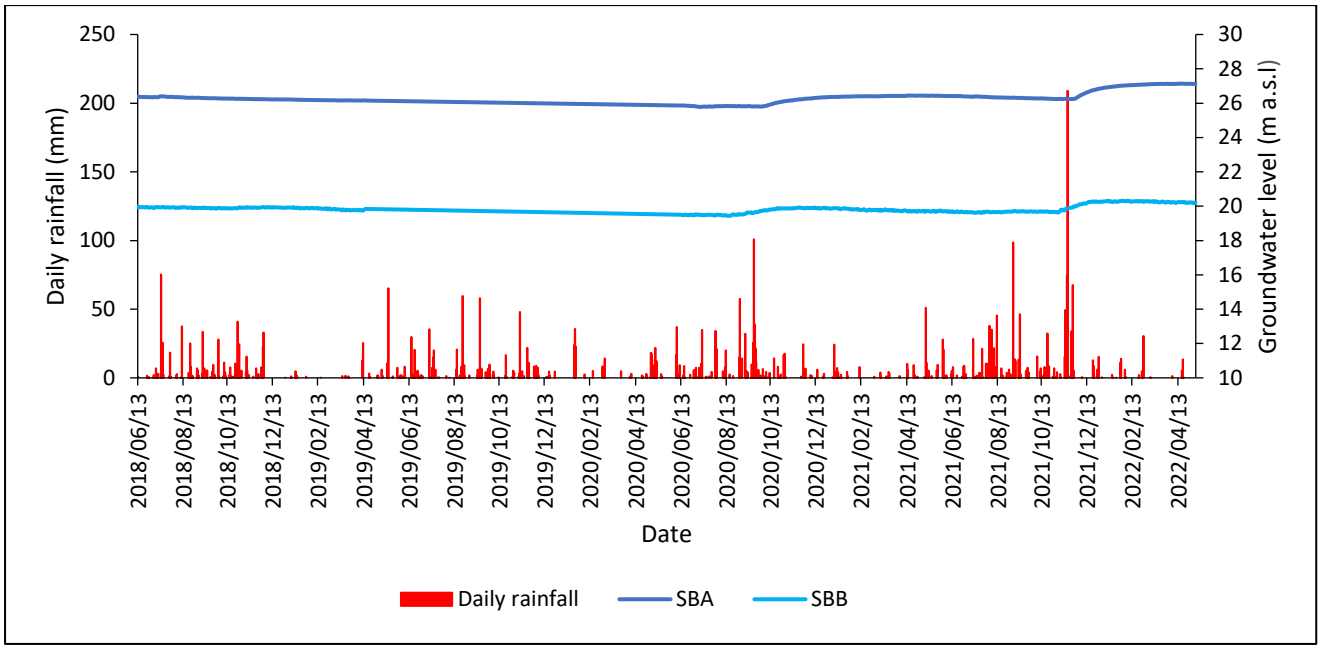

Figure 5-12 Groundwater levels of SBB and SBA boreholes vs Daily rainfall amount from Vasi Science Centre weather station

5.5 Revealing aquifer interconnectivity from well logs

In this study, shallow and deep well geology was analysed to asses if the soils allow any movement of water, which then allows the interconnection between aquifers and the water level to see if the shallow and the deep aquifer will behave the same during the recharge. The geology from each nested well is shown figure 5-13, 14 and 15.

Figure 5-13, 14 and 15 is a well-to-well geological cross-section obtained from Terrastest, (2019). The well-to-well cross-section shows the different geological materials and some of their properties that lies beneath a surface and some of their properties such as colour, texture, grain size, and depth at which changes occurred. Each layer has a significant amount of sandy sediment, which allows the movement of water from the upper aquifer to the lower aquifer.

Sandy sediments vary in all layers of the aquifers. The presence of a distinct clay or other impermeable layer is not evident from the available well-log revealing the lack of evidence to conclude multiple aquifers separated by confining layers.

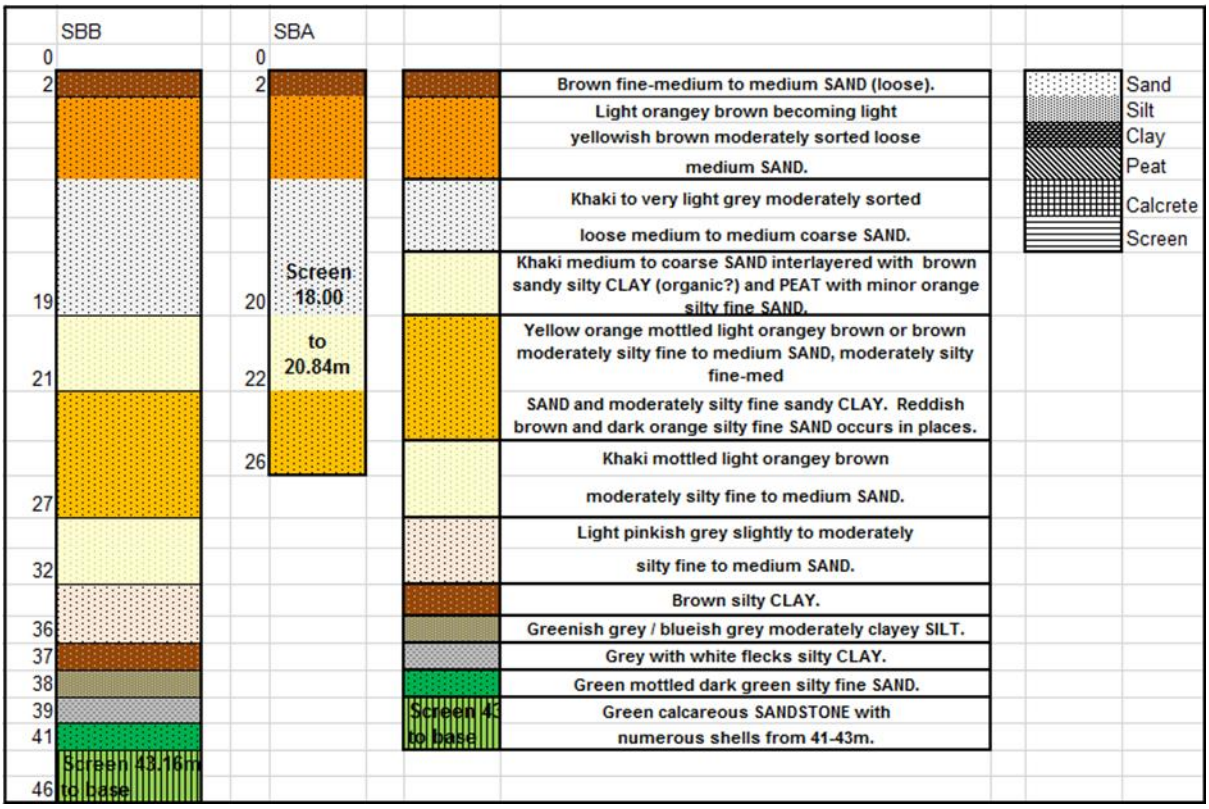

Figure 5-13 Geological cross section of SBA and SBB (Terrastest, 2019)

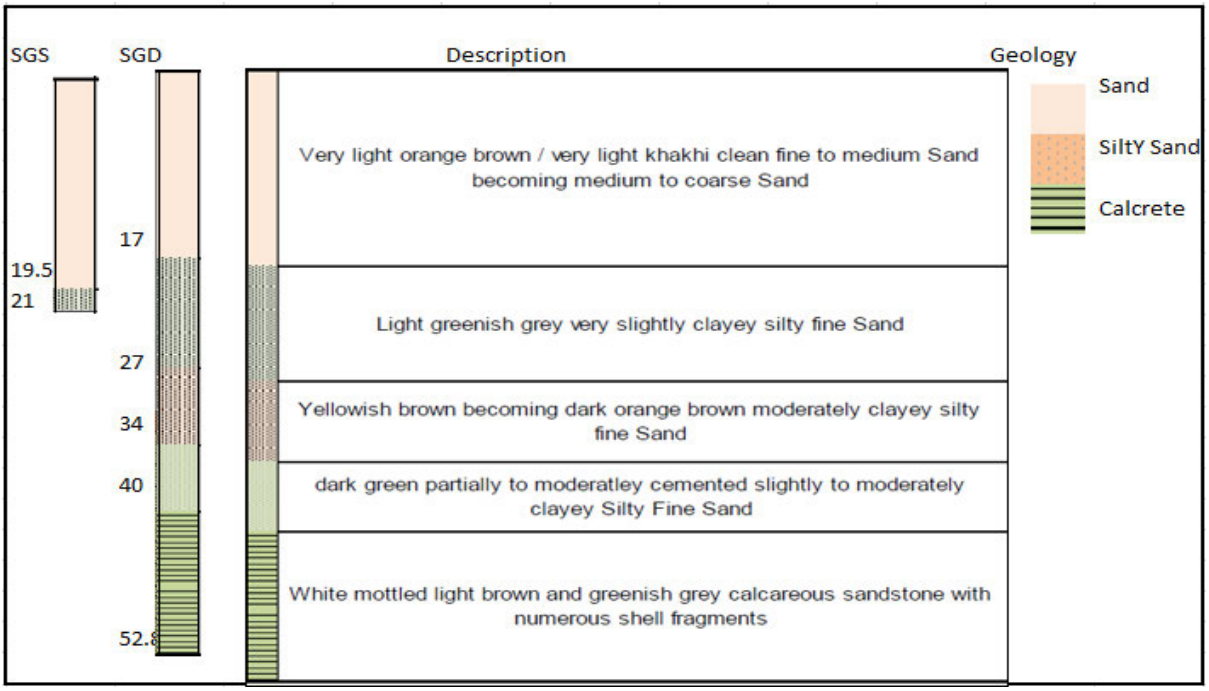

Figure 5-14 Geological cross section of SGD and SGS (Terrastest, 2019)

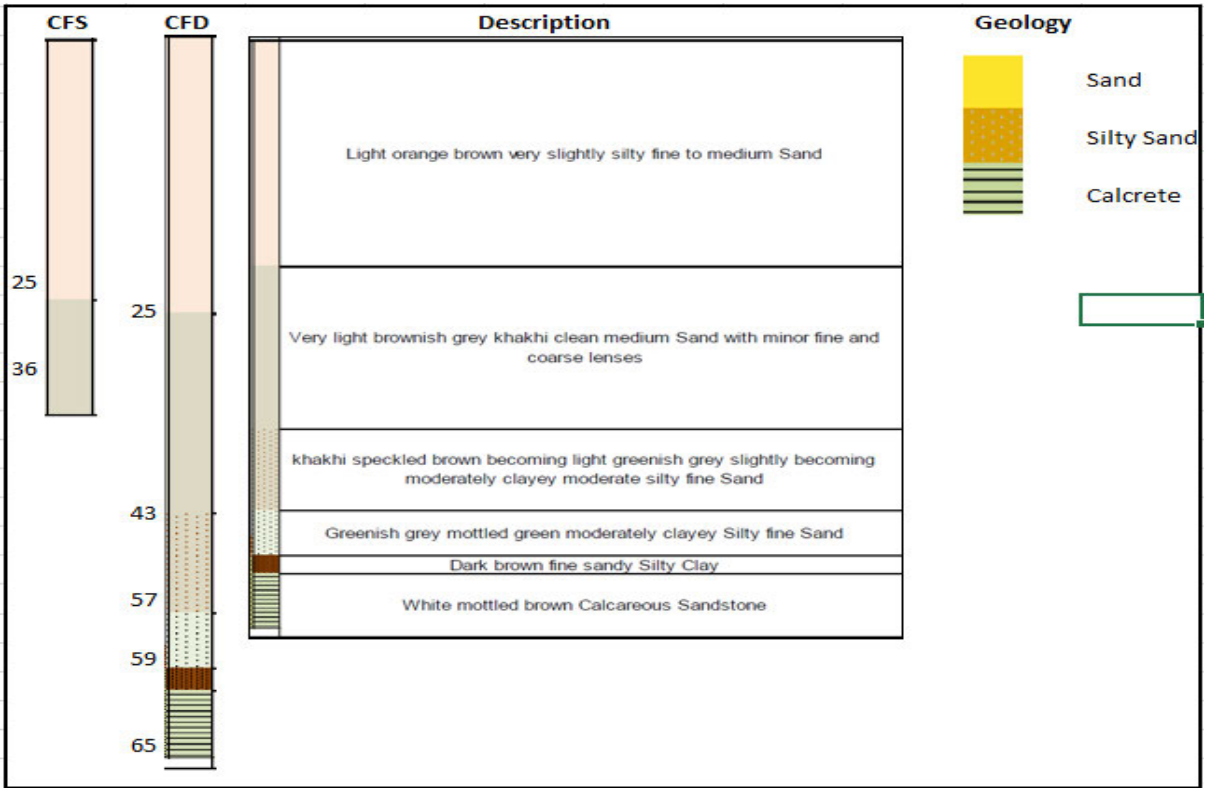

Figure 5-15 Geological cross section of CFD and CFS (Terrastest, 2019)

5.6 Evidence from field chemistry (EC)

The chemistry of water is commonly used to determine the source of groundwater as well as problems with its quality (Kumar *et al*., 2013). According to Clark and Fritz (1997), hydrochemcal analysis are effective tools to determine the origin of mixed waters in groundwater and surface water system. To determine the relationship between groundwater and rainfall hydro chemical parameter electrical conductivity (EC) was measured in various boreholes including the nested ones. The pattern observed for most inland boreholes shows a declined in EC as rainfall amounts increased. After the heavy April rains, the differences are visible.

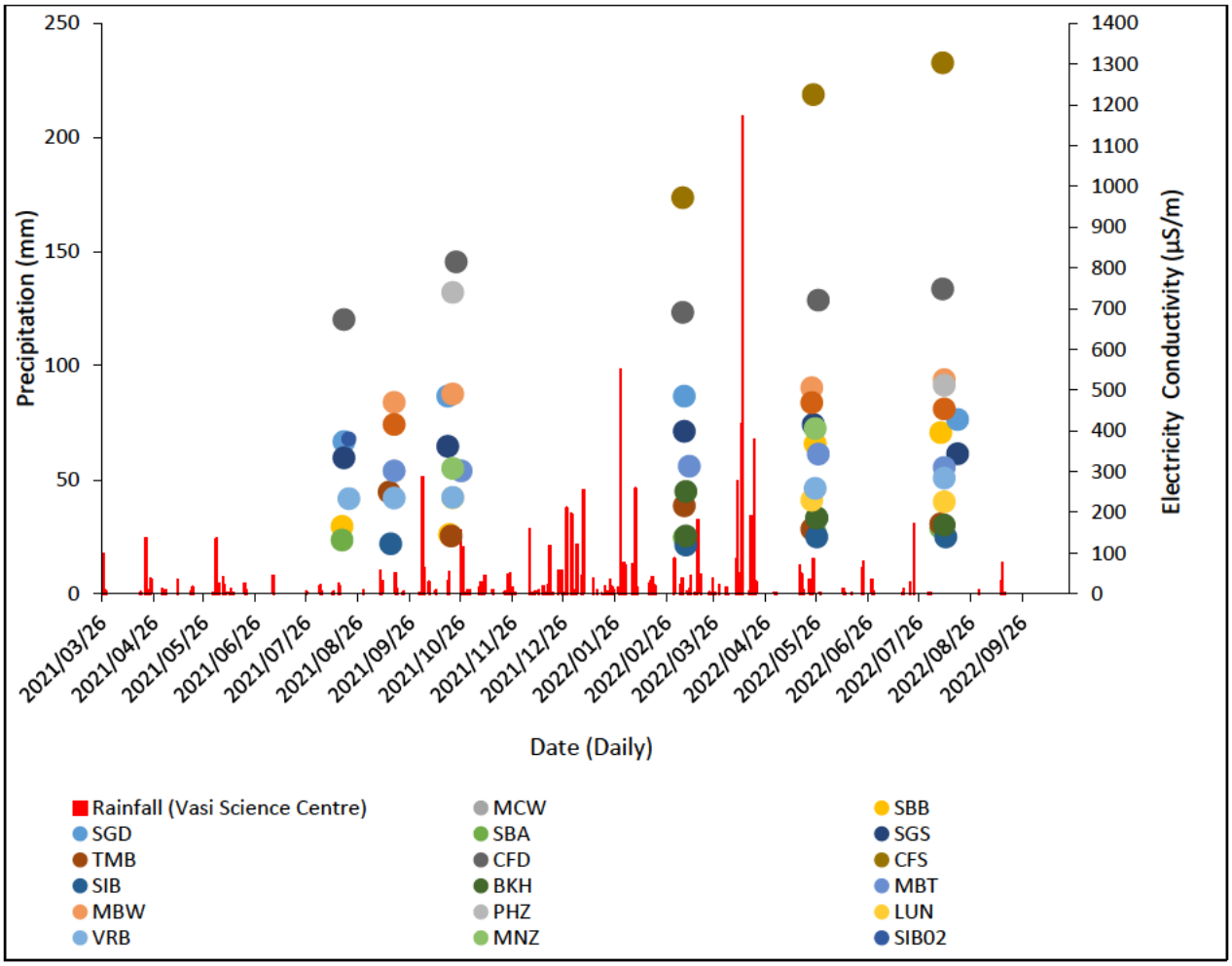

Figure 5-16 Electrical conductivity for all groundwater sampled for this study

The electrical conductivity from the nested boreholes (Figure 5-17) showed the similar pattern of response between the shallow and the deep boreholes. For the inland boreholes, the EC decreased with the increased rainfall amount/after the rainy month of April 2022. However, maximum concentrations of EC were observed in coastal boreholes (CFS and CFD) after the heavy April rains. The shallowest CFS borehole shows a sharp rise in EC compared to the deeper equivalent (CFD). The increased EC in the CFS and CFD boreholes are remarkably higher than the increase in the other nested boreholes located inland. The sharp increase in EC in the CFD and CFS boreholes following the April rainfall may be caused by the salts from dry deposition and sea spray accumulating on the soil during the dry season/months in the coastal environment. These boreholes are very close to the Sea Coast. Moving toward the inland boreholes, the dry deposition and sea spray decreases, and consequently the increase in EC is marked in SBA and SBB boreholes following the heavy rains of April. The increase in EC following heavy rains was not observed in the furthest borehole pairs, which are located tens of Km away from the Coast.

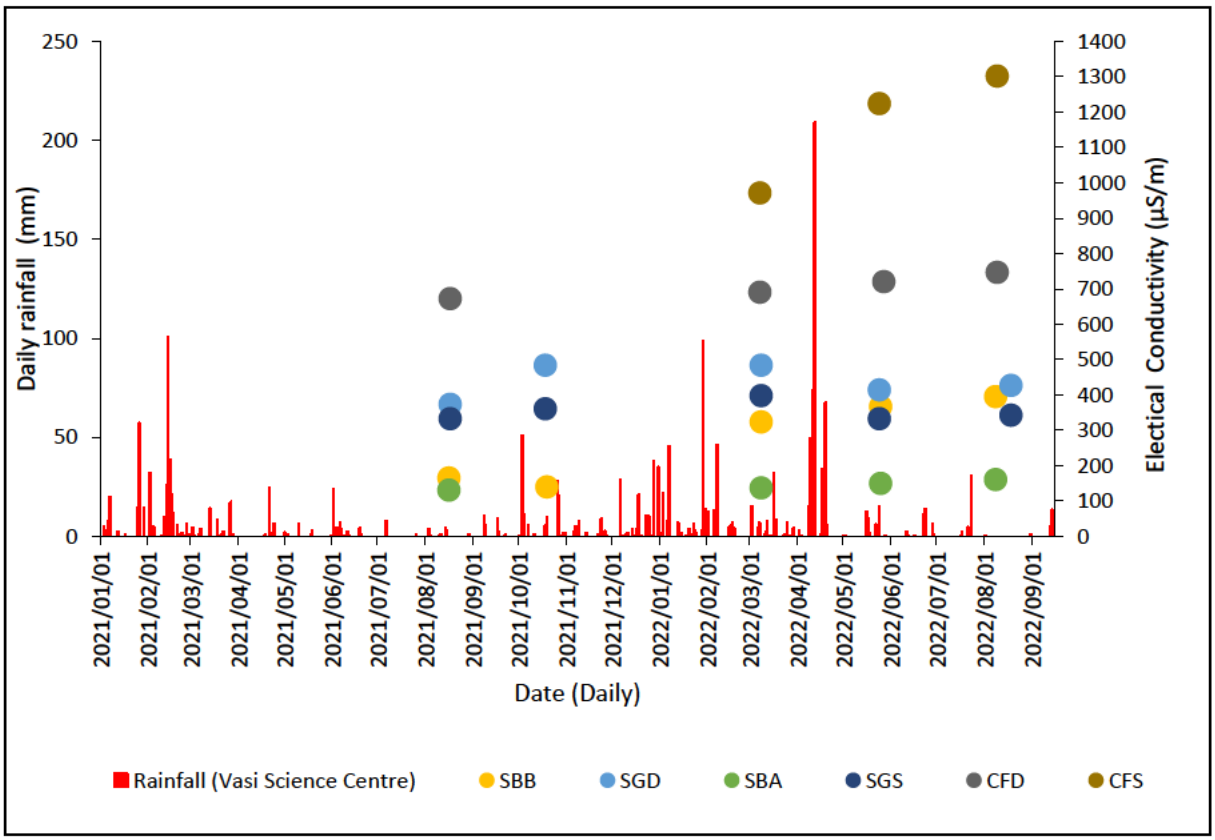

Figure 5-17 Electrical conductivity for all groundwater sampled for this study

6 DISCUSSION

This chapter presents the discussion of the results. The key findings of the research and their implication for conceptual model development and water resources management are discussed. It is to be recalled that the main objectives of the study were to first determine the groundwater recharge mechanism. Secondly to determine interconnectivity between the aquifers, thirdly to construct a conceptual groundwater flow model.

6.1 Groundwater Recharge mechanism

The amount effect showed a strong correlation of ~R= 0.75 between the rainfall amount and its $\delta^{18}O$. Comparing the rainfall amount and its $\delta^{18}O$ to the groundwater isotope signals, the minimum rainfall amount that recharges the aquifer is 30 mm/day and above. The 30 mm/day is evident in the inland boreholes. This finding supports the hypothesis that heavy rainfall contributes to aquifer replenishment. Observing the coastal dunes, however, all rainfall, large or small, would contribute to groundwater recharge (evidently in MBT BH). The isotopic signatures of CFD and CFS BH (group 1) did not indicate any recharge from rainfall. They had similar isotopic signatures to the lake, indicating that the lake water recharges them. Even though their isotopic signal could not be traced from the amount effect, it is believed that they are recharged by rainfall.

Climate change is predicted to alter rainfall patterns in various parts of the world (IPCC *et al*., 2021). Heavy rainfalls and tropical cyclones are projected to increase frequency and intensity (Ziervogel *et al*., 2014; IPCC *et al*., 2021). Examples of extreme events increasing frequency and intensity can be observed with the Cut-off lows rainfall, the cut-off lows from 1987, 2007, 2019, and the recent event of 12 April 2022. The April 2022 rainfalls had an impact on recharging the groundwater, which supports that the groundwater is recharged from exceptionally higher rainfalls.

The groundwater samples showed depletion, indicating they had undergone substantial evaporation before recharge. The plausible mechanism for the substantial evaporation before recharge could be groundwater recharge from floods and ponded water in wetlands. The wetlands cover 60% of the MPC region (SANBI, 2016). These wetlands are being converted

to farms, affecting the soil texture and increasing infiltration. Nevertheless, the destruction of wetlands in the study by farming may negatively affect the ecosystem. Concerning groundwater, coveting the wetlands to farmlands would increase recharge, substantiated with additional monitoring work.

6.2 Aquifer interconnectivity

The tracer data (stable isotopes, EC and direction) response show an interconnection between aquifers. Both shallow and deep boreholes had different heads but responded in similar patterns, this indicates that the leaky aquifer is present. All this indicates a plausible conceptual model with the aquifers separated by the leaky layers with substantial water exchange but the pressure in the boreholes may still be different. With the obtained results, a multi-layered leaky aquifer conditions may be the best representation of the aquifer system in the MPC. Then with respect of the existing number of models such as MODFLOW and conceptual models constructed for MPC which accounts for separated aquifers, must accounted for aquifers separated by leaky aquifer, two-layer aquifer.

6.3 Conceptual Modelling

All geological, hydrological, physical, hydrochemical, and environmental isotope data from the Lake Sibaya Catchment were analysed to construct a conceptual recharge and flow model for the Lake Sibaya area (Figure 6-1 and Figure 6-3). As the results isotope data revealed that in the western section and northern section of the catchment, groundwater flows to the lake where groundwater head is above the lake stage, whereas along the southern section, the present of mixing between lake and groundwater isotopic compositions indicates that the lake recharges the aquifer (Figure 6-1). Isotope data also revealed groundwater flows into the eastern section of the Lake. The depleted isotopic signatures of groundwater indicating they have undergone evaporation before recharge. This indicated the groundwater recharged from the water pool/flood water (Figure 6-2).

Isotope data, well log, electic conductivity, groundwater level data were also used to constrain the link between aquifer-to-aquifer interconnection, the result revealed they are connected (Figure 6-2).

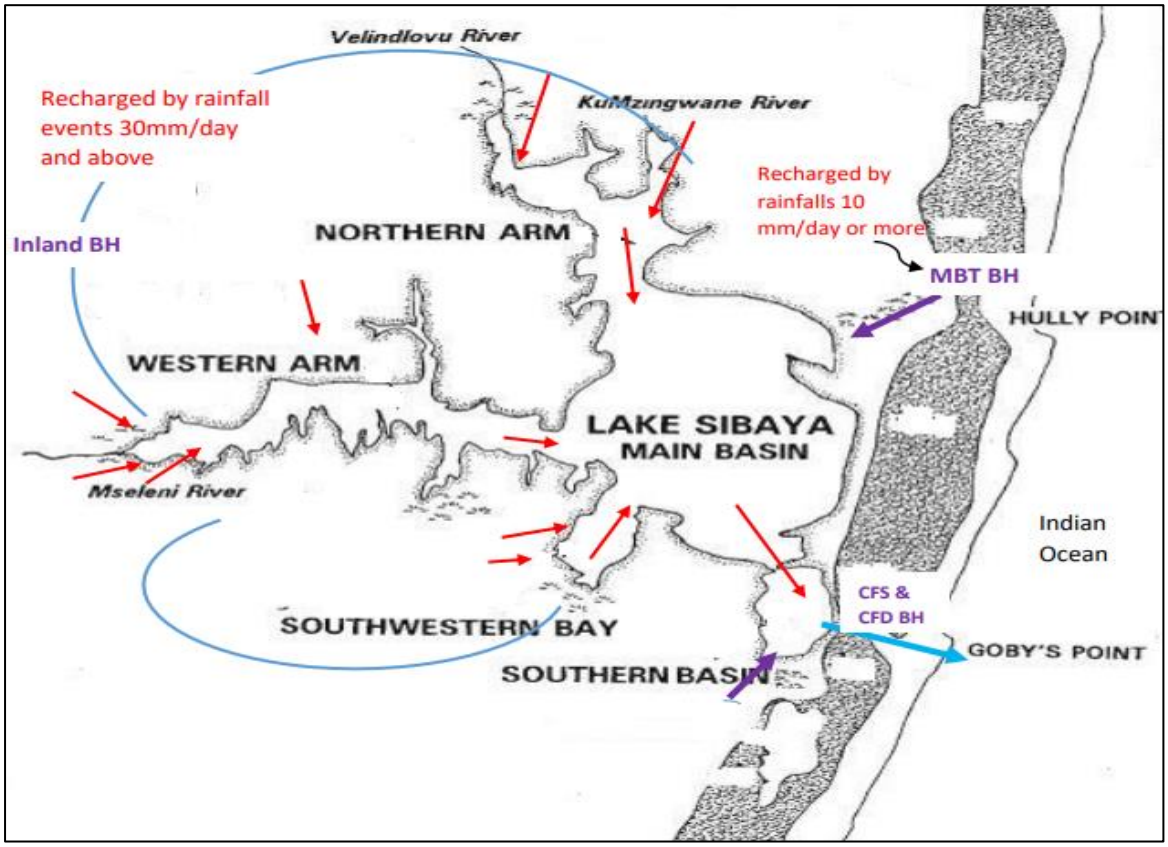

Figure 6-1 Figure showing the movement of water within the surroundings of the lake Sibaya

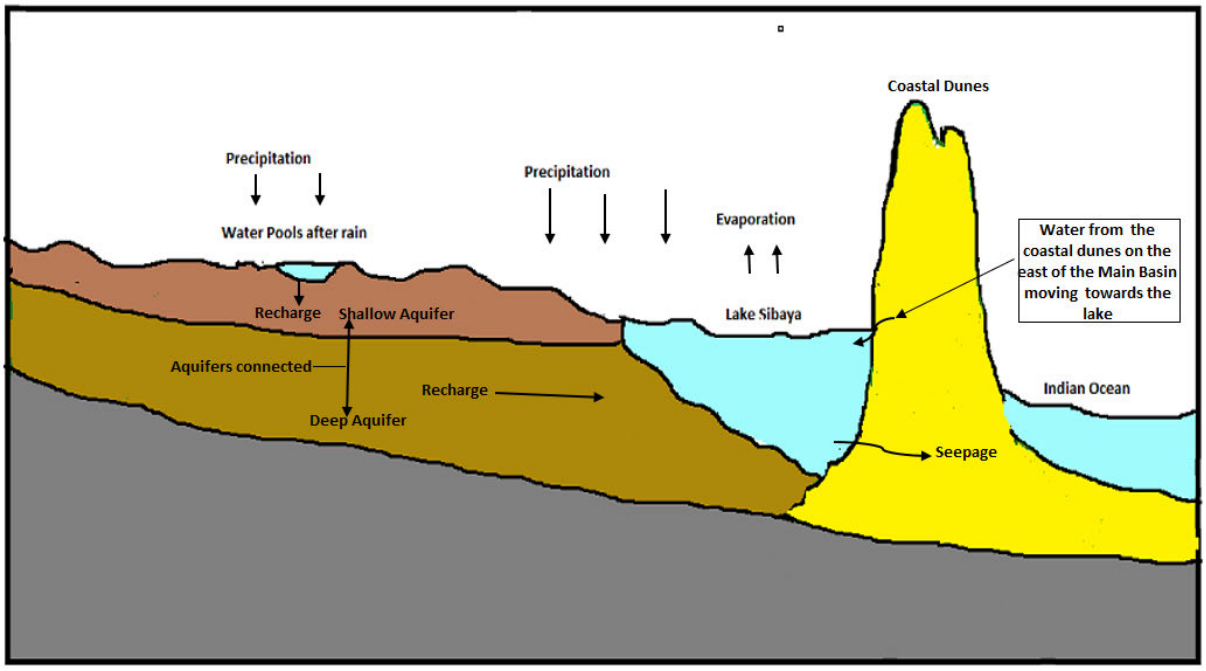

Figure 6-2 Hydrogeological Conceptual Map of Lake Sibaya Catchment.

7 CONCLUSION AND IMPLICATIONS

Environmental isotope, hydrological and hydrogeological data were integrated and interpreted to understand better the relationship between the rainfall and groundwater recharge and aquifer-aquifer interactions and develop a conceptual model within the study area. The dependence of groundwater recharge was determined in this study using isotope data through rainfall and groundwater sampling in different study area sites. The groundwater-level observations and isotopic signatures for precipitation and groundwater revealed that recharge occurs exclusively during rainy seasons and is associated with heavy rainfall events (>30 mm/day). Based on environmental isotopes, groundwater level observations, and EC data, well-log data revealed that aquifers are connected, indicating a two aquifer layer must be accounted for during modelling.

Implications for future water availability

Extreme rainfall events such as tropical storms, cyclones, cut-off lows and mesoscale convective systems (MCS) are the principal sources of groundwater recharge. The future of Lake Sibaya hydrology is tied to this regional climate. However, the local land cover will also have an impact on a feature of local importance: the land property (soil, micro topography), which allows the temporal accumulation of rainwaters in pools. Conversion of wetlands/pools to farmlands could increase groundwater recharge, similar to the observation in the Sahel region in Africa. This reveals that natural conservation goals may be different from hydrological goals. Elsewhere in Africa, there is an inference that future rainfall intensification is beneficial to groundwater recharge because of the selectiveness of recharge. The same is observed in MPC. While rainfall intensification is predicted under IPCC for most of Africa, and increased recharge can be insinuated, the prediction of water availability in the MPC largely depends on the frequency of extreme rainfall events activity. The implication for future modelling, more detailed, hydraulic testing of each aquifer layer by separating the others and generate more data is required to confirmed the connectivity between aquifers.

8. References

Aggarwal, P. K., Alduchov, O., Araguás Araguás, L., Dogramaci, S., Katzlberger, G., Kriz, K., and Purcher, A. (2007). New capabilities for studies using isotopes in the water cycle. *Eos, Transactions American Geophysical Union*, *88*(49), 537-538.

Anderson, M. P., Woessner, W. W., and Hunt, R. J. (1992). Applied groundwater modeling: Simulation of flow and adjective transport. *Academic Press Inc., San Diego, CA. Journal of Hydrology*, *140*, 393-395.

Ala-Aho, P., Soulsby, C., Pokrovsky, O. S., Kirpotin, S. N., Karlsson, J., Serikova, S., and Tetzlaff, D. (2018). Using stable isotopes to assess surface water source dynamics and hydrological connectivity in a high-latitude wetland and permafrost influenced landscape. *Journal of Hydrology*, *556*, 279-293.

Allison, G. B. (1988). A review of some of the physical, chemical and isotopic techniques available for estimating groundwater recharge. *Estimation of natural groundwater recharge*, 49-72.

Baalousha, H. (2009). Fundamentals of groundwater modelling. *Groundwater: Modelling, Management and Contamination; Konig, LF, Weiss, JL, Eds*, 149-166.

Bagheri, R., Bagheri, F., Karami, G. H., and Jafari, H. (2019). Chemo-isotopes (^{18}O & ^{2}H) signatures and HYSPLIT model application: clues to the atmospheric moisture and air mass origins. *Atmospheric Environment*, *215*, 116892.

Beekman, H. E., and Xu, Y. (2003). Review of groundwater recharge estimation in arid and semi-arid Southern Africa. *Council for Scientific and Industrial Research (South Africa) and University of the Western Cape Report*.

Betancur, T. (2012). Conceptual models in hydrogeology, methodology and results. In *Hydrogeology-A global perspective*. IntechOpen.

Blamey, R. C., and Reason, C. J. C. (2009). Numerical simulation of a mesoscale convective system over the east coast of South Africa. *Tellus A: Dynamic Meteorology and Oceanography*, *61*(1), 17-34.

Blamey, R. C., and Reason, C. J. C. (2013). The role of mesoscale convective complexes in southern Africa summer rainfall. *Journal of climate*, *26*(5), 1654-1668.

Blasch, K. W., and Bryson, J. R. (2007). Distinguishing sources of ground water recharge by using δ^2H and $\delta^{18}O$. *Groundwater*, *45*(3), 294-308.

Boerner, A., and Weaver, C. (2012). Nebraska recharge estimation from chloride mass balance.

Boas, T.,and Mallants, D. (2022). Episodic extreme rainfall events drive groundwater recharge in arid zone environments of central Australia. *Journal of Hydrology: Regional Studies*, *40*, 101005.

Botha, G. A. (1997). The Maputaland Group: a provisional lithostratigraphy for coastal KwaZulu-Natal. In *Maputaland focus on the Quaternary evolution of the southeast African coastal plain. International Union for Quaternary Research Workshop Abstracts, Council for Geoscience, Private Bag X* (Vol. 112).

Botha, G. (2015). The Maputaland Corridor: A Coastal Geomorphological Treasure. In *Landscapes and Landforms of South Africa* (pp. 121-128). Springer, Cham.

Botha G, Haldorsen S, and Porat N (2013) Geological history. In: Perissinotto R, Stretch DD, Taylor RH (eds) Ecology and conservation of estuarine ecosystems: Lake St Lucia as a global model. Cambridge University Press, Cambridge, UK

Bopape, M. J. M., Sebego, E., Ndarana, T., Maseko, B., Netshilema, M., Gijben, M., and Mkhwanazi, M. (2021). Evaluating South African weather service information on idai tropical cyclone and KwaZulu-natal flood events. *South African Journal of Science*, *117*(3-4), 1-13.

Bopape, M. J. M., Cardoso, H., Plant, R. S., Phaduli, E., Chikoore, H., Ndarana, T., and Rakate, E. (2021). Sensitivity of Tropical Cyclone Idai simulations to cumulus parametrization schemes. *Atmosphere*, *12*(8), 932.

Carnie, T. (2020). The slow death of Lake Sibaya. *Water Wheel*, *19*(2), 22-27.

Chand, S. S., Walsh, K. J., Camargo, S. J., Kossin, J. P., Tory, K. J., Wehner, M. F., and Murakami, H. (2022). Declining tropical cyclone frequency under global warming. *Nature Climate Change*, *12*(7), 655-661.

Cherry, M., Gilmore, T., Mittelstet, A., Gastmans, D., Santos, V., and Gates, J. B. (2020). Recharge seasonality based on stable isotopes: Nongrowing season bias altered by irrigation in Nebraska. *Hydrological Processes, 34*(7), 1575-1586.

Clark, I. D., and Fritz, P. (1997). *Environmental isotopes in hydrogeology*. CRC press.

Craig, H. (1961). Isotopic variations in meteoric waters. *Science, 133*(3465), 1702-1703.

Cuthbert, M. O., Taylor, R. G., Favreau, G., Todd, M. C., Shamsudduha, M., Villholth, K. G.,and Kukuric, N. (2019). Observed controls on resilience of groundwater to climate variability in sub-Saharan Africa. *Nature, 572*(7768), 230-234.

Dimova, N. T., Burnett, W. C., Chanton, J. P., and Corbett, J. E. (2013). Application of radon-222 to investigate groundwater discharge into small shallow lakes. *Journal of Hydrology, 486*,112-122.

Dingle, R. V., Siesser, W. G., and Newton, A. R. (1983). *Mesozoic and Tertiary geology of southern Africa* (p. 375). Rotterdam: AA Balkema.

Döll, P., and Fiedler, K. (2008). Global-scale modeling of groundwater recharge. *Hydrology and Earth System Sciences, 12*(3), 863-885.

Dores, D., Glenn, C. R., Torri, G., Whittier, R. B. and Popp, B. N. (2020). Implications for groundwater recharge from stable isotopic composition of precipitation in Hawai'I during the 2017–2018 La Niña. *Hydrological Processes, 34*(24), 4675-4696.

Dube, K., Nhamo, G., and Chikodzi, D. (2022). Flooding trends and their impacts on coastal communities of Western Cape Province, South Africa. *GeoJournal, 87*(Suppl 4), 453-468.

Favre, A., Hewitson, B., Tadross, M., Lennard, C., and Cerezo-Mota, R. (2012).Relationships between cut-off lows and the semiannual and southern oscillations. *Climate dynamics, 38*, 1473-1487.

Fetter, C. W., 2001, Applied Hydrogeology, Fourth Edition, Upper Saddle River, New Jersey, 598p.

Gibson, J. J., Fekete, B. M.,and Bowen, G. J. (2010). Stable isotopes in large-scale hydrological applications. *Isoscapes: Understanding movement, pattern, and process on Earth through isotope mapping*, 389-405.

Fitchett, J. M., and Grab, S. W. (2014). A 66-year tropical cyclone record for south-east Africa: temporal trends in a global context. *International Journal of Climatology*, *34*(13), 3604-3615.

Freeze, R. Allan and John Cherry (1979): Groundwater; Prentice-Hall.

Galle, S., Grippa, M., Peugeot, C., Moussa, I. B., Cappelaere, B., Demarty, J., and Wilcox, C. (2018). AMMA-CATCH, a critical zone observatory in West Africa monitoring a region in transition. *Vadose Zone Journal*, *17*(1), 1-24.

Gat, J. R. (2010). *Isotope hydrology: a study of the water cycle* (Vol. 6). World scientific.

Garstang, M., Kelbe, B. E., Emmitt, G. D., and London, W. B. (1987). Generation of convective storms over the escarpment of northeastern South Africa. *Monthly weather review*, *115*(2), 429-443.

Grab, S. W., and Nash, D. J. (2023). A new flood chronology for KwaZulu-Natal (1836–2022): the April 2022 Durban floods in historical context. *South African Geographical Journal*, 1-22.

Grundling, A.T., Van den Berg, E.C. and. Price, J.S. (2013) Assessing the distribution of wetlands over wet and dry periods and land-use change on the MPC, north-eastern KwaZulu-Natal, South Africa. South African Journal of Geomatics 2:120–138.

Grundling, A. T., Van den Berg, E. C., and Pretorius, M. L. (2014). *Influence of Regional Environmental Factors on the Distribution, Characteristics and Functioning of Hydrogeomorphic Wetland Types on the MPC, KwaZulu-Natal, South Africa: Report to the Water Research Commission*. Water Research Commission.

Hart, L. A., Bowker, M. B., Tarboton, W., & Downs, C. T. (2014). Species composition, distribution and habitat types of Odonata in the iSimangaliso Wetland Park, KwaZulu-Natal, South Africa and the associated conservation implications. *PLoS One*, *9*(3), e92588.

Harrington, G. A., Gardner, W. P., and Munday, T. J. (2014). Tracking groundwater discharge to a large river using tracers and geophysics. *Groundwater*, *52*(6), 837-852.

He, B. J., Zhao, D., Dong, X., Xiong, K., Feng, C., Qi, Q., and Pathak, M. (2022). Perception, physiological and psychological impacts, adaptive awareness and knowledge, and climate justice under urban heat: A study in extremely hot-humid Chongqing, China. *Sustainable Cities and Society*, *79*, 103685

He X, Li P, Wu J, Wei M, Ren X, Wang D (2020) Poor groundwater quality and high potential health risks in the Datong Basin, northern China: research from published data. Environ Geochem Health.

Healy, R.W. (2010) *Estimating Groundwater Recharge*. First Edition. Cambridge University Press. ISBN: 978-0521863964

Hill, B. J. (1979). Bathymetry, morphometry and hydrology of Lake Sibaya. *Lake Sibaya. Monographiae Biologicae*, *36*, 34-41.

Hill, B. J. (1969). The bathymetry and possible origin of Lakes Sibaya, Nhlange and Sifungwe in Zululand (Natal). *Transactions of the Royal Society of South Africa*, *38*(3), 205-216.

Hobday, DK* and Orme, A. (1974). The Port Durnford Formation: a major Pleistocen barrier-lagoon complex along the Zululand coast. South African Journal of Geology, 77(2), 141-149. IAEA/WMO (2023).

Hiscock, K. M. (2005). Hydrogeology, principles and practice, Kevin M. Hiscock.

Hunt, R. J., Coplen, T. B., Haas, N. L., Saad, D. A., and Borchardt, M. A. (2005). Investigating surface water–well interaction using stable isotope ratios of water. *Journal of Hydrology*, *302*(1-4), 154-172.

IPCC, 2021: Summary for Policymakers [H.-O. Pörtner, D.C. Roberts, E.S. Poloczanska, K. Mintenbeck, M. Tignor, A. Alegría, M. Craig, S. Langsdorf, S. Löschke, V. Möller, A. Okem (eds.)]. In: Climate Change 2021: Impacts, Adaptation, and Vulnerability. Contribution of Working Group II to the Sixth Assessment Report of the Intergovernmental Panel on Climate Change [H.-O. Pörtner, D.C. Roberts, M. Tignor, E.S. Poloczanska, K. Mintenbeck, A. Alegría, M. Craig, S. Langsdorf, S. Löschke, V. Möller, A. Okem, B. Rama (eds.)]. Cambridge University Press. In Press.

Global Network of Isotopes in Precipitation. The GNIP Database. Accessible at: https://nucleus.iaea.org/wiser

Jana, S., Rajagopalan, B., Alexander, M. A., and Ray, A. J. (2018). Understanding the dominant sources and tracks of moisture for summer rainfall in the southwest United States. *Journal of Geophysical Research: Atmospheres*, *123*(10), 4850-4870.

Janse van Rensburg, SJ. 2019b. Where Has All the Water Gone? Science Matters. Vol. 2 Issue 2. National Research Foundation, Pretoria, South Africa.

Jasechko, S., Birks, S. J., Gleeson, T., Wada, Y., Fawcett, P. J., Sharp, Z. D., and Welker, J. M.(2014). The pronounced seasonality of global groundwater recharge. *Water Resources Research*, *50*(11), 8845-8867.

Kelbe, Bruce, and Talita Germishuyse. "Groundwater/surface water relationships with specific reference to Maputaland." *Water Research Commission Report* 1168/1 (2010): 10.

Kelbe, B., and Taylor, R. (2011). Analyses of the hydrological linkage between Mfolozi/Msunduzi estuary and lake St Lucia. *A review of studies on the Mfolozi Estuary and associated floodplain, with emphasis on information required by management for future reconnection of the river to the St Lucia system. WRC report no. KV*, *255*(10).

Kelbe, B. E., Grundling, A. T., and Price, J. S. (2016). Modelling water-table depth in a primary aquifer to identify potential wetland hydrogeomorphic settings on the northern MPC, KwaZulu-Natal, South Africa. *Hydrogeology journal*, *24*(1), 249-265.

Kelbe, B. E., Taylor, R. H., Haldorsen, S., Perissinotto, R., and Stretch, D. D. (2013). Groundwater hydrology. *Ecology and Conservation of Estuarine Ecosystems: Lake St Lucia as a Global Model. Cambridge University Press, Cambridge*, 151-167.

Kendall, C., and McDonnell, J. J. (Eds.). (2012). *Isotope tracers in catchment hydrology*. Elsevier.

Kiptum, C. K., Mbakaa, P., and Mwangi, J. K. (2017). Application of groundwater vistas in modelling groundwater flow in Keiyo Highlands. *Africa Environmental Review Journal*, *2*(2), 33-45.

Kock, A., Taylor, J. C., and Malherbe, W. (2019). Diatom community structure and relationship with water quality in Lake Sibaya, KwaZulu-Natal, South Africa. *South African Journal of Botany*, *123*, 161-169.

Kotchoni, D. V., Vouillamoz, J. M., Lawson, F. M., Adjomayi, P., Boukari, M., and Taylor, R. G. (2019). Relationships between rainfall and groundwater recharge in seasonally humid Benin: a comparative analysis of long-term hydrographs in sedimentary and crystalline aquifers. *Hydrogeology Journal*, *27*(2), 447-457.

Kruger, G. P.,and Meyer, R. (1988). A sedimentological model for the northern Zululand coastal plain. In *Ext. abstr. 22nd Earth Sci. Congress, Geol. Soc. S. Africa* (pp. 423-426).

Kruseman, G. P., De Ridder, N. A., & Verweij, J. M. (1970). *Analysis and evaluation of pumping test data* (Vol. 11, p. 200). Wageningen, The Netherlands: International institute for land reclamation and improvement.

Kulsawat, W., and Nochit, P. (2019, November). Stable isotopes relationship between precipitation and surface water, Phitsanulok. In *Journal of Physics: Conference Series* (Vol. 1380, No. 1, p. 012162). IOP Publishing.

Laurance, W. F. (2004). Forest-climate interactions in fragmented tropical landscapes. *Philosophical Transactions of the Royal Society of London. Series B: Biological Sciences*, *359*(1443), 345-352.

Leblanc, M. J., Favreau, G., Massuel, S., Tweed, S. O., Loireau, M., and Cappelaere, B. (2008). Land clearance and hydrological change in the Sahel: SW Niger. *Global and Planetary Change*, *61*(3-4), 135-150.

Leketa, K. C. (2011). *Flow characteristics of groundwater systems: An investigation of hydraulic parameters* (Doctoral dissertation, University of the Free State).

Le Maitre, D. C., Seyler, H., Holland, M., Smith-Adao, L., Nel, J. L., Maherry, A., and Witthüser, K. (2018). *Identification, Delineation and Importance of the Strategic Water Source Areas of South Africa, Lesotho and Swaziland for Surface Water and Groundwater. Report No* (p. 4). TT 743/1/18, Water Research Commission, Pretoria.

Lemma, B., Kebede Gurmessa, S., Nemomissa, S., Otte, I., Glaser, B., and Zech, M. (2020). Spatial and temporal 2H and 18O isotope variation of contemporary precipitation in the Bale Mountains, Ethiopia. *Isotopes in environmental and health studies*, *56*(2), 122-135.Li, P., He, X., and Guo, W. (2019). Spatial groundwater quality and potential health risks due to nitrate ingestion through drinking water: a case study in Yan'an City on the Loess Plateau of northwest China. *Human and ecological risk assessment: an international journal*, *25*(1-2), 11-31.

Li, J., Pang, Z., Kong, Y., Wang, S., Bai, G., Zhao, H., and Yang, Z. (2018). Groundwater isotopes biased toward heavy rainfall events and implications on the local meteoric water line. *Journal of Geophysical Research: Atmospheres*, *123*(11), 6259-6266.

Lin, L., Lin, H., and Xu, Y. (2014). Characterisation of fracture network and groundwater preferential flow path in the Table Mountain Group (TMG) sandstones, South Africa. *Water SA*, *40*(2), 263-272.

Liu, Z., Bowen, G. J., and Welker, J. M. (2010). Atmospheric circulation is reflected in precipitation isotope gradients over the conterminous United States. *Journal of Geophysical Research: Atmospheres*, *115*(D22).

MacDonald, A. M., Lark, R. M., Taylor, R. G., Abiye, T., Fallas, H. C., Favreau, G., and West, C. (2021). Mapping groundwater recharge in Africa from ground observations and implications for water security. *Environmental Research Letters*, *16*(3), 034012

Makiwane, N. (2019). Characterisation of the deep aquifers of South Africa-the Karoo Supergroup and Table Mountain Group (Doctoral dissertation, University of the Free State).

Malherbe, J., Engelbrecht, F. A., and Landman, W. A. (2013). Projected changes in tropical cyclone climatology and landfall in the Southwest Indian Ocean region under enhanced anthropogenic forcing. *Climate dynamics*, *40*, 2867-2886.

Malherbe J, Engelbrecht FA, Landman WA, and Engelbrecht CJ (2012) Tropical systems from the southwest Indian Ocean making landfall over the Limpopo River Basin, southern Africa: a historical perspective.

Manna, F., Walton, K. M., Cherry, J. A., and Parker, B. L. (2017). Mechanisms of recharge in a fractured porous rock aquifer in a semi-arid region. *Journal of Hydrology*, *555*, 869-880.

Maréchal, J. C., Dewandel, B., Ahmed, S., Galeazzi, L., & Zaidi, F. K. (2006). Combined estimation of specific yield and natural recharge in a semi-arid groundwater basin with irrigated agriculture. *Journal of Hydrology*, *329*(1-2), 281-293.

Maud, RR* and Orr, W. (1975). Aspects of post-Karroo geology in the Richards Bay area. *South African Journal of Geology*, *78*(1), 101-109.

Mawren, D., Hermes, J., and Reason, C. J. C. (2022). Marine heat waves and tropical cyclones-Two devastating types of coastal hazard in South-eastern Africa. *Estuarine, Coastal and Shelf Science*, *277*, 108056.

Merz, S. K. (2012). Australian groundwater modelling guidelines. *Waterlines report series*.

Meyer, R., Talma, A. S., Duvenhage, A. W. A., Eglington, B. M., Taljaard, J., Botha, J. P., Van der Voort, I. (2001). Geohydrological investigation and evaluation of the Zululand coastal aquifer. *Water Research Commission Report*, *221*(1), 01

Miller, W. R. (1998). The bathymetry, sedimentology and seismic stratigraphy of Lake Sibaya-Northern KwaZulu-Natal (Doctoral dissertation).

Miller, WR. 2001. The bathymetry, sedimentology and seismic stratigraphy of Lake Sibaya, Northern KwaZulu-Natal. Bulletin 131. Council for Geoscience, Pretoria, RSA.

Mohammadzadeh, H., Eskandari Mayvan, J., and Heydarizad, M. (2020). The effects of moisture sources and local parameters on the 18O and 2H contents of precipitation in the west of Iran and the east of Iraq. *Tellus B: Chemical and Physical Meteorology*, *72*(1), 1-15.

Mondal, N. C., Singh, V. S., and Rangarajan, R. (2009). Aquifer characteristics and its modeling around an industrial complex, Tuticorin, Tamil Nadu, India: a case study. *Journal of earth system science*, *118*, 231-244.

Mook, W. G. "Introduction to Isotope Hydrology, Volume 25 in the series: International Contributions to Hydrogeology." (2006).

Morake, D. M., Blamey, R. C., and Reason, C. J. C. (2021). Long-lived mesoscale convective systems over eastern South Africa. *Journal of Climate*, *34*(15), 6421-6439.

Moya, C. E., Raiber, M., Taulis, M., and Cox, M. E. (2016). Using environmental isotopes and dissolved methane concentrations to constrain hydrochemical processes and inter-aquifer mixing in the Galilee and Eromanga Basins, Great Artesian Basin, Australia. *Journal of Hydrology*, *539*, 304-318.

Mpenyana-Monyatsi, L., Onyango, M. S., and Momba, M. N. B. (2012). Groundwater quality in a South African rural community: A possible threat to public health. *Pol J Environ Stud*, *21*(5), 1349-58.

Mpungose, N., Thoithi, W., Blamey, R. C., and Reason, C. J. C. (2022). Extreme rainfall events in southeastern Africa during the summer. *Theoretical and Applied Climatology*, *150*(1-2), 185-201.

Mukherjee, S. "Hydrostratigraphy." *YES Bulletin* 1 (2011): 10-13.

Müller, T., Jurikova, H., Gutjahr, M., Tomašových, A., Schlögl, J., Liebetrau, V., and Eisenhauer, A. (2020). Ocean acidification during the early Toarcian extinction event: Evidence from boron isotopes in brachiopods. *Geology*, *48*(12), 1184-1188.

Mutoti, M. I. (2015). Estimating groundwater recharge using chloride mass balance in the upper Berg River catchment, South Africa.

New, M., Hewitson, B., Stephenson, D. B., Tsiga, A., Kruger, A., Manhique, A., and Lajoie, R. (2006). Evidence of trends in daily climate extremes over southern and West Africa. *Journal of Geophysical Research: Atmospheres*, *111*(D14).

Nicholson, S. L., Pike, A. W., Hosfield, R., Roberts, N., Sahy, D., Woodhead, J., and Fleitmann, D. (2020). Pluvial periods in Southern Arabia over the last 1.1 million-years. *Quaternary Science Reviews*, *229*, 106112.

Ntanganedzeni, B., and Nobert, J. (2021). Flood risk assessment in Luvuvhu River, Limpop province, South Africa. *Physics and Chemistry of the Earth, Parts A/B/C*, *124*, 102959.

Oxtobee, J. P., and Novakowski, K. (2002). A field investigation of groundwater/surface water interaction in a fractured bedrock environment. *Journal of Hydrology*, *269*(3-4), 169-193.

Owor, M., Taylor, R. G., Tindimugaya, C., and Mwesigwa, D. (2009). Rainfall intensity and groundwater recharge: empirical evidence from the Upper Nile Basin. *Environmental Research Letters*, *4*(3), 035009.

Pandey, S., Singh, D., Denner, S., Cox, R., Dickinson, C., Gallagher, M., and Gossmann, S. (2020). Inter-aquifer connectivity between Australia's Great Artesian Basin and the overlying Condamine Alluvium: an assessment and its implications for the basin's groundwater management. *Hydrogeology Journal*, *28*(1), 125-146.

Paces, J. B., and Wurster, F. C. (2014). Natural uranium and strontium isotope tracers of water sources and surface water–groundwater interactions in arid wetlands–Pahranagat Valley, Nevada, USA. *Journal of hydrology*, *517*, 213-225.

Ping, J., Nichol, C., and Wei, X. (2014). Quantification of groundwater recharge using the chloride mass balance method in a semi-arid mountain terrain, South Interior British Columbia, Canada. *J Chem Pharm Res*, *6*(1), 383-388.

Porat, N., and Botha, G. (2008). The luminescence chronology of dune development on the MPC, southeast Africa. *Quaternary Science Reviews*, *27*(9-10), 1024-1046.

Priestley, S. C., Wohling, D. L., Keppel, M. N., Post, V. E., Love, A. J., Shand, P., and Kipfer, R. (2017). Detecting inter-aquifer leakage in areas with limited data using hydraulics and multiple environmental tracers, including 4 He, 36 Cl/Cl, 14 C and 87 Sr/86 Sr. *Hydrogeology Journal*, *25*(7), 2031-2047.

Qian, J., Wang, L., Ma, L., Lu, Y., Zhao, W., and Zhang, Y. (2016). Multivariate statistical analysis of water chemistry in evaluating groundwater geochemical evolution and aquifer connectivity near a large coalmine, Anhui, China. *Environmental Earth Sciences*, *75*(9), 747.

Reason, C. J. C., Allan, R. J., Lindesay, J. A., and Ansell, T. J. (2000). ENSO and climatic signals across the Indian Ocean basin in the global context: Part I, Interannual

composite patterns. *International Journal of Climatology: A Journal of the Royal Meteorological Society*, *20*(11), 1285-1327.

Risi, C., Bony, S., and Vimeux, F. (2008). Influence of convective processes on the isotopic composition ($\delta^{18}O$ and δD) of precipitation and water vapor in the tropics: 2. Physical interpretation of the amount effect. *Journal of Geophysical Research: Atmospheres*, *113*(D19).

Salako, A. O., and Adepelumi, A. A. (2018). Aquifer, classification, and characterization. *Aquifers-matrix and fluids*, 11-31

South African National Landcover Datasets:

https://egis.environment.gov.za/sa_national_land_cover_datasets

Scanlon, B. R., Rateb, A., Anyamba, A., Kebede, S., MacDonald, A. M., Shamsudduha, M., and Xie, H. (2022). Linkages between GRACE water storage, hydrologic extremes, and climate teleconnections in major African aquifers. *Environmental Research Letters*, *17*(1), 014046.

Seddon, D., Kashaigili, J. J., Taylor, R. G., Cuthbert, M. O., Mwihumbo, C., and MacDonald, A. M. (2021). Focused groundwater recharge in a tropical dryland: Empirical evidence from central, semi-arid Tanzania. *Journal of Hydrology: Regional Studies*, *37*, 100919.

Simmers, I. (1998). Groundwater recharge: an overview of estimation 'problems' and recent developments. *Geological Society, London, Special Publications*, *130*(1), 107-115.

Singleton, A. T., and Reason, C. J. C. (2007). Variability in the characteristics of cut-off low-pressure systems over subtropical southern Africa. *International Journal of Climatology: A Journal of the Royal Meteorological Society*, *27*(3), 295-310.

Space, M. L., Ingraham, N. L., and Hess, J. W. (1991). The use of stable isotopes in quantifying groundwater discharge to a partially diverted creek. *Journal of Hydrology*, *129*(1-4), 175-193.

Smithers, J. C., Gray, R. P., Johnson, S., and Still, D. (2017). Modelling and water yield assessment of Lake Sibhayi. *Water SA*, *43*(3), 480-491.

Su, Z., Wu, J., He, X., and Elumalai, V. (2020). Temporal changes of groundwater quality within the groundwater depression cone and prediction of confined groundwater

salinity using Grey Markov model in Yinchuan area of northwest China. *Exposure and Health*, *12*(3), 447-468.

Taylor, R. G., Todd, M. C., Kongola, L., Maurice, L., Nahozya, E., Sanga, H., and MacDonald, A. M. (2013). Evidence of the dependence of groundwater resources on extreme rainfall in East Africa. *Nature Climate Change*, *3*(4), 374-378.

Talma, A. S., and Van Wyk, E. (2013). Rainfall and groundwater isotope atlas. *The use of isotope hydrology to characterize and assess water resources in southern Africa*, 83-110.

Terrastest, 2019. Report to PID on Lake Sibaya Monitoring Boreholes feasibility and implementation Report. Terrastest (pty) LTD. Reference: 41730.

Thomas, B. F., Behrangi, A., and Famiglietti, J. S. (2016). Precipitation intensity effects on groundwater recharge in the southwestern United States. *Water*, *8*(3), 90.

Torri, G., Ma, D., and Kuang, Z. (2017). Stable water isotopes and large-scale vertical motions in the tropics. *Journal of Geophysical Research: Atmospheres*, *122*(7), 3703-3717.

Van der Schyff, M., Kanyerere, T., Israel, S., and Vermaak, N. (2020). Using multiple tracers and geological techniques to determine the connectivity between aquifer systems, West Coast, South Africa. *Physics and Chemistry of the Earth, Parts A/B/C*, *118*, 102863.

Van Tonder, G., Riemann, K., and Dennis, I. (2002). Interpretation of single-well tracer tests using fractional-flow dimensions. Part 1: Theory and mathematical models. *Hydrogeology Journal*, *10*, 351-356.

Van Wyk, E. (2010). *Estimation of episodic groundwater recharge in semi-arid fractured hard rock aquifers* (Doctoral dissertation, University of the Free State).

Været, L., Kelbe, B., Haldorsen, S., and Taylor, R. H. (2009). A modelling study of the effects of land management and climatic variations on groundwater inflow to Lake St Lucia, South Africa. *Hydrogeology journal*, *17*(8), 1949.

Viljoen, M. F., and Booysen, H. J. (2006). Planning and management of flood damage control: the South African experience. *Irrigation and Drainage: The journal of the International Commission on Irrigation and Drainage*, *55*(S1), S83-S91.

Xu, Y., and Beekman, H. E. (2019). Groundwater recharge estimation in arid and semi-arid southern Africa. *Hydrogeology Journal*, *27*(3), 929-943.

Weaver, J., Biegalski, S., and Buchholz, B. (2009). Assessment of non-traditional isotopic ratios by mass spectrometry for analysis of nuclear activities. *Journal of radioanalytical and nuclear chemistry*, *282*(3), 709-713.

Weight, W. (2008). *Hydrogeology field manual*. McGraw-Hill Education.

Weitz, J., and Demlie, M. (2014). Conceptual modelling of groundwater–surface water interactions in the Lake Sibaya Catchment, Eastern South Africa. *Journal of African Earth Sciences*, *99*, 613-624.

Weitz, J., and Demlie, M. (2015). Hydrogeological system analyses of the Lake Sibaya Catchment, north-eastern South Africa. *South African Journal of Geology*, *118*(1), 91-107.

Weitz, JC. 2016. Hydrogeological and Three-Dimensional Numerical Groundwater Flow Modelling of the Lake Sibaya catchment, Northern KwaZulu-Natal, South Africa Unpublished PhD in Hydrogeology Dissertation. College of Agriculture, Engineering and Science. University of KwaZulu-Nata, Durban, RSA.

Whyte, SR. 1999. A geochemical investigation of the Lake Sibiya system, Northern Zululand.

Unpublished MSc in Environmental Geochemistry Dissertation. Department of Geological Sciences, University of Cape Town, Cape Town, RSA.

Worthington, P. F. (1978). Groundwater conditions in the Zululand coastal plain around Richards Bay. *CSIR Report, FIS*, *182*.

Wright, C. I., Miller, W. R., and Cooper, J. A. G. (2000). The late Cenozoic evolution of coastal water bodies in Northern KwaZulu-Natal, South Africa. *Marine Geology*, *167*(3-4), 07-229.

Wu J, Zhang Y, Zhou H (2020) Groundwater chemistry and groundwater quality index incorporating health risk weighting in Dingbian County, Ordos basin of northwest China. Geochemistry. https://doi.org/10.1016/j.chemer.2020.125607

Wu, J., Zhang, R., and Yang, J. (1996). Analysis of rainfall-recharge relationships. *Journal of Hydrology*, *177*(1-2), 143-160.

Zomlot, Z., Verbeiren, B., Huysmans, M., and Batelaan, O. (2017). Trajectory analysis of land use and land cover maps to improve spatial–temporal patterns, and impact assessment on groundwater recharge. *Journal of Hydrology*, *554*, 558-569.

APENDIX

Appendix A: Table showing isotopic data for groundwater samples collected

Date	Site Name	Source	$\delta^{18}O$ (‰)	$\delta^{2}H$ (‰)
2021/10/19	MCW	Groundwater	-4.165	-18.23
2021/10/19	TMB	Groundwater	-4.661	-23.20
2021/10/19	MNZ	Groundwater	-3.064	-10.63
2021/10/18	SGD	Groundwater	-3.505	-13.80
2021/10/22	ZEB	Groundwater	-3.182	-12.26
2021/10/19	SBB	Groundwater	-3.632	-14.12
2021/10/22	PHZ	Groundwater	-4.306	-19.74
2021/10/22	JIK	Groundwater	-3.682	-13.79
2021/10/22	LUN	Groundwater	-3.908	-17.26
2021/10/19	NJI	Groundwater	-3.553	-15.18
2021/10/21	VRB	Groundwater	-4.186	-19.13
2021/10/19	MBW	Groundwater	-4.104	-19.43
2021/10/18	SGS	Groundwater	-3.672	-14.570
2022/03/07	SGS01	Groundwater	-3.843	-14.09
2022/03/09	SIB01	Groundwater	-4.046	-20.25
2022/03/10	NJI01	Groundwater	-3.484	-16.54
2022/03/08	SBB01	Groundwater	-3.376	-13.49
2022/03/07	SGD01	Groundwater	-3.188	-12.87
2022/03/08	SBA01	Groundwater	-3.283	-11.39
2022/03/11	ZEB01	Groundwater	-3.002	-11.33
2022/03/08	MBW01	Groundwater	-4.081	-19.62
2022/03/11	LUN01	Groundwater	-3.830	-19.19
2022/03/10	PHZ01	Groundwater	-3.855	-19.25
2022/03/08	MCW01	Groundwater	-3.968	-19.18
2022/03/08	MNZ01	Groundwater	-3.050	-10.47
2022/08/09	SGD01	Groundwater	-3.813	-14.20
2022/08/09	SGS01	Groundwater	-3.962	-15.53
2022/08/11	BKH01	Groundwater	-3.628	-11.53
2022/08/08	SBA01	Groundwater	-4.037	-12.89
2022/08/08	SBB01	Groundwater	-4.461	-16.45
2022/08/11	SIB01	Groundwater	-5.267	-22.34
2022/08/11	ZEB01	Groundwater	-4.243	-15.03
2022/08/10	MBW01	Groundwater	-4.965	-22.07
2022/08/10	NJI01	Groundwater	-4.481	-18.89
2022/08/10	PHZ01	Groundwater	-4.609	-19.56
2022/08/10	VRB01	Groundwater	-4.813	-20.51
2022/08/07	TMB01	Groundwater	-5.243	-25.04
2022/08/10	MTH01	Groundwater	-4.635	-19.65
2022/08/11	MNZ01	Groundwater	-3.712	-11.89

2022/08/08	MCW01	Groundwater	-4.793	-19.40
2022/05/26	SIB	Groundwater	-4.846	-21.54
2022/05/23	NJI	Groundwater	-4.350	-17.82
2022/05/23	SGS	Groundwater	-4.128	-16.19
2022/05/23	MTH	Groundwater	-4.644	-20.44
2022/05/25	MNZ	Groundwater	-3.757	-12.68
2022/05/23	SGD	Groundwater	-3.990	-14.25
2022/05/25	VRB	Groundwater	-4.582	-19.76
2022/05/23	ZEB	Groundwater	-3.695	-13.15
2022/05/26	BKH	Groundwater	-3.803	-13.67
2022/05/23	TMB	Groundwater	-5.199	-24.20
2022/05/25	SBA	Groundwater	-4.076	-12.92
2022/05/25	MCW	Groundwater	-4.528	-18.28
2022/05/25	SBB	Groundwater	-3.955	-14.56
2022/05/23	MBW	Groundwater	-4.698	-20.90
2021/08/20	SGD03	Groundwater	-3.558	-14.60
2021/08/17	SGS03	Groundwater	-3.651	-15.46
2021/08/16	MNZ03	Groundwater	-3.725	-10.92
2021/08/16	MCW02	Groundwater	-4.604	-18.86
2021/09/17	MTH02	Groundwater	-4.935	-21.25
2021/09/14	BKH02	Groundwater	-3.734	-10.05
2021/08/20	SIBO2	Groundwater	-4.595	-17.32
2022/05/25	MNZ02	Groundwater	-3.173	-10.95
2022/03/07	CFS01	Groundwater	2.176	18.11
2022/03/07	CFD01	Groundwater	2.153	18.24
2021/10/23	CFD(33m)	Groundwater	2.629	20.62
2021/10/23	CFS(34m)	Groundwater	2.369	19.52
2022/08/09	CFS01	Groundwater	1.312	16.63
2022/08/10	CFD01	Groundwater	1.268	16.74
2022/05/27	CFD	Groundwater	1.286	16.59
2022/05/25	CFS	Groundwater	1.222	16.63
2022/08/10	MBT01	Groundwater	-2.751	-7.47
2021/09/15	MBT02	Groundwater	-2.534	-6.53
	MBT	Groundwater	-2.292	-5.61
2021/10/26	MBT	Groundwater	-1.898	-4.68
2022/03/11	MBT01	Groundwater	-1.92	-5.78

Appendix B: Table showing EC spreadsheet.

Date	Sampling Points	Water resource	EC(µS/m)
2021-08-16	Old Mac(MCW)	Groundwater	150

2021-10-19	Old Mac(MCW)	Groundwater	153
2022-03-08	Old Mac(MCW)	Groundwater	142
2022-05-25	Old Mac(MCW)	Groundwater	164
2022-08-08	Old Mac(MCW)	Groundwater	161
2021-08-16	SBB	Groundwater	166
2021-10-19	SBB	Groundwater	146
2022-05-25	SBB	Groundwater	368
2022-08-08	SBB	Groundwater	396
2021-08-16	SIBO1A	Groundwater	132
2022-03-08	SIBO1A	Groundwater	138
2022-05-25	SIBO1A	Groundwater	151
2022-08-08	SIBO1A	Groundwater	162
2021-08-17	SGD	Groundwater	374
2021-10-18	SGD	Groundwater	485
2022-03-08	SGD	Groundwater	485
2022-05-24	SGD	Groundwater	415
2022-08-18	SGD	Groundwater	428
2022-05-24	Cfshallow	Groundwater	1225
2022-08-09	Cfshallow	Groundwater	1303
2022-03-07	Cfshallow	Groundwater	972
2022-03-07	CFDeep	Groundwater	691
2022-05-27	CFDeep	Groundwater	721
2021-10-23	CFDeep	Groundwater	815
2022-08-09	CFDeep	Groundwater	748
2021-08-17	CFDeep	Groundwater	673
2021-08-17	SGShallow	Groundwater	334
2021-10-18	SGShallow	Groundwater	362
2022-03-08	SGShallow	Groundwater	399
2022-05-24	SGShallow	Groundwater	316
2022-08-18	SGShallow	Groundwater	344
2021-09-13	TMB	Groundwater	250
2021-10-20	TMB	Groundwater	142
2022-08-08	TMB	Groundwater	172
2022-03-08	TMB	Groundwater	216
2022-05-23	TMB	Groundwater	159
2022-03-09	Sileza	Groundwater	120
2022-05-26	Sileza	Groundwater	140
2022-08-11	Sileza	Groundwater	140
2021-09-14	Sileza	Groundwater	123
2022-03-09	BKH	Groundwater	142
2022-05-26	BKH	Groundwater	186
2022-08-10	BKH	Groundwater	169
2022-03-09	BKH	Groundwater	251
2022-05-26	BKH	Groundwater	186
2022-03-11	MBT	Groundwater	313
2021-09-16	MBT	Groundwater	302
2021-10-26	MBT	Groundwater	302
2022-05-27	MBT	Groundwater	343

2022-08-10	MBT	Groundwater	310
2022-08-10	ZEB	Groundwater	242
2021-10-21	ZEB	Groundwater	152
2021-10-21	NJI	Groundwater	142
2022-05-23	NJI	Groundwater	141
2022-08-10	NJI	Groundwater	153
2022-03-10	NJI	Groundwater	161
2021-09-16	MBW	Groundwater	470
2021-10-21	MBW	Groundwater	491
2022-08-10	MBW	Groundwater	526
2022-05-23	MBW	Groundwater	506
2021-10-21	PHZ	Groundwater	740
2022-08-10	PHZ	Groundwater	512
2021-10-21	LUN	Groundwater	236
2022-08-10	LUN	Groundwater	226
2022-05-23	LUN	Groundwater	230
2022-05-23	EZB	Groundwater	123
2021-09-16	VRB	Groundwater	235
2022-08-10	VRB	Groundwater	284
2021-10-21	VRB	Groundwater	237
2021-08-20	VRB	Groundwater	234
2022-05-25	VRB	Groundwater	259
2021-10-21	MNZ	Groundwater	308
2022-05-25	MNZ	Groundwater	406
2021-08-20	SIB02	Groundwater	380
2021-09-16	MTH	Groundwater	416
2022-05-23	MTH	Groundwater	469
2022-08-10	MTH	Groundwater	454

Appendix C: Table showing $\delta^{18}O$ and $\delta^{2}H$ (‰) for the nested boreholes

Deep				Shallow			Difference (δ18O)	Difference (δ2H)
Date	Code	$\delta^{18}O$ (‰)	$\delta^{2}H$ (‰)	Code	$\delta^{18}O$ (‰)	$\delta^{2}H$ (‰)		
2021/10/23	CFD	2.629	20.62	CFS	2.369	19.52	-0.26	-1.1
2022/03/07	CFD	2.153	18.24	CFS	2.176	18.11	0.023	-0.13
2022/05/25	CFD	1.286	16.59	CFS	1.222	16.63	-0.064	0.04
2022/08/09	CFD	1.268	16.74	CFS	1.312	16.63	0.044	-0.11
2021/09/17	SGD	-3.558	-14.6	SGS	-3.651	-15.46	-0.093	-0.86
2021/10/18	SGD	-3.505	-13.8	SGS	-3.672	-14.57	-0.167	-0.77
2022/03/07	SGD	-3.188	-12.87	SGS	-3.843	-14.09	-0.655	-1.22
2022/05/23	SGD	-3.99	-14.25	SGS	-4.128	-16.19	-0.138	-1.94
2022/08/09	SGD	-3.813	-14.2	SGS	-3.962	-15.53	-0.149	-1.33
2021/10/19	SBB	-3.632	-14.12	SBA	-	-	3.632	14.12
2022/03/08	SBB	-3.376	-13.49	SBA	-3.283	-11.39	0.093	2.1
2022/05/25	SBB	-3.955	-14.56	SBA	-4.076	-12.92	-0.121	1.64
2022/08/09	SBB	-4.461	-16.45	SBA	-4.037	-12.89	0.424	3.56

Appendix D: Table showing isotopic composition of rainfall samples collected

Date	Rain_mm_Tot	δ18O (‰)
2021/06/18	3	-2.934
2021/10/18	5.588	-1.079
2021/10/26	27.94	0.398
2021/10/30	1.778	-1.577
2021/11/21	0.762	-0.422
2021/11/23	8.38	-1.674
2021/11/24	51.05	-3.273
2021/12/14	3.556	-2.460
2021/12/17	3.81	-2.441
2021/12/25	10.16	-0.558
2021/12/27	0.254	-2.842
2021/12/31	35.05	-3.127
2022/01/03	21.59	-1.931
2022/01/06	7.874	-2.136
2022/01/22	0.254	-1.142
2022/02/18	4.064	-1.288
2022/03/02	15.49	-2.128
2022/03/02	15.49	-1.161
2022/03/16	32.26	-3.824
2022/03/18	8.38	-3.706
2022/03/26	0.51	-2.018
2022/04/08	15.24	-2.125
2022/04/09	49.28	-4.445
2022/04/10	9.14	-2.596
2022/04/11	74.17	-6.125
2022/04/12	209	-6.540
2022/04/17	34.04	-2.745
2022/04/18	67.56	-9.559
2022/04/19	67.56	-6.539
2022/04/25	60	-4.769
2022/05/22	6.096	-3.978
2022/05/24	15.24	-6.097

Appendix E: Table showing groundwater level data

Date_(Daily)	CF01A	CF01B	Date (Daily)	SGS	SGD
2021/11/13	4.6463	5.1331	2021/01/01	9.4396	9.3416
2021/11/14	4.6490	5.1341	2021/01/02	9.4565	9.3582
2021/11/15	4.6545	5.1375	2021/01/03	9.4641	9.3645
2021/11/16	4.6518	5.1337	2021/01/04	9.4594	9.3607
2021/11/17	4.6436	5.1280	2021/01/05	9.4534	9.3550

2021/11/18	4.6350	5.1175	2021/01/06	9.4512	9.3512
2021/11/19	4.6402	5.1273	2021/01/07	9.4589	9.3647
2021/11/20	4.6427	5.1300	2021/01/08	9.4559	9.3667
2021/11/21	4.6432	5.1314	2021/01/09	9.4496	9.3629
2021/11/22	4.6384	5.1273	2021/01/10	9.4458	9.3604
2021/11/23	4.6374	5.1261	2021/01/11	9.4421	9.3583
2021/11/24	4.6322	5.1222	2021/01/12	9.4405	9.3564
2021/11/25	4.6323	5.1223	2021/01/13	9.4425	9.3584
2021/11/26	4.6331	5.1218	2021/01/14	9.4471	9.3654
2021/11/27	4.6404	5.1259	2021/01/15	9.4432	9.3608
2021/11/28	4.6396	5.1218	2021/01/16	9.4362	9.3520
2021/11/29	4.6271	5.1071	2021/01/17	9.4425	9.3548
2021/11/30	4.6317	5.1108	2021/01/18	9.4495	9.3595
2021/12/01	4.6301	5.1093	2021/01/19	9.4461	9.3556
2021/12/02	4.6243	5.1012	2021/01/20	9.4423	9.3519
2021/12/03	4.6220	5.1021	2021/01/21	9.4456	9.3546
2021/12/04	4.6246	5.1055	2021/01/22	9.4405	9.3505
2021/12/05	4.6179	5.1017	2021/01/23	9.4384	9.3480
2021/12/06	4.6139	5.0996	2021/01/24	9.4289	9.3415
2021/12/07	4.6033	5.0925	2021/01/25	9.4551	9.3767
2021/12/08	4.6076	5.0957	2021/01/26	9.5354	9.4338
2021/12/09	4.6051	5.0924	2021/01/27	9.5554	9.4477
2021/12/10	4.6010	5.0874	2021/01/28	9.5709	9.4587
2021/12/11	4.6031	5.0876	2021/01/30	9.5932	9.4789
2021/12/12	4.6014	5.0840	2021/01/31	9.5992	9.4850
2021/12/13	4.6018	5.0840	2021/02/01	9.5965	9.4851
2021/12/14	4.6084	5.0880	2021/02/02	9.6229	9.5116
2021/12/15	4.6075	5.0874	2021/02/03	9.6305	9.5213
2021/12/16	4.6044	5.0982	2021/02/04	9.6298	9.5225
2021/12/17	4.6182	5.1168	2021/02/05	9.6275	9.5208
2021/12/18	4.6330	5.1309	2021/02/06	9.6278	9.5222
2021/12/19	4.6304	5.1269	2021/02/07	9.6287	9.5242
2021/12/20	4.6217	5.1205	2021/02/08	9.6324	9.5284
2021/12/21	4.6115	5.1115	2021/02/09	9.6348	9.5345
2021/12/22	4.6105	5.1094	2021/02/10	9.6369	9.5323
2021/12/23	4.5943	5.0953	2021/02/11	9.6350	9.5300
2021/12/24	4.5973	5.0985	2021/02/12	9.6393	9.5260
2021/12/25	4.6032	5.1038	2021/02/13	9.6447	9.5322
2021/12/26	4.5984	5.0975	2021/02/14	9.6493	9.5367
2021/12/27	4.5980	5.0942	2021/02/15	9.6553	9.5466
2021/12/28	4.6100	5.1009	2021/02/16	9.6599	9.5550
2021/12/29	4.6009	5.0943	2021/02/17	9.6776	9.5736

2021/12/30	4.6064	5.0964	2021/02/18	9.6783	9.5757
2021/12/31	4.6194	5.1039	2021/02/19	9.6733	9.5715
2022/01/01	4.6267	5.1142	2021/02/20	9.6867	9.5858
2022/01/02	4.6153	5.1036	2021/02/21	9.6822	9.5796
2022/01/03	4.6249	5.1143	2021/02/22	9.6913	9.5889
2022/01/04	4.6163	5.1080	2021/02/23	9.7056	9.6037
2022/01/05	4.6157	5.1107	2021/02/24	9.7102	9.6071
2022/01/06	4.6088	5.1050	2021/02/25	9.7196	9.6158
2022/01/07	4.6224	5.1159	2021/02/26	9.7332	9.6291
2022/01/08	4.6218	5.1153	2021/02/27	9.7456	9.6396
2022/01/09	4.6303	5.1203	2021/02/28	9.7508	9.6422
2022/01/10	4.6391	5.1267	2021/03/01	9.7642	9.6516
2022/01/11	4.6373	5.1239	2021/03/02	9.7676	9.6527
2022/01/12	4.6371	5.1233	2021/03/03	9.7679	9.6495
2022/01/13	4.6531	5.1374	2021/03/04	9.7706	9.6505
2022/01/14	4.6527	5.1375	2021/03/05	9.7742	9.6531
2022/01/15	4.6597	5.1442	2021/03/06	9.7754	9.6540
2022/01/16	4.6601	5.1459	2021/03/07	9.7784	9.6564
2022/01/17	4.6620	5.1499	2021/03/08	9.7843	9.6626
2022/01/18	4.6599	5.1498	2021/03/09	9.7781	9.6584
2022/01/19	4.6587	5.1508	2021/03/10	9.7766	9.6560
2022/01/20	4.6568	5.1511	2021/03/11	9.7738	9.6526
2022/01/21	4.6582	5.1536	2021/03/12	9.7729	9.6581
2022/01/22	4.6613	5.1577	2021/03/13	9.7827	9.6701
2022/01/23	4.6631	5.1603	2021/03/14	9.7886	9.6738
2022/01/24	4.6638	5.1605	2021/03/15	9.7905	9.6732
2022/01/25	4.6651	5.1604	2021/03/16	9.7926	9.6713
2022/01/26	4.6658	5.1602	2021/03/17	9.7860	9.6639
2022/01/27	4.6659	5.1586	2021/03/18	9.7895	9.6676
2022/01/28	4.6688	5.1592	2021/03/19	9.7883	9.6649
2022/01/29	4.6869	5.1763	2021/03/20	9.7821	9.6585
2022/01/30	4.6836	5.1738	2021/03/21	9.7803	9.6579
2022/01/31	4.6769	5.1686	2021/03/22	9.7825	9.6618
2022/02/01	4.6730	5.1673	2021/03/23	9.7814	9.6630
2022/02/02	4.6639	5.1615	2021/03/24	9.7818	9.6644
2022/02/03	4.6552	5.1557	2021/03/25	9.7792	9.6640
2022/02/04	4.6450	5.1497	2021/03/26	9.7798	9.6677
2022/02/05	4.6577	5.1610	2021/03/27	9.7712	9.6582
2022/02/06	4.6654	5.1674	2021/03/28	9.7639	9.6503
2022/02/07	4.6719	5.1722	2021/03/29	9.7669	9.6540
2022/02/08	4.6736	5.1717	2021/03/30	9.7656	9.6502
2022/02/09	4.6735	5.1697	2021/03/31	9.7603	9.6451
2022/02/10	4.6715	5.1680	2021/04/01	9.7539	9.6372
2022/02/11	4.6752	5.1705	2021/04/02	9.7467	9.6292

2022/02/12	4.6758	5.1703	2021/04/03	9.7473	9.6301
2022/02/13	4.6807	5.1728	2021/04/04	9.7453	9.6307
2022/02/14	4.6749	5.1682	2021/04/05	9.7460	9.6331
2022/02/15	4.6796	5.1719	2021/04/06	9.7403	9.6308
2022/02/16	4.6714	5.1777	2021/04/07	9.7337	9.6258
2022/02/17	4.6589	5.1665	2021/04/08	9.7302	9.6225
2022/02/18	4.6640	5.1735	2021/04/09	9.7245	9.6194
2022/02/19	4.6627	5.1724	2021/04/10	9.7186	9.6125
2022/02/20	4.6595	5.1680	2021/04/11	9.7159	9.6092
2022/02/22	4.6517	5.1597	2021/04/12	9.7125	9.6048
2022/02/24	4.6584	5.1589	2021/04/13	9.7115	9.6032
2022/02/25	4.6628	5.1597	2021/04/14	9.7070	9.5958
2022/02/26	4.6659	5.1600	2021/04/15	9.7064	9.5953
2022/02/27	4.6755	5.1655	2021/04/16	9.7026	9.5914
2022/02/28	4.6749	5.1631	2021/04/17	9.7141	9.6010
2022/03/01	4.6699	5.1588	2021/04/18	9.7191	9.6046
2022/03/02	4.6775	5.1661	2021/04/19	9.7141	9.6016
2022/03/03	4.6684	5.1579	2021/04/20	9.7039	9.5922
2022/03/04	4.6600	5.1515	2021/04/21	9.7043	9.5932
2022/03/05	4.6535	5.1465	2021/04/22	9.7009	9.5895
2022/03/06	4.6597	5.1495	2021/04/23	9.6963	9.5914
2022/03/07	4.6533	5.1422	2021/04/24	9.7002	9.5937
2022/03/08	4.6536	5.1477	2021/04/25	9.7016	9.5943
2022/03/09	4.6597	5.1433	2021/04/26	9.6940	9.5864
2022/03/10	4.6497	5.1398	2021/04/27	9.6890	9.5808
2022/03/11	4.6485	5.1394	2021/04/28	9.6885	9.5782
2022/03/12	4.6515	5.1404	2021/04/29	9.6789	9.5672
2022/03/13	4.6542	5.1410	2021/04/30	9.6753	9.5622
2022/03/14	4.6516	5.1380	2021/05/01	9.6841	9.5662
2022/03/15	4.6626	5.1500	2021/05/02	9.6829	9.5679
2022/03/16	4.6696	5.1563	2021/05/03	9.6853	9.5701
2022/03/17	4.6591	5.1476	2021/05/04	9.6844	9.5697
2022/03/18	4.6583	5.1488	2021/05/05	9.6805	9.5668
2022/03/19	4.6514	5.1431	2021/05/06	9.6771	9.5630
2022/03/20	4.6453	5.1398	2021/05/07	9.6726	9.5613
2022/03/21	4.6406	5.1366	2021/05/08	9.6700	9.5595
2022/03/22	4.6361	5.1326	2021/05/09	9.6675	9.5570
2022/03/23	4.6314	5.1273	2021/05/10	9.6669	9.5559
2022/03/24	4.6340	5.1275	2021/05/11	9.6646	9.5520
2022/03/25	4.6379	5.1269	2021/05/12	9.6606	9.5468
2022/03/26	4.6432	5.1315	2021/05/13	9.6544	9.5387
2022/03/27	4.6435	5.1288	2021/05/15	9.6525	9.5317
2022/03/28	4.6432	5.1272	2021/05/16	9.6524	9.5312
2022/03/29	4.6439	5.1264	2021/05/17	9.6509	9.5277
2022/03/30	4.6451	5.1278	2021/05/18	9.6497	9.5289
2022/03/31	4.6395	5.1248	2021/05/19	9.6507	9.5278

2022/04/01	4.6366	5.1238	2021/05/20	9.6482	9.5270
2022/04/02	4.6253	5.1151	2021/05/21	9.6409	9.5176
2022/04/03	4.6207	5.1111	2021/05/22	9.6413	9.5220
2022/04/04	4.6170	5.1083	2021/05/23	9.6469	9.5293
2022/04/05	4.6121	5.1037	2021/05/24	9.6462	9.5291
2022/04/06	4.6079	5.1003	2021/05/25	9.6437	9.5265
2022/04/07	4.6086	5.0993	2021/05/26	9.6434	9.5246
2022/04/08	4.6287	5.1162	2021/05/27	9.6400	9.5190
2022/04/09	4.6354	5.1194	2021/05/28	9.6360	9.5137
2022/04/10	4.6405	5.1232	2021/05/29	9.6352	9.5094
2022/04/11	4.6475	5.1265	2021/05/30	9.6324	9.5039
2022/04/12	4.6677	5.1417	2021/05/31	9.6297	9.5020
2022/04/13	4.6722	5.1445	2021/06/01	9.6309	9.5031
2022/04/14	4.6778	5.1494	2021/06/02	9.6363	9.5114
			2021/06/03	9.6297	9.5030
			2021/06/04	9.6283	9.5042
			2021/06/05	9.6272	9.5036
			2021/06/06	9.6237	9.5016
			2021/06/07	9.6219	9.4998
			2021/06/08	9.6206	9.4976
			2021/06/09	9.6189	9.4956
			2021/06/10	9.6157	9.4923
			2021/06/11	9.6112	9.4890
			2021/06/12	9.6128	9.4862
			2021/06/13	9.6072	9.4798
			2021/06/14	9.6025	9.4748
			2021/06/15	9.6000	9.4713
			2021/06/16	9.6002	9.4697
			2021/06/17	9.5979	9.4677
			2021/06/18	9.6006	9.4690
			2021/06/19	9.5995	9.4705
			2021/06/20	9.6003	9.4743
			2021/06/21	9.5999	9.4756
			2021/06/22	9.5989	9.4772
			2021/06/23	9.5944	9.4747
			2021/06/24	9.5924	9.4742
			2021/06/25	9.5910	9.4722
			2021/06/26	9.5890	9.4692
			2021/06/27	9.5880	9.4655
			2021/06/28	9.5863	9.4645
			2021/06/29	9.5780	9.4568
			2021/06/30	9.5801	9.4608
			2021/07/01	9.5752	9.4618
			2021/07/02	9.5749	9.4585
			2021/07/03	9.5778	9.4639
			2021/07/04	9.5682	9.4561

			2021/07/05	9.5722	9.4620
			2021/07/06	9.5752	9.4673
			2021/07/07	9.5743	9.4682
			2021/07/08	9.5717	9.4667
			2021/07/09	9.5656	9.4605
			2021/07/10	9.5691	9.4635
			2021/07/11	9.5653	9.4605
			2021/07/12	9.5640	9.4585
			2021/07/13	9.5567	9.4513
			2021/07/14	9.5592	9.4518
			2021/07/15	9.5633	9.4585
			2021/07/16	9.5551	9.4513
			2021/07/17	9.5545	9.4516
			2021/07/18	9.5496	9.4497
			2021/07/19	9.5506	9.4525
			2021/07/20	9.5481	9.4527
			2021/07/21	9.5454	9.4531
			2021/07/22	9.5434	9.4522
			2021/07/23	9.5423	9.4553
			2021/07/24	9.5377	9.4503
			2021/07/25	9.5372	9.4477
			2021/07/26	9.5334	9.4420
			2021/07/27	9.5297	9.4373
			2021/07/28	9.5296	9.4350
			2021/07/29	9.5276	9.4338
			2021/07/30	9.5247	9.4321
			2021/07/31	9.5243	9.4314
			2021/08/01	9.5232	9.4311
			2021/08/02	9.5208	9.4285
			2021/08/03	9.5160	9.4264
			2021/08/04	9.5135	9.4259
			2021/08/05	9.5120	9.4244
			2021/08/06	9.5100	9.4216
			2021/08/07	9.5046	9.4159
			2021/08/08	9.5059	9.4170
			2021/08/09	9.5007	9.4084
			2021/08/10	9.4971	9.4030
			2021/08/11	9.5026	9.4087
			2021/08/12	9.4991	9.4024
			2021/08/13	9.4947	9.3975
			2021/08/14	9.4979	9.3983
			2021/08/15	9.4993	9.3991
			2021/08/16	9.4947	9.3951
			2021/08/17	9.4931	9.3943
			2021/08/18	9.4834	9.3943
			2021/08/19	9.4768	9.3879

			2021/08/20	9.4800	9.3922
			2021/08/21	9.4804	9.3922
			2021/08/22	9.4777	9.3875
			2021/08/23	9.4808	9.3883
			2021/08/24	9.4743	9.3843
			2021/08/25	9.4736	9.3776
			2021/08/26	9.4754	9.3785
			2021/08/27	9.4705	9.3722
			2021/08/28	9.4691	9.3704
			2021/08/29	9.4774	9.3786
			2021/08/30	9.4795	9.3813
			2021/08/31	9.4746	9.3770
			2021/09/01	9.4678	9.3705
			2021/09/02	9.4680	9.3731
			2021/09/03	9.4598	9.3655
			2021/09/04	9.4603	9.3689
			2021/09/05	9.4586	9.3674
			2021/09/06	9.4567	9.3642
			2021/09/07	9.4565	9.3605
			2021/09/08	9.4646	9.3686
			2021/09/09	9.4649	9.3663
			2021/09/10	9.4612	9.3608
			2021/09/11	9.4601	9.3586
			2021/09/12	9.4577	9.3558
			2021/09/13	9.4554	9.3534
			2021/09/14	9.4504	9.3495
			2021/09/15	9.4457	9.3450
			2021/09/16	9.4494	9.3513
			2021/09/17	9.4473	9.3496
			2021/09/18	9.4509	9.3543
			2021/09/19	9.4507	9.3536
			2021/09/20	9.4473	9.3541
			2021/09/21	9.4404	9.3448
			2021/09/22	9.4478	9.3516
			2021/09/23	9.4451	9.3499
			2021/09/24	9.4409	9.3434
			2021/09/25	9.4355	9.3376
			2021/09/26	9.4320	9.3350
			2021/09/27	9.4286	9.3314
			2021/09/28	9.4219	9.3257
			2021/09/29	9.4237	9.3296
			2021/09/30	9.4297	9.3362
			2021/10/01	9.4280	9.3368
			2021/10/02	9.4326	9.3452
			2021/10/03	9.4273	9.3409
			2021/10/04	9.4348	9.3497

			2021/10/05	9.4342	9.3511
			2021/10/06	9.4306	9.3472
			2021/10/07	9.4317	9.3503
			2021/10/08	9.4276	9.3436
			2021/10/09	9.4229	9.3414
			2021/10/10	9.4176	9.3315
			2021/10/11	9.4269	9.3409
			2021/10/12	9.4301	9.3444
			2021/10/13	9.4226	9.3410
			2021/10/14	9.4130	9.3322
			2021/10/15	9.4054	9.3272
			2021/10/16	9.4015	9.3234
			2021/10/17	9.3941	9.3202
			2021/10/18	9.4163	9.3374
			2021/10/19	9.4194	9.3373
			2021/10/20	9.4201	9.3357
			2021/10/21	9.4192	9.3336
			2021/10/22	9.4097	9.3220
			2021/10/23	9.4040	9.3161
			2021/10/24	9.3949	9.3065
			2021/10/25	9.4107	9.3215
			2021/10/26	9.4104	9.3272
			2021/10/27	9.4190	9.3307
			2021/10/28	9.4123	9.3304
			2021/10/29	9.4083	9.3280
			2021/10/30	9.4057	9.3251
			2021/10/31	9.4094	9.3296
			2021/11/01	9.4089	9.3270
			2021/11/02	9.4027	9.3270
			2021/11/03	9.4031	9.3226
			2021/11/04	9.4063	9.3246
			2021/11/05	9.4065	9.3260
			2021/11/06	9.3965	9.3154
			2021/11/07	9.4019	9.3177
			2021/11/08	9.3968	9.3100
			2021/11/09	9.4061	9.3219
			2021/11/10	9.4013	9.3150
			2021/11/11	9.4019	9.3144
			2021/11/13	9.3953	9.3160
			2021/11/14	9.3944	9.3143
			2021/11/15	9.3952	9.3175
			2021/11/16	9.3907	9.3144
			2021/11/17	9.3872	9.3098
			2021/11/18	9.3740	9.3002
			2021/11/19	9.3909	9.3126
			2021/11/20	9.3951	9.3169

			2021/11/21	9.3996	9.3165
			2021/11/22	9.3955	9.3166
			2021/11/23	9.3969	9.3123
			2021/11/24	9.3949	9.3119
			2021/11/25	9.3959	9.3104
			2021/11/26	9.3974	9.3156
			2021/11/27	9.3991	9.3189
			2021/11/28	9.3942	9.3123
			2021/11/29	9.3883	9.2991
			2021/11/30	9.3812	9.3011
			2021/12/01	9.3801	9.3002
			2021/12/02	9.3679	9.2914
			2021/12/03	9.3738	9.2944
			2021/12/04	9.3765	9.2971
			2021/12/05	9.3738	9.2930
			2021/12/06	9.3820	9.2960
			2021/12/07	9.3720	9.2891
			2021/12/08	9.3755	9.2906
			2021/12/09	9.3737	9.2875
			2021/12/10	9.3674	9.2825
			2021/12/11	9.3672	9.2827
			2021/12/12	9.3630	9.2795
			2021/12/13	9.3615	9.2796
			2021/12/14	9.3690	9.2856
			2021/12/15	9.3654	9.2830
			2021/12/16	9.3617	9.2862
			2021/12/17	9.3808	9.3060
			2021/12/18	9.3943	9.3178
			2021/12/19	9.3902	9.3140
			2021/12/20	9.3869	9.3083
			2021/12/21	9.3804	9.3004
			2021/12/22	9.3779	9.2986
			2021/12/23	9.3696	9.2884
			2021/12/24	9.3716	9.2892
			2021/12/25	9.3780	9.2944
			2021/12/26	9.3685	9.2871
			2021/12/27	9.3649	9.2851
			2021/12/28	9.3727	9.2940
			2021/12/29	9.3691	9.2868
			2021/12/30	9.3666	9.2874
			2021/12/31	9.3785	9.3053
			2022/01/01	9.4207	9.3341
			2022/01/02	9.4211	9.3324
			2022/01/03	9.4369	9.3495
			2022/01/04	9.4389	9.3470
			2022/01/05	9.4478	9.3520

			2022/01/06	9.4465	9.3514
			2022/01/07	9.4545	9.3568
			2022/01/08	9.4524	9.3581
			2022/01/09	9.4526	9.3566
			2022/01/10	9.4536	9.3635
			2022/01/11	9.4476	9.3549
			2022/01/12	9.4444	9.3524
			2022/01/13	9.4525	9.3648
			2022/01/14	9.4483	9.3560
			2022/01/15	9.4489	9.3589
			2022/01/16	9.4444	9.3583
			2022/01/17	9.4435	9.3543
			2022/01/18	9.4381	9.3495
			2022/01/19	9.4340	9.3450
			2022/01/20	9.4301	9.3408
			2022/01/21	9.4274	9.3379
			2022/01/22	9.4242	9.3343
			2022/01/23	9.4236	9.3342
			2022/01/24	9.4154	9.3278
			2022/01/25	9.4081	9.3221
			2022/01/26	9.4019	9.3174
			2022/01/27	9.3910	9.3105
			2022/01/28	9.3844	9.3067
			2022/01/29	9.3932	9.3202
			2022/01/30	9.3875	9.3145
			2022/01/31	9.3752	9.3040
			2022/02/01	9.3698	9.2989
			2022/02/02	9.3608	9.2898
			2022/02/03	9.3507	9.2802
			2022/02/04	9.3442	9.2717
			2022/02/05	9.3575	9.2844
			2022/02/08	9.3547	9.2883
			2022/02/20	9.3499	9.2773
			2022/02/21	9.3432	9.2647
			2022/02/22	9.3464	9.2654
			2022/02/25	9.3471	9.2673
			2022/02/26	9.3487	9.2655
			2022/03/01	9.3495	9.2648
			2022/03/04	9.3546	9.2613
			2022/03/05	9.3539	9.2567
			2022/03/07	9.3537	9.2540
			2022/03/08	9.3646	9.2608
			2022/03/09	9.3652	9.2596
			2022/03/10	9.3617	9.2580
			2022/03/13	9.3586	9.2604
			2022/03/14	9.3564	9.2591

			2022/03/15	9.3695	9.2727
			2022/03/16	9.3751	9.2809
			2022/03/17	9.3686	9.2739
			2022/03/18	9.3717	9.2768
			2022/03/19	9.3678	9.2727
			2022/03/20	9.3653	9.2691
			2022/03/21	9.3652	9.2676
			2022/03/24	9.3582	9.2620
			2022/03/27	9.3603	9.2716
			2022/03/28	9.3573	9.2713
			2022/03/29	9.3534	9.2702
			2022/03/30	9.3549	9.2727
			2022/03/31	9.3543	9.2719
			2022/04/01	9.3544	9.2711
			2022/04/02	9.3490	9.2648
			2022/04/03	9.3464	9.2619
			2022/04/04	9.3449	9.2605
			2022/04/05	9.3428	9.2578
			2022/04/06	9.3410	9.2553
			2022/04/07	9.3392	9.2543
			2022/04/08	9.3539	9.2729
			2022/04/09	9.3598	9.2814
			2022/04/10	9.3691	9.2903
			2022/04/11	9.3648	9.2960
			2022/04/12	9.4168	9.3402
			2022/04/13	9.4480	9.3687
			2022/04/14	9.4712	9.3914
			2022/04/15	9.4924	9.4127
			2022/04/16	9.5094	9.4291
			2022/04/17	9.5408	9.4661
			2022/05/01	9.8695	9.7340
			2022/05/02	9.8866	9.7455
			2022/05/03	9.9004	9.7536
			2022/05/05	9.9290	9.7724
			2022/05/07	9.9525	9.7917